Evolved for success in novel environments: The round goby genome

Authors

Irene Adrian-Kalchhauser[1], Anders Blomberg[2*], Tomas Larsson[3*], Zuzana Musilova[4*], Claire R Peart[5*], Martin Pippel[6*], Monica Hongroe Solbakken[7*], Jaanus Suurväli[8*], Jean-Claude Walser[9*], Joanna Yvonne Wilson[10*], Magnus Alm Rosenblad[2,11§], Demian Burguera[4§], Silvia Gutnik[12§], Nico Michiels[13§], Mats Töpel[2§], Kirill Pankov[10§], Siegfried Schloissnig[14§], Sylke Winkler[6§]

Author contributions

* equal contribution, section lead authors, listed alphabetically

§ co-authors with equal contribution, listed alphabetically

Affiliations

[1] Program Man-Society-Environment, Department of Environmental Sciences, University of Basel, Vesalgasse 1, 4051 Basel, Switzerland

[2] Department of Chemistry and Molecular Biology, University of Gothenburg, Medicinaregatan 9C, 41390 Gothenburg, Sweden

[3] Department of Marine Sciences, University of Gothenburg, Medicinaregatan 9C, 41390 Gothenburg, Sweden

[4] Department of Zoology, Charles University, Vinicna 7, CZ-128 44 Prague, Czech Republic

[5] Division of Evolutionary Biology, Faculty of Biology, Ludwig-Maximilians-Universität München, Grosshaderner Strasse 2, 82152 Planegg-Martinsried, Germany

[6] Max Planck Institute of Molecular Cell Biology and Genetics, Pfotenhauerstrasse 108, 01307 Dresden, Germany

[7] Centre for Ecological and Evolutionary Synthesis, University of Oslo, Blindernveien 31, 0371 Oslo, Norway

[8] Institute for Genetics, University of Cologne, Zülpicher Strasse 47a, D-50674 Köln, Germany

[9] Genetic Diversity Centre, ETH, Universitätsstrasse 16, 8092 Zurich, Switzerland

[10] Department of Biology, McMaster University, 1280 Main Street West, Hamilton, ON, Canada

[11] NBIS Bioinformatics Infrastructure for Life Sciences, University of Gothenburg, Medicinaregatan 9C, 41390 Gothenburg, Sweden

[12] Biocenter, University of Basel, Klingelbergstrasse 50/70, 4056 Basel, Switzerland

[13] Institute of Evolution and Ecology, University of Tuebingen, Auf der Morgenstelle 28, 72076 Tübingen, Germany

[14] Research Institute of Molecular Pathology (IMP), Vienna BioCenter (VBC), 1030 Vienna, Austria.

Corresponding author

Irene Adrian-Kalchhauser

email: irene.adrian-kalchhauser@unibas.ch

mail: University of Basel, Vesalgasse 1, 4051 Basel

phone: +41 61 2070410

Keywords

PacBio, *Neogobius melanostomus,* invasive species, fish, genomics, evolution, adaptation, gene duplication, vision, olfaction, innate immunity, detoxification, osmoregulation, epigenetics

Abstract

Since the beginning of global trade, hundreds of species have colonized territories outside of their native range. Some of these species proliferate at the expense of native ecosystems, i.e., have become invasive. Invasive species constitute powerful *in situ* experimental systems to study fast adaptation and directional selection on short ecological timescales. They also present promising case studies for ecological and evolutionary success in novel environments.

We seize this unique opportunity to study genomic substrates for ecological success and adaptability to novel environments in a vertebrate. We report a highly contiguous long-read based genome assembly for the most successful temperate invasive fish, the benthic round goby (*Neogobius melanostomus)*, and analyse gene families that may promote its impressive ecological success.

Our approach provides novel insights from the large evolutionary scale to the small species-specific scale. We describe expansions in specific cytochrome P450 enzymes, a remarkably diverse innate immune system, an ancient duplication in red light vision accompanied by red skin fluorescence, evolutionary patterns in epigenetic regulators, and the presence of genes that may have contributed to the round goby's capacity to invade cold and salty waters.

A recurring theme across all analyzed gene families are gene expansions. This suggests that gene duplications may promote ecological flexibility, superior performance in novel environments, and underlie the impressive colonization success of the round goby. *Gobiidae* generally feature fascinating adaptations and are excellent colonizers. Further long-read genome approaches across the goby family may reveal whether the ability to conquer new habitats relates more generally to gene copy number expansions.

Introduction

Since the beginning of global trade and the colonial period, hundreds of species have colonized territories outside their native range. A fraction of those species proliferates at the expense of native species and ecosystems, i.e., they are invasive. While invasive species present challenges for biodiversity and ecosystem conservation, they also constitute exciting eco-evolutionary models for adaptation and ecological success in novel or changing environments (1–4).

The benthic round goby *Neogobius melanostomus* (**Figure 1A**) is one of the most widespread invasive fish species. Since 1990, round gobies have been detected in over 20 countries outside their native Ponto-Caspian range. In some regions of Europe and North America, they have become the most common fish species (5–7) (**Figure 1B**). Lasting impacts on biodiversity and on ecosystems have been observed (see (8) for a summary of the impacts). In recent years, the round goby has therefore become a novel model for ecology, behavior and evolution (**Figure 1C**).

The round goby effortlessly outcompetes native species with similar ecology, and is therefore a promising candidate to study fundamental questions on long-term ecological and evolutionary success. Round goby sequence data are presently restricted to a handful of phylogenetic markers (9–15). However, genome analyses have previously provided significant insights into fish ecology and evolution. Examples are genome compaction (16), the transition from fin to limb (17), loss of major parts of adaptive immunity (18), or effects of genome duplication (19). We therefore expect relevant insights into round goby biology and into success in novel environments from the round goby genome sequence.

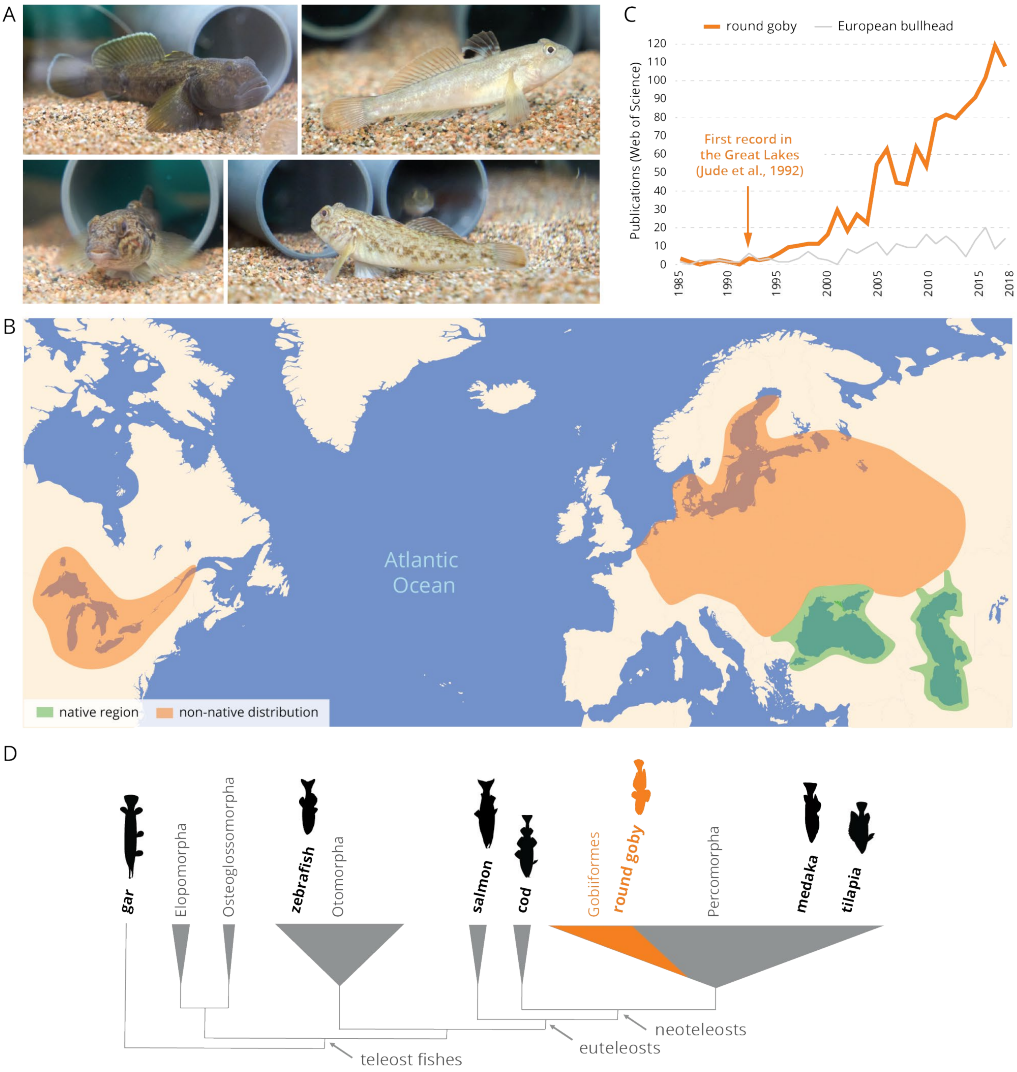

Figure 1

The round goby, a benthic invasive fish species. A *Wild-caught round goby in aquaria. Individuals are usually brightly colored or spotted with a characteristic black dot on the first dorsal fin. During the reproductive season, territorial males develop a black body color (first panel).* ***B*** *The growing scientific relevance of the species is reflected by records in Web of Science (orange) when compared to a non-invasive fish with similar ecology (European bullhead, Cottus gobio; grey).* ***C*** *Current distribution of round goby. The round goby has spread from its native region (green) to many European rivers and lakes, the Baltic Sea, the Great Lakes and their tributaries (orange).* ***D*** *Phylogenetic position of the round goby among fishes.*

103 The survival of an individual in a novel environment depends on how well it can perceive, react to, and
104 accommodate to its new surroundings. In this study, we therefore explore a high quality and
105 contiguous genome assembly of the round goby for genes related to three categories: environmental
106 perception, reaction to environmental conditions, and long-term accommodation to novel
107 environments. We focus on gene families that have been hypothesized to play a role in the
108 colonization of novel environments and on gene families that may relate to round goby invasion
109 ecology.
110
111 For environmental perception, we investigated genes responsible for sensory perception in fishes. We
112 specifically focused on the opsin genes for visual perception, as well as on the olfactory receptors for
113 odor perception. Vision in fishes is often specifically adapted to environmental conditions, such as
114 darkness in deep water (20), modified color spectrum in turbid water (21, 22), habitat color (23), or
115 specific light regimes or light compositions (24–26). The overall spectral sensitivity range of teleost
116 fishes exceeds the human visual range and, in many cases, includes the UV (23) and far-red (27)
117 spectrum. Similarly, olfaction is an essential chemoreception sense for fish, allowing for fast responses
118 to predators and alarm cues as well as for intra-species communication. Pheromones have play an
119 important role in the round goby (28–30), and males attract females into their nests by releasing them
120 (31). A particularly specialized sense of smell therefore may provide an advantage during initial
121 population establishment in novel environments.
122
123 We further investigated genes that may mediate responses to novel environments, namely genes
124 involved in detoxification, ion transport and the immune system. The round goby occurs even in
125 chemically contaminated harbors (32–34) and appears to tolerate xenobiotic compounds well. This
126 suggests that the round goby may be particularly well equipped to degrade and eliminate chemical
127 pollutants. We therefore analyze the cytochrome P450 gene superfamily, which is a particularly
128 important and conserved part of the xenobiotic response (35). The round goby also tolerates a wide
129 range of salinities (0 to 25 PSU / ‰) and temperatures (0°C-30°C) and occurs at latitudes ranging
130 from <40° N in the Ponto-Caspian region to >60° N in the Baltic Sea. Most fishes tolerate only a
131 narrow range of salinities (36); the round goby however belongs to a specialized group, the euryhaline
132 fish species, which thrive in fresh and brackish environments and includes estuarine species and
133 migratory species such as salmon. We study the genetic basis of osmoregulation and osmolyte

134 production in round goby to gain insights into the evolution of salinity and cold tolerance, and to
135 possibly predict future range expansions. Invasive species encounter an array of previously unknown
136 pathogens when they colonize a habitat, and invasion success may be related to a species' ability to
137 tackle novel immune challenges (37). Intriguingly, the round goby displays a low parasite load at the
138 invasion front (38). We therefore characterize key factors of the innate and the adaptive immune
139 system.
140
141 We also investigated conserved gene regulators because such genes might be involved in long-term
142 adaptation to a novel environment. Mechanisms such as DNA methylation and histone modifications
143 promote long- and short-term gene expression regulation and therefore mediate adaptations to altered
144 conditions at the cellular level (39), but also regulate genome-scale evolutionary processes such as
145 the distribution of meiotic recombination events (40) or transposon activity (41), and provide stochastic
146 variability as basis for selection (42). Epigenetic variants have been proposed to cause fitness-relevant
147 differences in gene expression and phenotype (43, 44). The ecological flexibility of the round goby has
148 been linked to enhanced gene expression plasticity in response to environmental stimuli (45) and to
149 their ability to pass information on water temperature to their offspring through maternal RNA (46). To
150 understand the features of core epigenetic regulators in the round goby, we focused on two widely
151 conserved and well characterized parts of the epigenetic machinery: the histone-methylating PRC2
152 complex and the DNA methylases. Both mechanisms are thought to restrict developmental plasticity,
153 downregulate gene expression (at least in mammals), and have been linked to plastic responses,
154 behavioral changes, and environmental memory (47–51).
155
156 Finally, we take advantage of the high genome contiguity to investigate sex determination using RAD
157 sequencing data. Fish display a wide variety of sex determination mechanisms, ranging from sex
158 chromosomes to multilocus genetic sex determination to environmental sex determination (52), and
159 sex determination in the round goby has not previously been investigated.

Results

1. The round goby genome

The round goby genome assembly ("RGoby_Basel_V2", BioProject accession PRJNA549924, BioSample SAMN12099445, GenBank genome accession VHKM00000000, release date July 22 2019) consists of 1364 contigs with a total length of 1.00 Gb (1'003'738'563 bp), which is within the expected size range (53–55). It is assembled to high contiguity (NG50 at 1'660'458 bp and N50 at 2'817'412 bp). GC content is 41.60%. An automated Maker gene annotation predicts a total of 38,773 genes and 39,166 proteins, of which 30,698 are longer than 100 amino acids (**Table 1**; annotation track available as **Supplemental_Material_S1**). The genome does not appear to contain a sex chromosome or a large sex determining region, since a RAD-tag dataset from 40 females and 40 males with an estimated resolution of 25,000 – 45,000 bp does not contain any sex-specific loci.

Approximately 47% of the genome assembly is masked as various types of repetitive sequences by RepeatMasker in the Maker annotation pipeline. The genome consists of approximately 9% predicted interspersed repeats (**Supplemental_Table_S1**), which is much lower than for zebrafish (*Danio rerio*, total genome size 1427.3Mb, 46% predicted as interspersed repeats) but higher than for the more closely related three-spined stickleback (*Gasterosteus aculeatus*, total genome size 446.6Mb, 3.2% predicted as interspersed repeats). Among interspersed repeats, the long terminal repeat (LTR) retrotransposon family is the most common in many species including fish (Repbase, https://www.girinst.org/repbase/). RepeatMasker identifies 0.9% LTR retrotransposons in the round goby genome, but separately run *de novo* predictions with LTRfinder and LTRharvest (**Supplemental_Table_S1)** indicate an underestimation of LTR retrotransposons and interspersed repeats by this approach. The latter approaches estimate that the proportion of LTR retrotransposons in the round goby genome is 11.2% (3.8% LTRs with target-site-repeats; LTRfinder) or 4.9% (LTRharvest), respectively.

In addition to the genome sequence, we provide raw short read sequencing data from various published and ongoing projects. They include RNA sequencing data from early cleavage embryos

190 (46), DNA methylation capture data from adult male brains (47), as well as RAD tags from two local
191 Swiss populations and ATAC seq reads from brain and liver (unpublished; **Table 1**).
192
193 **Table 1. Round goby genome assembly and annotation statistics.**

Assembly	
Number of contigs	1364
Total genome length (bp)	1,003,738,563
Longest contig (bp)	19,396,355
Smallest contig (bp)	21,178
N50 contig length (bp)	2,817,412
Annotation	
Number of genes	38,773
Genomic repeat content (%)	47
G + C (%)	41.60
LTR retrotransposons (%)	4.9 - 11.2
Accession	NCBI BioProject PRJNA549924 Accession VHKM00000000
Additional sequencing data	
RNA (Adrian-Kalchhauser 2018)	Embryonic transcriptome (1-32 cell stages) from 16 clutches NCBI BioProject PRJNA547711 NCBI SRA SRR9317352 - SRR9317366
DNAme (Somerville 2019)	Brain DNA methylation data from 15 males NCBI BioProject PRJNA515617 NCBI SRA SRR8450505 - SRR8450528
RADseq (unpublished)	RAD Seq data from 120 individuals NCBI BioProject PRJNA547536 NCBI SRA SRR9214152 - SRR9214154
ATACseq (unpublished)	ATAC Seq data of liver and brain from 50 individuals NCBI BioProject PRJNA551348 NCBI SRA SRR9714857 - SRR9714901

194
195 **2. Sensory perception genes: Vision**
196
197 Vertebrates perceive color with cone cells expressing one of four types of opsin proteins (usually
198 sensitive to the red, green, blue, and ultraviolet part of the spectrum) and dim light with rod cells
199 expressing the rod opsin. The UV and blue light is detected by the short-wavelength sensitive SWS1
200 and SWS2 opsins, the green part of the spectrum is perceived mostly by the rhodopsin-like RH2
201 opsins, and the red color by the long-wavelength sensitive LWS opsins. Rod cells are active in the
202 dim-light conditions and contain the rod opsin RH1 (56). Gene duplications and losses of the opsin
203 genes during fish evolution correlate to certain extent with adaptations to specific environments (20,
204 57).

We identified two cone opsin gene duplications in the round goby genome. Firstly, the genome features a recent duplication of the green-sensitive RH2 gene. RH2 duplications are a common phenomenon in fish (**Figure 2**). Secondly, the genome features an ancient duplication of the long-wave red-sensitive LWS gene. The event can be traced most likely to the ancestor of all teleosts, or possibly even to the ancestor of Neopterygii (**Figure 2**; see **Supplemental_Fig_S1** for full tree). As expected, the round goby genome further contains one dim-light rod opsin (RH1) gene, two blue-sensitive SWS2 genes (57), and as previously reported for gobies, lacks the UV/violet-sensitive SWS1 gene (20, 25, 57).

The proposed ancestral position of the red opsin gene duplication is supported by three lines of evidence. First, the monophyly of all other teleost + gar LWS genes is strongly supported by the Bayesian analysis (Bayesian posterior probability value = 1). Second, the distant phylogenetic position is supported by trees based on individual exons, which indicate a low probability of a compromised phylogenetic signal, e.g. due to the partial gene conversion. Three of four exons cluster at the same position as the whole gene, while the fourth exon (exon 4) cluster with the genes resulting from a more recent teleost-specific LWS duplication specific to *Astyanax* and *Scleropages* (58) (**Supplemental_Fig_S2**). Third, the choice of outgroup (parietopsin or pinopsin) does not affect the position of the LWS2 gene. Together, these analyses suggest either (1) the presence of an ancient gene duplication event of the LWS gene in the ancestor of teleost and holostean fishes (i.e. *Neopterygii*) which was retained only in the goby family, or (2) a teleost-specific event, possibly identical to that reported for characins and bony tongues (58), with a subsequent concerted goby-specific sequence diversification in exons 2, 3 and 5.

The spectral sensitivity of photopigments, i.e. their excitation wavelength can be modified by substitutions in certain key amino acids (59). We find that round goby LWS1 and LWS2 differ in the key spectral tuning site at amino acid 277 (position 261 of bovine rhodopsin, **Table 2)** suggesting a sensitivity shift of 10 nm.

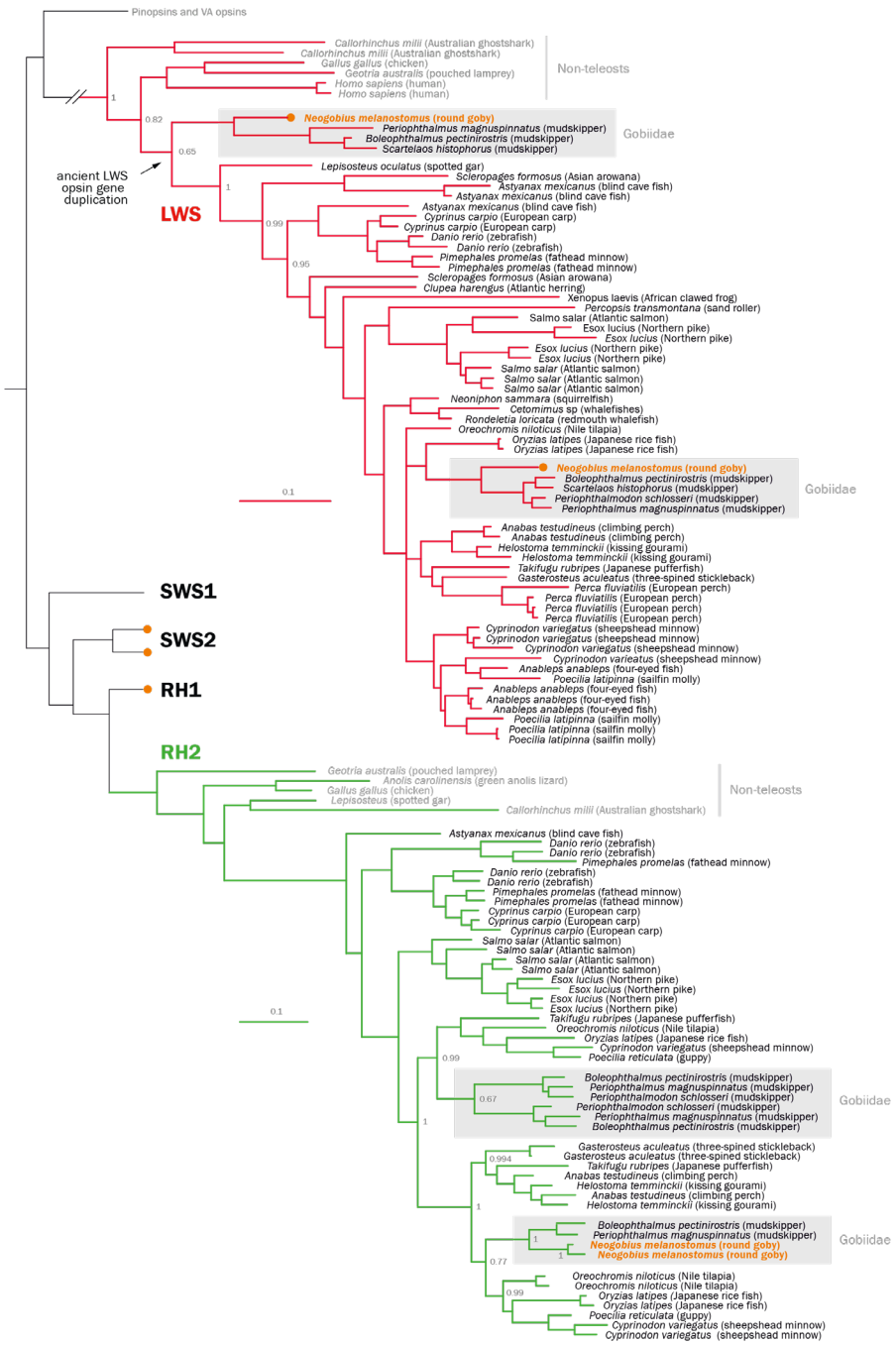

Figure 2

Phylogenetic tree of vertebrate opsin gene sequences. *Maximum-likelihood phylogenetic tree based on the cone and rod visual opsins and using VA opsins and pinopsins as outgroup. The round goby genome contains two LWS gene copies, which seem to be the results of an ancient gene duplication event, and two more recently duplicated RH2 gene copies. Round goby is indicated in orange. Red opsin branches are indicated in red. Green opsin branches are indicated in green. Non-teleost species and the outgroup (VA opsins and pinopsins) are indicated in grey. Grey boxes highlight Gobiidae.*

To find a possible link to the ecological significance of the red opsin duplication, we checked for the presence of red skin fluorescence in the round goby. Interestingly, round goby individuals of both sexes and of all sizes (n=10) feature weakly red fluorescent crescents above the eyes (**Figure 3**). Whether such pattern has any relevance for the putatively enhanced vision in the red spectrum remains elusive.

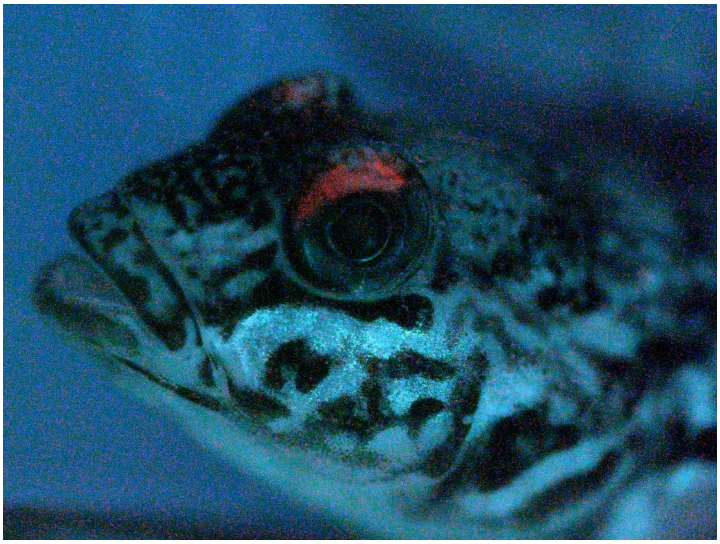

Figure 3

Red fluorescence in the round goby. *Round gobies exhibit red fluorescence above the eyes when exposed to green light.*

Table 2. Amino acid analysis of key tuning sites in Gobiidae red opsins proteins.

species	ecology	gene	key tuning amino acid site in round goby					max. spectral sensitivity (wavelength)	reference
			180	197	277	285	308		
		bovine rhodopsin equivalent site:	*164*	*181*	*261*	*269*	*292*		
Boleophthalmus pectinirostris	terrestrial mudskipper	LWS1	A	H	Y	T	A	553 nm	(25)
		LWS2	A	H	F	A	A	531 nm	
Periophthalmus magnuspinnatus	terrestrial mudskipper	LWS1	S	H	Y	T	A	560 nm	
		LWS2	A	H	F	T	A	546 nm	
Neogobius melanostomus	freshwater temperate rivers and lakes	LWS1	S	H	Y	T	A	560 nm	this study
		LWS2	S	H	F	T	A	550 nm*	this study
* = predicted by the key tuning sites, and Y261F shift of 10 nm; Yokoyama, 2008.									

254 **3. Sensory perception genes: Olfaction**

255

256 Olfactory receptors (OR) in vertebrates are 7-transmembrane-domain G-protein coupled
257 transmembrane proteins. They are expressed in neurons embedded in membranes of the olfactory
258 lamellae. Mammals usually have several hundred OR genes that cluster in two major types (~400 in
259 human, and ~1000 genes in mouse) (60). Teleost fishes possess fewer OR genes but feature a higher
260 diversity (5 kinds of type 2 ORs in teleosts as compared to 2 kinds of type 2 ORs in mammals) (61).
261 The binding properties of individual ORs, especially in fishes, are virtually unexplored.

262

263 We identified 112 putative olfactory receptor genes in the round goby genome. To put this result into
264 evolutionary context, all analyses were carried out in comparison with two Gobiidae species (blue-
265 spotted mudskipper and giant mudskipper) and two percomorph species (three-spined stickleback,
266 *Gasterosteus aculeatus* and Nile tilapia, *Oreochromis niloticus*; **Figure 4A**). The round goby presented
267 similar number of ORs (112) to the giant mudskipper (106) and stickleback (115), notably less than the
268 blue-spotted mudskipper (154) and near half the amount compared to Nile tilapia (214). We find that
269 all ORs belong to one of two transmembrane domain subtypes according to the Pfam database (7tm4
270 or 7tm1; **Figure 4B**; **Supplemental_Fig_S3**). This matches a previous large-scale phylogenetic
271 analysis which identified two main types of olfactory receptor genes in vertebrates (61). The functional
272 differences between the domain subtypes are unclear, but their different consensus sequences may
273 confer distinct biochemical properties.

274

275 Our analyses identify several cases of clade-specific gene expansions. Certain OR genes are
276 expanded in parallel in several lineages (**Figure 4C**). Likely, those expansion events are the result of
277 clade-restricted gene duplications, although a secondary role for gene conversion after species
278 divergence cannot be ruled out. While the Nile tilapia features the greatest overall amount of
279 expansions, the round goby presents the highest number of genes and expansions within the 7tm1
280 subfamily, a trend that is consistent in the other Gobiidae species (**Figure 4D**).

281

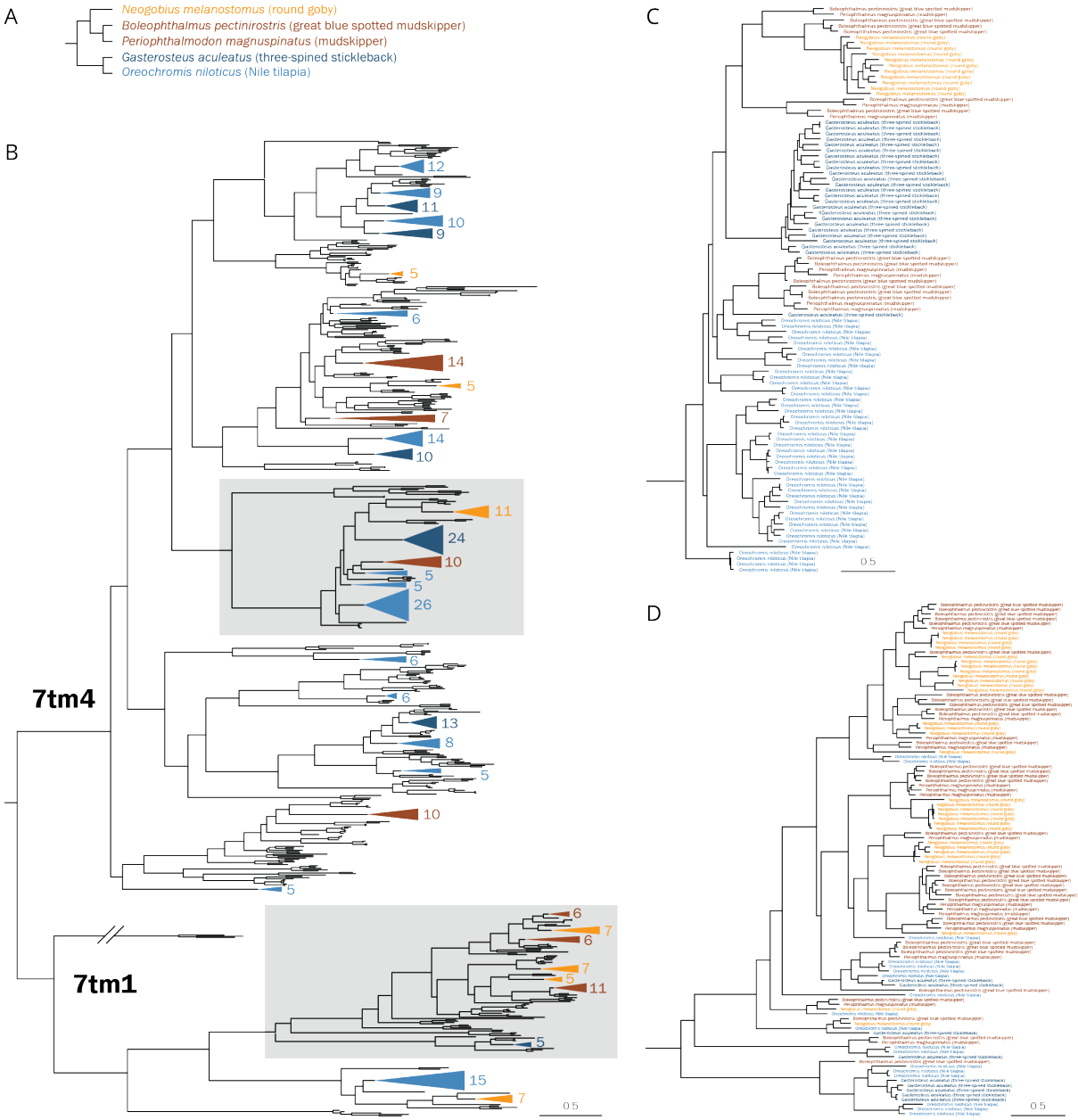

Figure 4

Phylogenetic tree of percomorph olfactory receptor protein sequences. A *Phylogenetic relationship among five analyzed percomorph species, i.e. three gobiids, one cichlid and one stickleback.* ***B*** *Maximum-likelihood phylogenetic tree constructed with adrenergic receptors as outgroup. Sequences were identified de novo except for nile tilapia (blue). Branches magnified in panels C and D are highlighted with grey boxes.* ***C*** *Branch of the 7tm4 family featuring large independent expansions in all species analyzed.* ***D*** *Branch of the 7tm1 family featuring several expansions in Gobiidae (red, orange) that are not paralleled in other percomorph species (blue).*

292 **4. Response to the environment: Detoxification**

293

294 The CYP gene superfamily is an essential part of the defensome, a collection of genes that provide
295 protection against harmful chemicals (35). Vertebrate genomes contain between 50-100 CYP genes.
296 The genomes of fugu and zebrafish, for example, encode 54 (62) and 94 (63) CYP genes respectively.
297 Expansions of individual CYP families occur in both mammals and fish. For example, zebrafish have
298 three times as many CYP2 family members (40) as most other vertebrate species (13-15), and similar
299 expansions of CYP2 genes have been observed in mice and rats (64).

300

301 We find that the round goby genome contains few CYP genes. We identify 25 complete or partial CYP
302 genes, as well as 21 gene fragments. Pseudogenes are common for CYP genes (62, 63, 65), which is
303 why strict annotation criteria are applied first before smaller fragments are considered. In total, the
304 genome contains approximately 50 CYP genes (**Supplemental_Table_S2**).

305

306 When including gene fragments, all expected CYP families are present in the round goby, and the
307 phylogenetic analyses show the expected relationships between gene families and between
308 vertebrates (**Figure 5**). Fish and most vertebrates have CYP genes from 17 families (CYP 1-5, 7, 8,
309 11, 17, 19, 20, 21, 24, 26, 27, 46 and 51) (62), while the CYP39 family occurs in humans and
310 zebrafish, but not in fugu (62, 63). In the round goby, the complete or partial genes could be assigned
311 to 9 CYP families (CYP 1- 4, 8, 19, 26, 27 and 51). The families CYP7, CYP11, CYP17 and CYP21
312 were present among the sequence fragments.

313

314 Contrary to expectations, the classical detoxification families CYP1-3 were not expanded (**Figure 5**).
315 CYP1, 2, 3 and to a lesser extent CYP4 proteins are responsible for the oxidative metabolism of
316 xenobiotic compounds (pollutants, drugs, etc.). In rodents and humans, the CYP1 family metabolizes
317 planar cyclic aromatic hydrocarbon compounds (reviewed in (66)), the CYP2 family metabolizes
318 structurally diverse drugs, steroids and carcinogens, the CYP4 family catalyzes the ω-hydroxylation of
319 the terminal carbon of fatty acids and xenobiotics, and CYP3 genes metabolize a range of structurally
320 different compounds in the liver and intestines. Over 50% of all pharmaceutical compounds are
321 metabolized by CYP3A genes in human. The goby genome contains three or four CYP1 genes: one
322 CYP1B gene, two CYP1C genes, and one CYP1A fragment. The latter lacks two main characteristics

323 (I- and K-helix) and could therefore be a pseudogene. As expected for a vertebrate (64), the genome
324 contains many CYP2 genes. The most important fish CYP2 families were represented, including
325 CYP2J, CYP2N, CYP2Y and CYP2AD. Finally, the round goby had a single CYP3A gene and a
326 potential CYP3A fragment. This is somewhat unusual because fish often feature species-specific
327 CYP3 subfamilies in addition to CYP3A. For example, medaka also contains CYP3B genes, zebrafish
328 CYP3C genes, and Acanthopterygii fish CYP3D genes (67).
329
330 We find that the round goby genome contains six CYP8 genes, which is more than expected based on
331 observations from the other gobies. The closely related large blue-spotted mudskipper has only two
332 CYP8 genes (XM_020924471 and XM_020919000.1; about 73-85% identity); no sequences were
333 found in other mudskipper species. Accordingly, we assume that the CYP8B genes have undergone
334 species-specific tandem duplications in the round goby, as is also known for the subfamilies CYP2AA,
335 CYP2X and CYP2K in zebrafish (64). Five round goby CYP8 genes locate to the same contig with
336 high sequence similarity (~90%), which is similar to zebrafish CYP8B1-3 that also colocalize on the
337 same chromosome (63). Misidentification of closely related CYP7, CYP8, and CYP39 genes as CYP8
338 is unlikely given the colocalization and high sequence similarity. The function of the expansion is
339 presently unclear, although expression patterns in zebrafish suggest a role in the early embryo (63). In
340 humans, CYP8 genes act as prostacyclin synthases that mediate steroid metabolic pathways in bile
341 acid production or prostaglandin synthesis (68). Based on structural similarities with yeast proteins,
342 CYP8 genes might also have E3 ubiquitin ligase activity. The almost identical crystal structures of
343 zebrafish and human CYP8A1 suggest similar functions in fish and mammals (69).

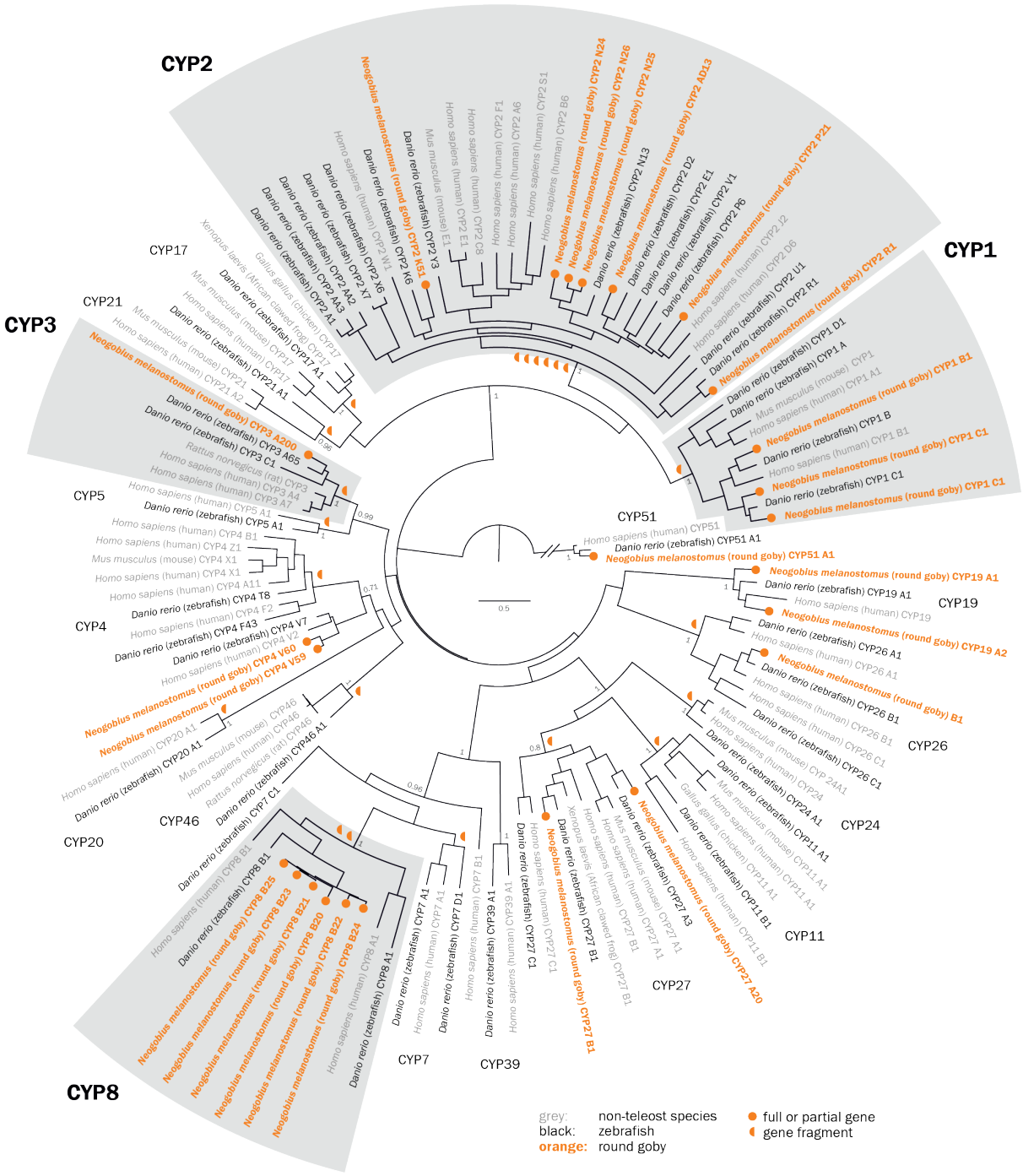

Figure 5.

Phylogenetic tree of vertebrate CYP protein sequences. *Maximum likelihood phylogenetic tree with 100 bootstraps, rooted with the CYP51 family. Detoxification genes CYP1-3 do not feature unusual expansions, while the CYP8 family is expanded to six members (grey boxes). Non-fish vertebrates are printed in grey. Fragments too short for tree building but attributable to a certain family are indicated by orange half circles next to the root of the respective family.*

353 **5. Response to the environment: Osmoregulation**

354

355 Osmotic homeostasis depends on passive ion and water uptake through cell membranes and the
356 intercellular space, on the active uptake or excretion of ions, and on the production and accumulation
357 of osmolytes. To understand the ability of round goby to tolerate a wide range of salinities, we
358 therefore compared the round goby repertoire of osmoregulatory genes to those of a stenohaline
359 freshwater species (zebrafish) and of euryhaline species (Nile tilapia, blue-spotted mudskipper and
360 three-spine stickleback).

361

362 Passive ion and water transport across membranes (transcellular permeability) depends on the
363 superfamily of aquaporin proteins. Aquaporins transport water (classical aquaporins), water and
364 glycerol (aquaglyceroporins), ammonia (aquaammoniaporins), or additional undescribed molecules
365 (unorthodox aquaporins; **Figure 6**). Primary sequences are only moderately conserved between the
366 classes (approximately 30% identity), but all aquaporins share six membrane-spanning segments and
367 five connecting loops. We find 15 aquaporin genes in the round goby, which compares to the number
368 in human (n=13) or zebrafish (n=20) and is lower than in the euryhaline Atlantic salmon (n=42) (70,
369 71). With 5 classical water aquaporins, 6 aquaglyceroporins, 2 aquaammonioporins, and 2 unorthodox
370 aquaporins, the round goby features the same types of aquaporins as freshwater stenohaline fish
371 (e.g., zebrafish) and highly euryhaline fish (e.g., tilapia; **Figure 6**).

372

373 Ion and water flow between cells in epithelia (paracellular permeability) is regulated by tight junctions,
374 of which claudin and occludin proteins are the most important components. Mammalian genomes
375 contain ~ 20 claudin genes, invertebrates such as *Caenorhabditis elegans* or *Drosophila melanogaster*
376 contain 4-5 genes, and fish often feature large expansions. For example, the fugu genome contains 56
377 claudins, of which some occur in clusters of > 10 genes (72). The round goby genome features 40
378 claudin paralogues, which is in line with numbers known from other fish. All human claudin genes were
379 represented as homologues (**Supplemental_Fig_S4**), and the round goby genome contains one
380 occludin gene in each of the two known subclades of the protein family (**Supplemental_Fig_S5**).

381

382

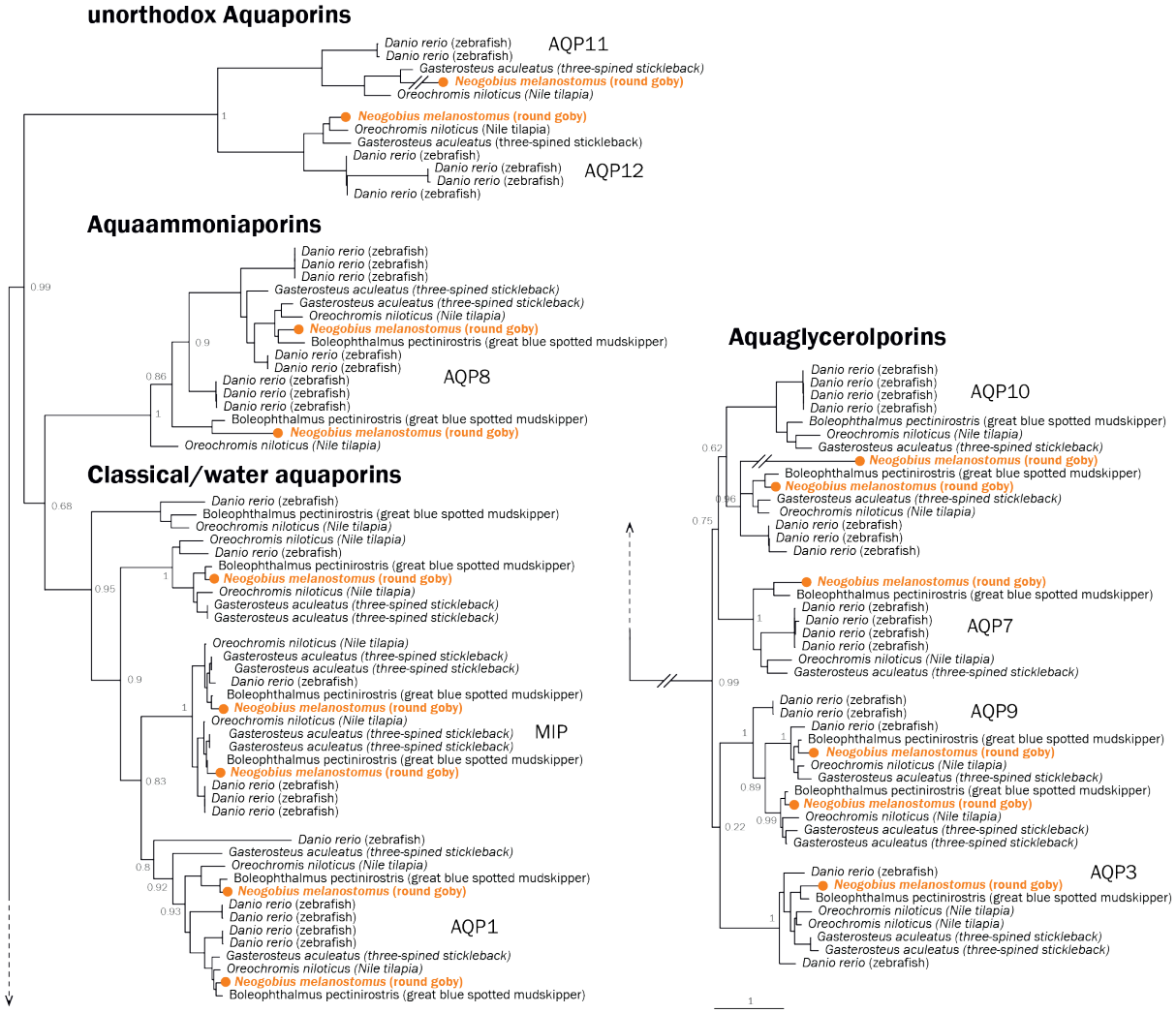

383

384 **Figure 6**

385 ***Phylogenetic tree of fish aquaporin proteins.*** *Maximum-likelihood tree with 100 bootstraps of round*

386 *goby (Neogobius melanostomus, orange) in relation to cyprinid zebrafish (Danio rerio) and*

387 *percomorph three spine stickleback (Gasterosteus aculeatus), nile tilapia (Oreochromis niloticus), and*

388 *great blue-spotted mudskipper (Boleophthalmus pectinirostris). Zebrafish was used as outgroup in*

389 *each aquaporin subfamiliy. The main classes of aquaporins are labeled with human genes names.*

390

391 In the kidney, intestine and gills, fish use active ion transport (mostly sodium transporters) to maintain

392 osmotic balance. Mechanisms mediating sodium uptake include electroneutral Na+/H+ exchange via

393 the NHE3b protein, Na+/Cl- cotransport via the NCC protein, and coupling of Na+ absorption with H+

394 secretion by a V-type H+-ATPase (73). We find 12 Na+/H+ exchanger genes, 5 Na+-K+-ATPase

395 catalytic alpha subunits and 6 Na+-K+-ATPase regulatory beta subunits in the round goby genome.

396 The round goby thus contains the same types of genes, but less copies, than either zebrafish or tilapia
397 (**Supplemental_Fig_S6**). We find that round goby, and also mudskippers, feature an interesting
398 distribution of Na+/Cl- co-transporters to subgroups; while most zebrafish and tilapia Na+/Cl- co-
399 transporters belong to the NKCC1 subgroup, Gobiidae feature more genes in the NKCC2 subgroup
400 (**Figure 7**).

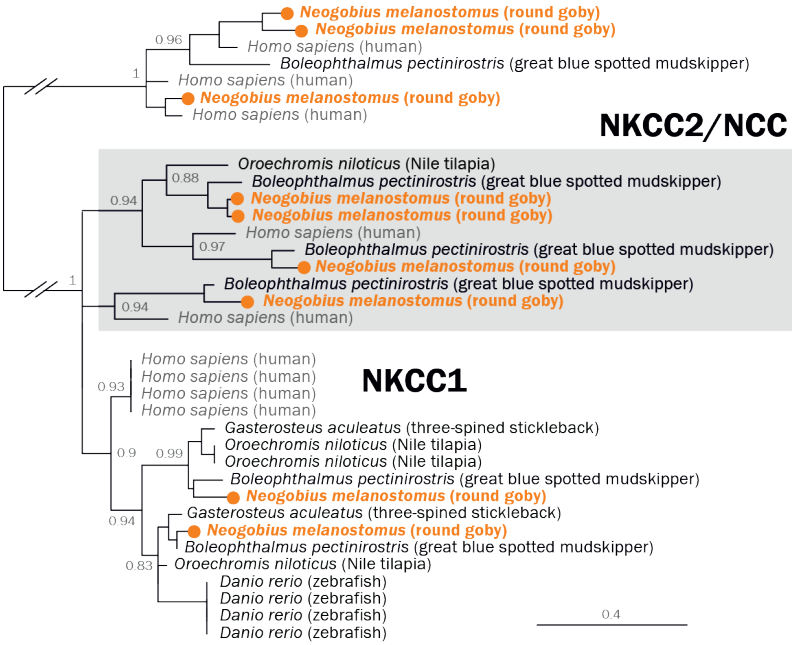

401

402 **Figure 7**

403 ***Phylogenetic tree of human and fish sodium/potassium/chloride co-transporter proteins***
404 ***(NKCC).*** *Maximum likelihood tree with 100 bootstraps of round goby (Neogobius melanostomus,*
405 *orange), zebrafish (Danio rerio), three spine stickleback (Gasterosteus aculeatus), nile tilapia*
406 *(Oreochromis niloticus), great blue-spotted mudskipper (Boleophthalmus pectinirostris) and as*
407 *contrast humans (Homo sapiens, grey). Potassium/chloride co-transporters (KCC) are used as*
408 *outgroup.*

409

410 Finally, fish produce osmolytes to actively take up and retain water. In particular, the cyclic polyol myo-
411 inositol is used by euryhaline teleosts to acclimate to high salinity. Two enzymes are required for its
412 production: myo-D inositol 3-phosphate synthase (MIPS) and inositol monophosphatase (IMPA). In
413 addition, some fish actively accumulate myo-inositol with a sodium/myo-inositol cotransporter (SMIT)
414 (74, 75). This transporter is of particular importance for marine fish exposed to high salt concentrations
415 (76, 77), while freshwater fish lack a SMIT gene (e.g. the freshwater stenohaline zebrafish lacks the

416 SMIT gene). The presence of SMIT has therefore been proposed to be a critical prerequisite for high
417 salinity tolerance in fish (78). We find that the round goby genome contains MIPS and IMPA, and
418 importantly, also a SMIT gene (**Supplemental_Fig_S7**).
419
420 **6. Response to the environment: Immune System**
421
422 It has been speculated that invasion success may relate to the ability to fight novel immune challenges
423 (37). We therefore characterized key genes related to the immune system, focusing on genes that
424 span both the innate and adaptive immune system such as pattern recognition receptors, selected
425 cytokines and chemokines, antigen presentation, T-cell surface receptors and antibodies
426 (**Supplemental_Table_S3; Supplemental_Table_S4**).
427
428 We find that the round goby genome features a classical adaptive immunity setup (**Table 3**).
429 Vertebrate adaptive immunity is characterized by the Major Histocompatibility Complex (MHC) class I
430 and MHC class II proteins and their regulators. MHCI presents antigens derived from a cell's
431 intracellular environment, while MHCII presents antigens derived from material engulfed by
432 macrophages, B-cells or dendritic cells (79). We find 26 full length MHCI sequences from the classic
433 U-lineage and one sequence from the teleost-specific Z-lineage (80) (**Supplemental_Table_S5**).
434 MHCII is represented by 8 alpha (2 fragments) and 9 beta copies (**Supplemental_Table_S6)**. The
435 uneven numbers may be attributed to assembly issues, but also, additional small fragments were not
436 further investigated (data not shown). We also identify the key MHC-supporting peptides Beta-2-
437 Microglobulin, *CD74*, *TAP1/2* and *tapasin*. Beta-2-Microglobulin (*B2M*) is present in two copies, one of
438 which contains several indels, a diverged region, and no stop codon and thus may be a pseudogene.
439 The round goby has two copies of *TAP2*, which promotes the delivery of peptides to MHCI (annotated
440 as *TAP2* and *TAP2T;* **Supplemental_Table_S4; Supplemental_Fig_S8**). Two *TAP2* genes have also
441 been described in zebrafish, and our results thus suggest this is conserved feature among teleosts
442 (81). In addition, we identify the MHC transcriptional regulators *CIITA* and *NLRC5*
443 (**Supplemental_Table_S3**). The presence of the thymus transcription factor *AIRE* and the T-cell
444 receptors *CD4* and *CD8* confirms the presence of helper T cells and cytotoxic T cells in the round
445 goby.
446

447 **Table 3**. Overview of manually annotated key adaptive immune genes

Gene	NEME annotation	Contig annotation	Start	End	Strand
CIITA	NEME_493	Contig_2585	3 985 719	3 993 128	Antisense
AICDA	NEME_58	Contig_447	597 424	599 014	sense
AIRE	NEME_9	Contig_79	14 106 230	14 113 573	antisense
B2M	NEME_421	Contig_2242	363 050	363 352	antisense
B2M_pseudo	NEME_421	Contig_2242	368 352	368 721	antisense
CD4	NEME_213	Contig_1334	340 445	348 248	sense
CD74	NEME_71	Contig_593	791 743	796 652	antisense
CD8a	NEME_729	Contig_3231	634 222	648 487	antisense
CD8b	NEME_729	Contig_3231	656 030	660 462	antisense
RAG1	NEME_106	Contig_787	4 690 414	4 695 142	sense
RAG2	NEME_106	Contig_787	4 699 042	4 700 651	antisense
TAP1	NEME_582	Contig_2864	694 776	722 339	sense
TAP2	NEME_387	Contig_2107	2 987 106	2 993 287	antisense
TAP2T	NEME_299	Contig_1786	3 697 645	3 704 089	sense
Tapasin	NEME_387	Contig_2107	3 111 989	3 119 308	sense

448

449 Similarly, the humoral adaptive immune response (also termed the B-cell mediated immune response)
450 is intact in the round goby. Humoral immunity in fish is characterized by three antibody isotypes
451 consisting of immunoglobulin heavy chains delta (IgD), mu (IgM), and tau (IgT). We identify a contig-
452 spanning immunoglobulin heavy chain locus (**Supplemental_Fig_S9**) containing 8 delta constant
453 domains, and 4 constant mu domains, as well as genes responsible for heavy chain recombination
454 and immunoglobulin hypermutation (*RAG1/2* and *AID(AICDA)*; **Table 3**; **Supplemental_Table_S3**).
455 There is no evidence for the presence of immunoglobulin tau constant domains, which are commonly
456 found in carps and salmonids (82).

457

458 While round goby adaptive immunity conforms to vertebrate standards, its innate immune repertoire
459 displays remarkable and unusual features. We find that all components of the inflammasome (a
460 signaling pathway involved in inflammatory responses; **Figure 8**) are expanded. Inflammasome
461 assembly is activated through pathogen pattern recognition receptors (83), and ultimately triggers a
462 local or systemic acute phase response by producing IL-1 family cytokines (83, 84) and/or promotes
463 cell death via pyroptosis (84). In the round goby genome, components of the entire cascade (pattern
464 recognition receptors, ASC adaptor proteins, IL-1, and acute phase proteins) are present in
465 unexpectedly large numbers (**Figure 8; Supplemental_Table_S8**). In the following, our findings are
466 described step-by-step from the cell surface down to the acute phase response.

467

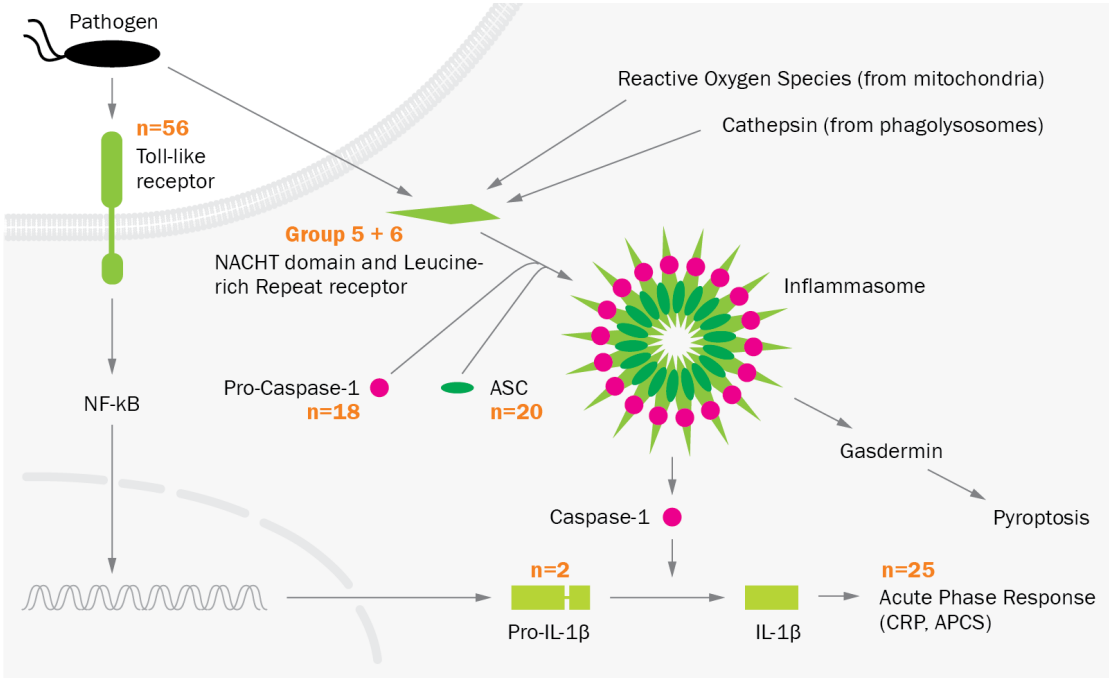

468

469 **Figure 8.**

470 ***The inflammasome pathway.*** *Several components of the pathway are expanded in the round goby*
471 *(gene numbers in round goby, or novel groups for NLRs, are indicated in orange). Pathogen-*
472 *associated patterns are recognized by pattern recognition receptors such as Toll-like receptors at the*
473 *cell surface, or NLRs in the cytoplasm. This interaction triggers the transcription of cytokine precursors*
474 *via NFkB, and the activation and assembly of inflammasome components (NLRs, Pro-Caspase-1, and*
475 *ASC). Inflammasome-activated Caspase-1 then initiates the maturation of cytokines and an acute*
476 *phase inflammatory response (CRP, APCS proteins), and / or pyroptosis through gasdermin.*

477

478 Perhaps the best studied pattern recognition receptors are the Toll-like Receptors (TLRs), pathogen-
479 recognizing molecules that are generally expressed either at the plasma membrane or on the
480 endosomal membranes. Sixteen TLR types with slightly differing ligand binding activities are
481 conserved across vertebrates, and most vertebrate genomes contain one to three copies of each type.
482 As expected for a teleost, the round goby genome does not contain the LPS-detecting TLR4 genes.
483 However, in total we find 56 TLRs, of which 40 appear to originate from an expansion of Toll-Like
484 Receptor 23-like genes (**Figure 9**). Small expansions of specific *TLRs* are somewhat common in fish
485 (85), and indeed, we find minor *TLR22* and *TLR23* expansions to 6-13 copies in the genomes of other
486 *Gobiidae*. However, the extent of the expansion of *TLR23* exceeds even what is observed for *TLR22*

487 in the relatives of cod (*Gadiformes*) (86). Phylogenetically, the identified TLR23 sequences form three
488 clades, of which two are specific to *Gobiidae*, while the third contains TLR23 sequences from other
489 teleosts as well (**Supplemental_Fig_S10**). In terms of genomic location, round goby TLRs 22 and 23
490 were distributed across several contigs with some copies arranged in tandem, which suggests several
491 independent duplication events.
492

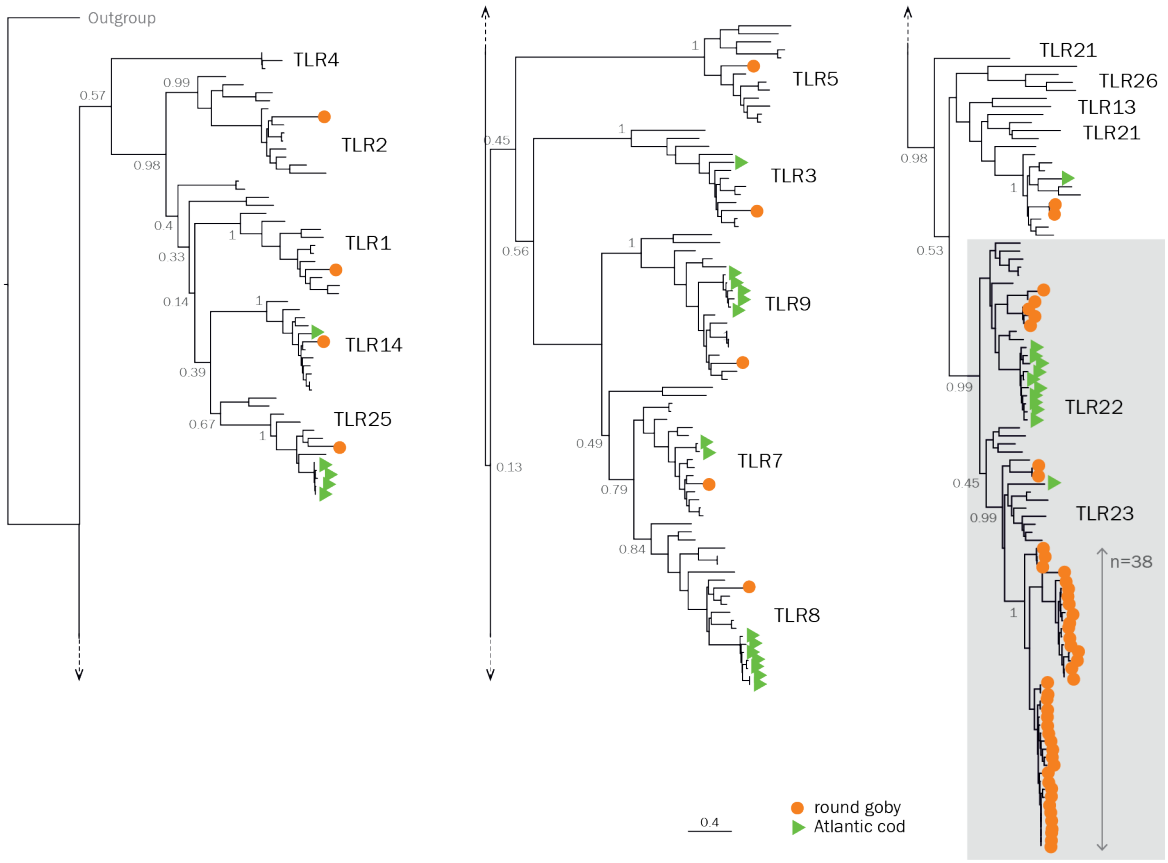

493 **Figure 9**

494 ***Phylogenetic tree of teleost Toll Like Receptor protein sequences.*** *A maximum likelihood*
495 *phylogenetic tree run with the JTT substitution model and 500 bootstrap replicates on the*
496 *transmembrane, linker and TIR domain of all TLRs found in a selected set of teleosts in the Ensembl*
497 *database, the Atlantic cod genome version 2, and all manually investigated Gobiiformes. A TLR*
498 *sequence from the lancelet Branchiostoma belcheri was used as an outgroup and the root was placed*
499 *upon its corresponding branch. Green triangles, Atlantic cod. Orange circles, round goby. Grey box,*
500 *TLR22 and TLR23.*
501

502 For intracellular pathogen recognition receptors of the NACHT domain and Leucine-rich Repeat

503 containing receptor (NLR) family, we identify two new, previously undescribed families (Group 5 and 6)

504 present in the round goby and also in the mudskipper *B. pectinirostris* (**Figure 10**).

505

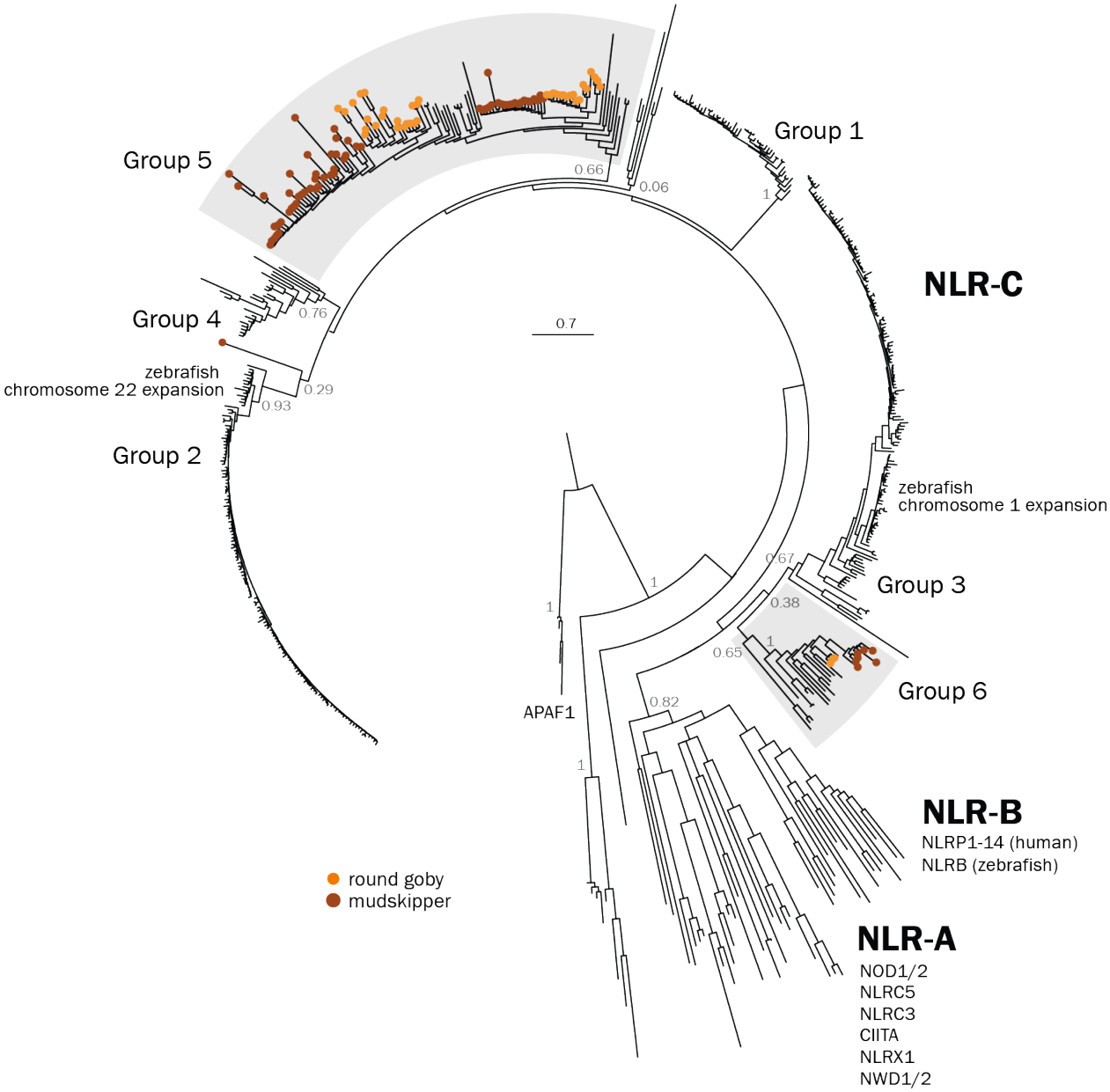

506 **Figure 10**

507 ***Phylogenetic tree of the NLR nucleotide-binding domain sequences*** *in round goby, great blue*

508 *dotted mudskipper, zebrafish and human. Maximum Likelihood phylogenetic tree with 500 bootstraps*

509 *rooted at the split between NB-ARC (found in APAF) and NACHT domains (present in all the other*

510 *NLRs). NB-ARC domains from APAF1 orthologs were used as an outgroup. Bootstrap values are*

511 *shown for nodes that determine an entire cluster. The tree resolves all three major classes of*

512 *vertebrate NLRs (NLR-A, NLR-B, NLR-C). NLR-A genes were conserved in all analyzed species, no*

513 *NLR-B genes were found from the gobies. Six groups of NLR-C genes were identified, four of which*
514 *are exclusive to zebrafish (Group 1-4) and two contain only sequences from gobies (Groups 5 and 6).*
515 *Within the goby-specific groups, lineage-specific expansions can be seen for both round goby*
516 *(orange) and mudskipper (brown).*
517
518 NLRs have diverse roles from direct pathogen recognition to transcriptional regulation of the MHC
519 (NLRs CIITA and NLRC5) and contribute to inflammasome activation. Mammalian genomes display
520 20-40 NLRs in families NLR-A and NLR-B, while fish also feature a fish-specific subfamily (NLR-C)
521 (87) and a much expanded NLR repertoire (e.g. 405 NLR-C genes in zebrafish) (88, 89). The round
522 goby genome contains at least 353 NLRs (**Supplemental_Table_S8**), which include 9 highly
523 conserved vertebrate NLRs (*NOD1*, *NOD2*, *NLRC3*, *NLRC5*, *NLRX1*, *NWD1*, *NWD2*, *APAF1*, *CIITA*)
524 as well as 344 NLR-C genes. Fish NLRs cluster into 6 groups of which 2 represent novel NLR-C
525 clades (groups 5 and 6, **Figure 10**). The novel groups are supported by phylogenetic analyses as well
526 as motif presence/absence (**Table 4)**. NLR-C groups are characterized by highly conserved versions
527 of the sequence motif Walker A. The most common sequence for Walker A observed in both goby
528 NLR-C groups, GVAGVGKT, is not associated with any of the four major NLR-C groups in zebrafish
529 (88). Also, NLR subtypes often carry group-specific combinations of the protein-protein interaction
530 domain PYD and/or B30.2 domain. This holds true for *Gobiidae* NLR-C groups, since only group 5
531 NLRs can carry an N-terminal PYD domain and/or a C-terminal B30.2 domain (88), similar to the
532 zebrafish Group 1 and 2 NLRs (**Table 4**). In contrast, some group 6 NLRs have C-terminal CARD
533 domains, which in both human and zebrafish are attached to specific inflammasome-associated NLR-
534 B genes (90). The round goby C-terminal CARD-containing NLRs are found on the same few scaffolds
535 and share a high degree of sequence similarity, indicative of a recent expansion. This expansion is
536 absent from mudskipper and thus restricted to the round goby lineage. Many other Group 6 NLRs are
537 fragmented, with large insertions in the middle of their conserved 2 kb exon
538 (**Supplemental_Table_S8**).
539
540

541 **Table 4.** Key features of each of the six NLR-C subgroups. x denotes a variable amino acid.

Group	Identified in this study	Walker A	Last residues of the largest exon	PYD?	B30.2?
1		GIAGVGKT	L(I/M)PVVKNT(T/R)RA	+	+
2		GVAGIGKS	LSAVIKTSKRA	+	+
3		GIAGIGKT	L(IP/TA)AV(R/S)NC(RK/TR/RR)A	-	+
4		GVAGIGKT	LPV(I/V)xxxx(A/V)x	-	-
5	x	GVAG(V/A/I)GKT	(L/M)PV(V/I)KASxK(A/V)	+	+
6	x	GVAG(V/A)GKT	L(I/V)P(A/V)VRNCRKA	-	-

542

543 Once activated, some NLRs (including those with a C-terminal CARD) can oligomerize and form an
544 inflammasome in order to activate specific caspases (usually Caspase 1, **Figure 8**). The interaction
545 between NLRs and the caspase are mediated by the adaptor protein ASC (also known as PYCARD),
546 which itself oligomerizes into large structures known as “specks” (91). Vertebrates have 1-2 copies of
547 ASC, which are characterized by a characteristic combination of a single PYD and CARD domain. In
548 the round goby genome, we find 20 cases of this domain combination. Since the genomes of other
549 gobies contain 1-2 PYD-ASC combinations, the expansion appears to be specific to the round goby
550 (**Figure 11A**). The effector protein Caspase 1 is present as one gene in humans and as two genes in
551 zebrafish. We find that the round goby genome features an expansion to 18 copies. Interestingly,
552 some of those genes appear to contain a CARD domain (as seen in mammals and several species of
553 fish) while others have PYD (as seen in zebrafish). This suggests that a caspase with both domains
554 may have existed in the common ancestor of fish and tetrapods, with most lineages having retained
555 only one of the two. However, phylogenetic analyses reveal that all round goby Caspase 1 genes are
556 the result of a single expansion event specific to this species (**Figure 11B**). An alternative explanation
557 for the presence of both PYD- and CARD-caspases 1 genes would be a recurrent acquisition of PYD
558 in different lineages. In any case, in addition to Caspase 1 genes, caspase 3 (a key component of
559 apoptosis which may be activated by Caspase 1) is also expanded to 5 copies. Caspase 4 and 5, on
560 the other hand, appear to be absent.

561

562 Finally, we find that genes encoding for two peptides produced in the course of inflammation, the
563 acute phase reactants C-reactive protein (CRP) and serum amyloid component P (APCS), are
564 expanded to a total of 25 copies (compared to 2-7 in fish, and 5-19 in the other *Gobiidae*). In fish, CRP
565 and APCS are closely related and cannot be distinguished based on BLAST scores or phylogeny. As

seen in other fish species, all investigated CRP/APCS sequences resolve into two major phylogenetic clades, with the mammalian sequences in a third (**Supplemental_Figure_S11**).

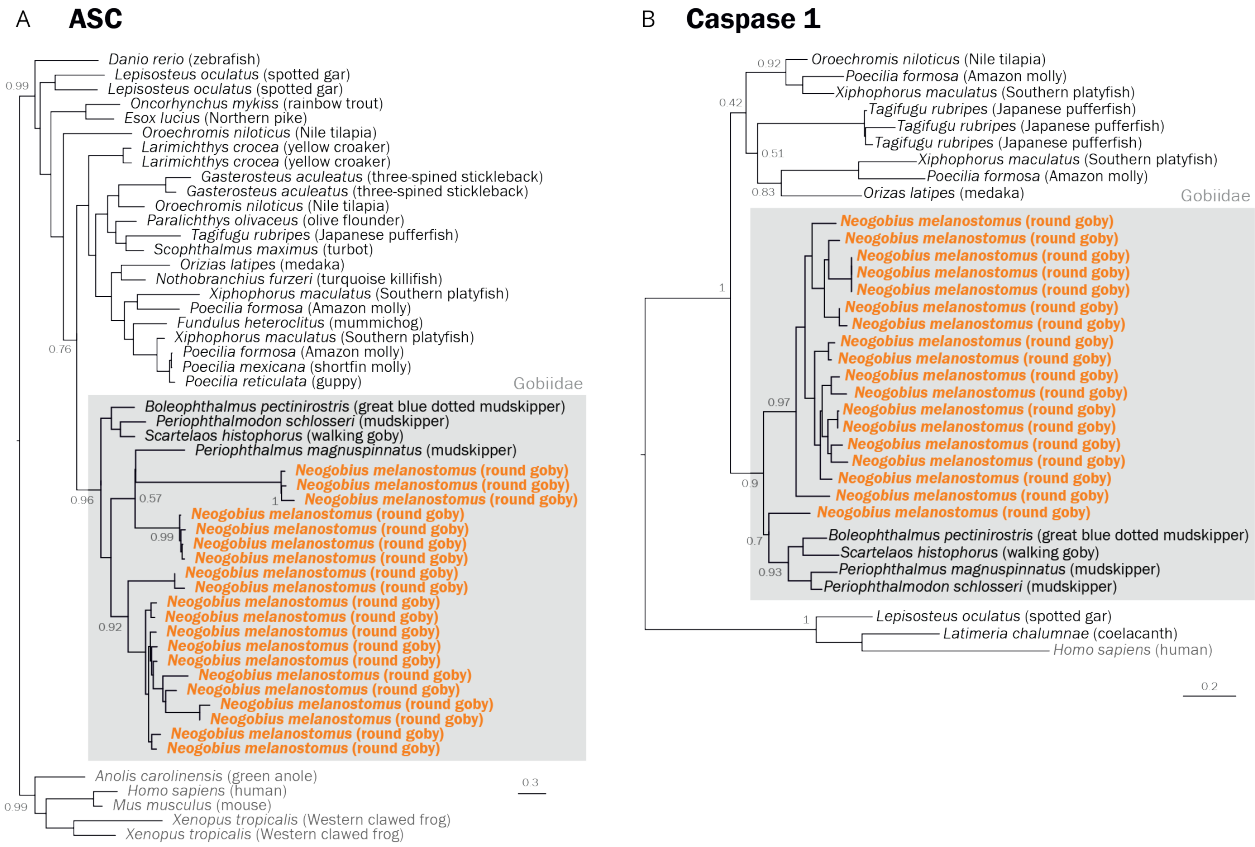

Figure 11

A Phylogenetic tree of gnathostome ASC protein sequences. *Maximum Likelihood phylogenetic tree with 500 bootstraps rooted at the split between tetrapods and ray-finned fish. Tetrapods were used as outgroup. Round goby is indicated in orange. Gobiidae are highlighted with a grey box. The goby sequences form a clear separate cluster (marked with the box), with a large expansion apparent in the round goby.* ***B Phylogenetic tree of gnathostome Caspase 1 protein sequences*** *The Caspase 1 tree comprises all protein sequences annotated as CASP1 in the investigated Gobiiformes genomes aligned together with reference sequences from Ensembl and GenBank. The root was placed on the branch containing the mammalian sequences.*

581 **7. Adaptation to novel environments: Epigenetic regulators**

582

583 The PRC2 complex establishes and maintains gene repression (92) and thus represents a plasticity-
584 restricting mechanism. The complex mediates di- and trimethylation of lysine 27 on histone H3 and
585 contains four proteins: a catalytic subunit (either *enhancer of zeste* EZH1 or EZH2), *suppressor of*
586 *zeste* SUZ12, *embryonic ectoderm development* EED and *RB Binding Protein 4* RBBP4 (50). In
587 mammals, the alternative catalytic subunits EZH1 and EZH2 have partially complementary roles (93,
588 94), and requirements for the two alternative catalytic subunits differ between species – in contrast to
589 mammals, zebrafish develop in the absence of either catalytic subunit (95, 96). We find that the round
590 goby genome contains the usual complement of PRC2 components: two copies of SUZ12 (of which
591 one appears quite diverged), one copy of EED, one copy of RBBP4, and two copies of EZH (with
592 multiple isoforms determined by RACE experiments). For SUZ12, EED, and RBBP4, sequence-based
593 identification was straightforward, and phylogenetic analyses followed the known phylogenetic
594 relationships of fish, mammals, and other vertebrates (**Supplemental_Fig_S12**). The catalytically
595 active subunits EZH1 and EZH2 do cluster with the closest species in the phylogeny, the mudskipper
596 *B. pectinirostris* (**Figure 12**), but the deeper relationships within EZH2 are poorly supported and may
597 suggest a complex evolutionary history.

598

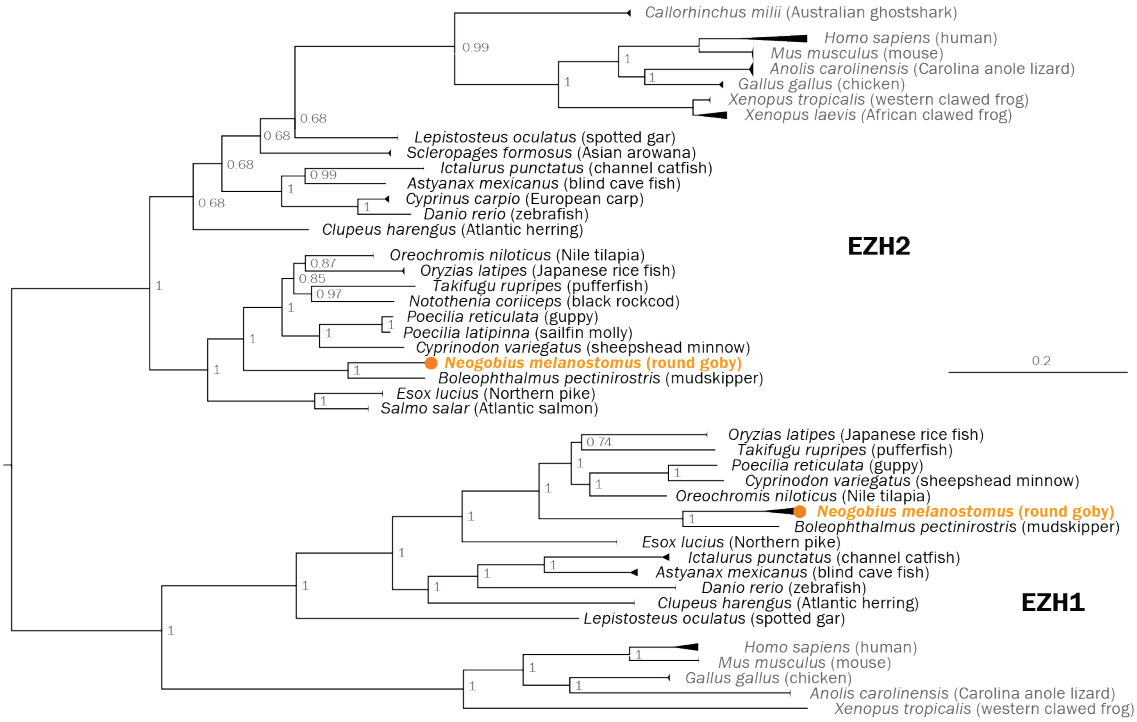

599

600 **Figure 12**

601 ***Phylogenetic tree of vertebrate EZH proteins.*** *Midpoint-rooted Bayesian phylogenetic tree. Note the*
602 *position of the Australian ghost shark (potential outgroup) within the poorly supported EZH2 branch.*
603 *When rooting with Australian ghost shark, teleost EZH2 genes cluster with EZH1 (data not shown).*
604 *Round goby is indicated in orange.*
605
606 Methylation marks similarly regulate gene expression and are deposited by conserved enzymes called
607 DNA methyltransferases (DNMTs). Mammals feature two types of DNMTs, DNMT3 (three genes A, B,
608 and L) and DNMT1 (one gene). The two types perform both *de novo* and maintenance methylation,
609 respectively, in a dynamic division of labor (97). Interestingly, fish feature a variable repertoire of
610 DNMT3 genes. Medaka, fugu, zebrafish, and carp have three, five, six, and twelve DNMT3 genes,
611 respectively (98). We find that the round goby genome features one DNMT1 that follows the expected
612 phylogenies, and five DNMT3 genes, of which two cluster with vertebrate DNMT3A sequences, and
613 three with vertebrate DNMT3B sequences (**Figure 13**). The number of DNMT3 genes in round goby
614 corresponds to that seen in in stickleback, fugu and tilapia (99). In general, the DNMT3 phylogeny is
615 not well supported, which limits conclusions about the evolution of specific DNMT3 genes.
616
617

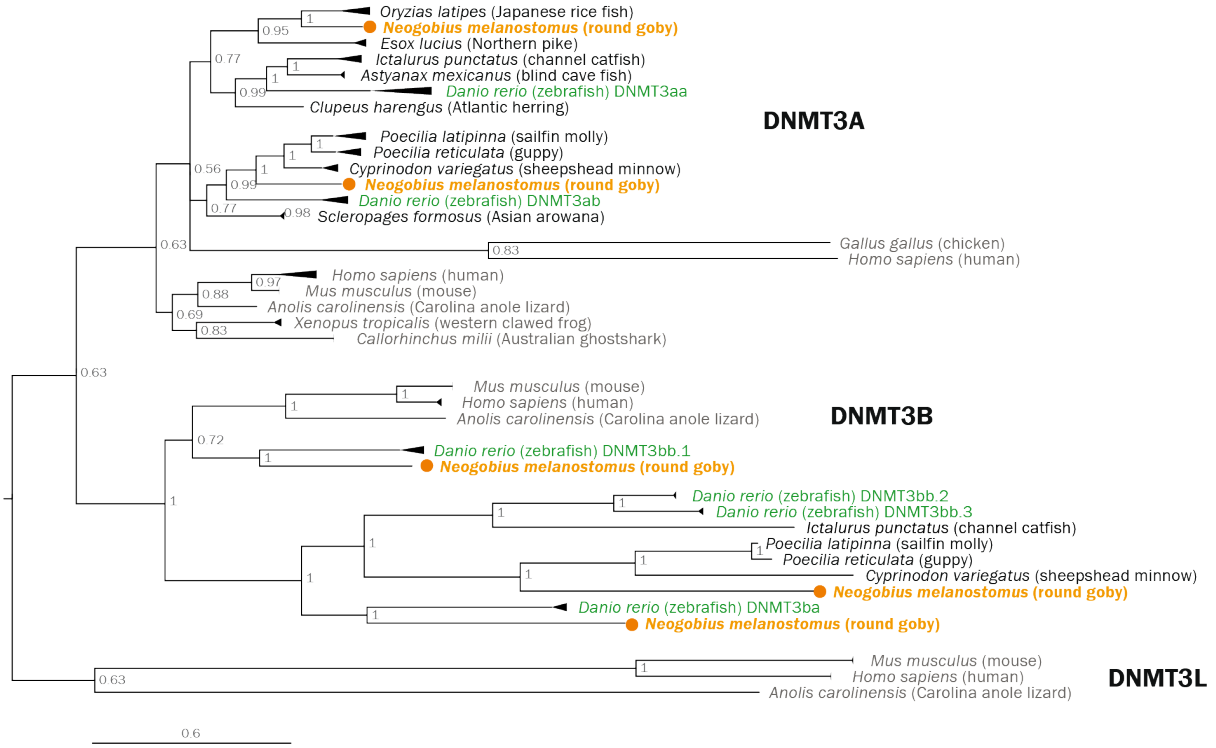

618
619 **Figure 13**

620 ***Phylogenetic tree of vertebrate DNMT3 proteins.*** *Midpoint-rooted Bayesian phylogenetic tree. The*
621 *Australian ghost shark (potential outgroup) is positioned among DNMT3A genes. Round goby is*
622 *indicated in orange. Zebrafish, the only other fish with well-annotated DNMT3 genes, is indicated in*
623 *green.*
624
625 **Discussion**
626
627 **General observations**
628
629 Our analyses depict a genome that, in many respects, is similar to other teleost genomes. There is no
630 evidence for recent genome duplications, and genome size, gene content and GC content are within
631 the ordinary range. Transposable elements can create genetic variation and mediate ecological
632 success (100), but repeat analyses do not reveal unusual transposon activities in the round goby.
633 Small genome size has been proposed to foster invasiveness (101), but the round goby genome is not
634 particularly small. Phylogenetic analyses reveal that many of the analyzed gene families conform to
635 expectations. For example, green opsin gene duplications and the loss of the UV opsin are observed
636 in many fish lineages (20). Similarly, the expected gene families and overall gene complements are
637 found for olfactory receptors, cytochrome P450, and osmoregulatory proteins, for adaptive immunity
638 and epigenetic regulators. Multilocus sex determination has previously been suggested for freshwater
639 gobies (102), and indeed our data suggest a multigenic and/or environmental sex determination
640 system for the round goby, rather than a large sex-determining region or a sex chromosome. Overall,
641 these findings support the validity of the sequencing and assembly approach, and suggest that
642 selected findings of interest are not artefacts. In addition, the round goby genome sequence also
643 reveals several novel and interesting findings of which some pertain to teleost genomes in general,
644 some to *Gobiidae*, and some to specific gene families, with possible implications for invasive potential.
645
646 **Environmental perception**
647
648 We find that the visual system of *Gobiidae* may be more efficient in the red parts of the light spectrum.
649 This is intriguing considering the benthic life style of gobies and their occurrence in turbid areas. In
650 clear waters, red light from the sun is the least abundant part of the spectrum (and virtually absent

below 15m of depth) because red light penetrates least through water, but many organisms convert the deeply penetrating green and blue wavelengths into red. Indeed, the eyes of gammarids, a common prey of round goby, strongly reflect red light (103). An enhanced red perception through an additional red opsin gene may thus be relevant for round goby predation success. In turbid waters, red is the most common part of the light spectrum because long wavelengths experience least scattering (21). Round gobies readily establish populations in turbid environments. The retention of two red opsin genes may thus possibly relate to the remarkable ability of the round goby to colonize turbid habitats. Our predictions based on the key amino-acid substitution suggest that LWS1 is expected to be most sensitive at 560 nm (same as one of the mudskipper gobies) (25), while LWS2 is expected to be most sensitive at 550 nm (59). Similar small differences in the sensitivity maximum can indeed result in functionally different spectral tuning palettes (e.g. during development or in different environmental conditions) (104).

The presence of red fluorescence on top of the eye in round goby is the first unequivocal description of fluorescence in a freshwater fish and might be interpreted as being associated with the ability to discriminate different shades of red colors. However, the fluorescence in the specimens investigated was quite weak. Unless fluorescence expression is stronger under natural conditions or in the ancestral population from which the invading populations stem, a visual function of the weak fluorescence observed here seems unlikely (see warnings by (105)). Fluorescence is, however, widespread and stronger among several marine gobies (106). Although the fluorescent "eyebrows" of the round goby show a striking similarity to those of some marine gobies, their function will remain unclear until properly tested. Social functions are possible – for example, in sand gobies, dark eyes indicate female readiness to spawn (107). Alternatively, they may simply provide camouflage for individuals buried in bright sand up to the eyes. Functional hypotheses for fluorescence, such as communication, camouflage and improved prey detection have been extensively reviewed by (108). The genetic tools now available for the round goby may allow for experimental manipulation of fluorescence expression, once the actual fluorophores that produce the fluorescent signal have been identified.

Response to the environment

682 With respect to ecological and physiological aspects of success and invasiveness, some findings on
683 CYP genes, on osmoregulation, and on innate immunity call for further attention. The mostly minimal
684 complement of cytochrome P450 proteins present in the round goby is unexpected considering the
685 occurrence of round goby in polluted areas (109, 110). The CYP1-3 gene complement for xenobiotic
686 metabolism is similar to other teleost genomes, and the ability of the round goby to survive in
687 contaminated environments must therefore have other reasons. Round goby may cope with
688 contaminations at the level of gene expression, either through higher basal expression values or by a
689 particularly rapid response to exposure (45). Alternatively, this species may have peculiarities in other,
690 not yet analyzed areas of the defensome (e.g. transporters). Analyses of the tissue expression of CYP
691 families 1, 2 and 3, and also the study of other defensome gene families, including the nuclear
692 receptors regulating CYP gene expression, transporters and conjugating enzyme families, may be
693 useful in this respect.
694
695 Another potentially relevant finding is the ability of the round goby to not only produce, but also
696 accumulate osmolytes. Species distribution constraints often arise from physiological limitations. The
697 round goby is one of the most geographically wide-ranging invasive fish species in Europe and North
698 America, and the ability to accumulate osmolytes may impact its range expansion in three ways.
699 Firstly, 0-25 PSU (common for coastal waters, but lower than the ocean) is the species' current limit
700 for unperturbed osmoregulation (111). However, the round goby's repertoire of key-genes in myo-
701 inositol production and accumulation might bestow the species with the potential to eventually tolerate
702 higher salinities, for example through the evolution of altered gene regulation patterns, and colonize
703 higher PSUs. Secondly, osmolytes improve water retention and thus desiccation tolerance. In this
704 context, myo-inositol accumulation may have contributed to overland dispersal. Overland dispersal of
705 eggs or larvae with boats or fishing gear involves air exposure, and indeed, round goby eggs
706 withstand desiccation for up to 48 hours (112). Finally, osmolytes essentially act as anti-freeze agents
707 and molecular chaperones, and contribute to cryoprotection in diverse organisms from bacteria (113)
708 to flies (114). Osmolytes may thus enable the round goby to combat a number of environmental
709 conditions and to colonize new areas. The surprising and unexpected ability of the round goby to
710 colonize cold areas well below its temperature optimum of 22°C, such as the Northern Baltic Sea, may
711 be linked to osmolyte production.
712

713 Lastly, the “strike fast, strike hard” innate immune system and the impressively large inflammation
714 machinery of the round goby may enhance the species’ colonization potential. Fish immunity appears
715 to be quite plastic. For example, cod have disposed of some core adaptive immunity components (18),
716 yellow croaker feature an expanded TNF repertoire (115), and channel catfish retain a high number of
717 recent duplications and SNPs in immune genes (116). Meanwhile, in salmonids, genes specifically
718 retained after the 4th whole genome duplication are not immune genes (117).
719
720 We find that the round goby genome contains multiple copies of genes for inflammasome assembly,
721 activation, and function. This is interesting because the fish inflammasome complex is much more
722 poorly characterized than that of mammals. Maturation of IL-1 by inflammasome-activated Caspase 1
723 cleavage in fish is a matter of debate, since teleost IL-1 proteins lack the conserved caspase cleavage
724 site present in mammalian IL-1b and IL-18 (118). However, as has been shown for zebrafish, Caspase
725 1 can also utilize an alternative site to cleave and mature IL-1 (90, 119). In any case, the caspases
726 also mediate cell death via pyroptosis and the presence of other components such as ASC, caspases
727 and pro-IL1 and pro-IL18 supports a role for inflammasomes in fish. Zebrafish ASC oligomerize and
728 form “specks” as seen in mammals (90). The molecular dynamics of inflammasome activation
729 therefore represent a potential future research avenue in the round goby.
730
731 In terms of ecological success, the round goby’s expanded repertoire of pathogen recognition
732 receptors may broaden the scope of its immune response and increase the range of detectable
733 ligands and pathogens. The expanded acute phase repertoire may also contribute to a fast response,
734 or inversely, may limit excessive cell damage. In humans, the acute phase protein CRP contains
735 inflammation as part of a negative feedback loop (120). Thus, the round goby may re-enter
736 homeostasis faster compared to other fish species with smaller CRP/APCS repertoires. The larger
737 acute phase repertoire may also function to limit the cellular damage caused by the potentially large
738 amount of inflammasome combinations the round goby can generate. In this context, we suggest
739 systematic investigations into a potential relation between inflammasome expansions and
740 invasiveness in *Gobiidae*, in combination with immune challenge experiments.
741
742 **Long-term adaptation**
743

744 We identify a potentially interesting evolutionary history for the conserved PRC2 component EZH in
745 fish, and add to the previous observation that the conserved *de novo* DNA methylation machinery
746 features a surprising diversity in fish. These results underscore the need for in-depth investigations
747 into the role and relevance of epigenetic regulation and transgenerational inheritance in teleosts. Our
748 findings support the emerging idea that epigenetic regulation in fish follows somewhat different rules
749 than in mammals. For the histone methylating complex PRC2, our results suggest interesting
750 phylogenetic relationships of EZH proteins in fish. EZH proteins act in tissue specific complexes
751 comprised of core SUZ12, EED, and RBBP4, but also AEBP2, PCL proteins and JARID2. These
752 proteins enhance PRC2 efficiency, contribute to recruitment to target sites, or inhibit the complex (50,
753 92). Small sequence changes can have strong effects on the entire complex, since the precise
754 interactions among the components and with other gene regulators impact its function and localization
755 (121–124). For example, species-specific insertions (125) are thought to regulate PRC2 recruitment
756 and/or exclusion from target genes (126). We suggest that the future incorporation of more sequences
757 of both EZH1 and EZH2 from a greater range of taxa and the inclusion of currently unannotated
758 versions of the genes associated with both the teleost specific whole genome duplication and lineage
759 specific duplications (96) would aid understanding of the evolutionary history of the entire complex. We
760 expect that studying PRC2 in non-mammalian vertebrates may reveal ancestral or less abundant
761 interactions, functions or also complex associations of PRC2.
762
763 Similarly, our results warrant an in-depth exploration of DNA methylation in fish. Originally, DNA
764 methylation evolved to distinguish own (methylated) DNA from foreign (non-methylated) DNA such as
765 introduced by viruses. Therefore, cytosines in CG base contexts are by default methylated. In
766 mammals, DNA methylation in CG dense regions (CG islands) is associated with gene repression.
767 However, DNA methylation also features species- and taxon-specific differences, even among
768 vertebrates, which are still greatly underappreciated. For example, non-methylated genome regions in
769 fish are unexpectedly CG-poor (127), fish differ from mammals with respect to the distribution of
770 methylated CpGs in the genome (128), algorithms developed on mammals fail to identify CpG islands
771 in fish (129), genome-wide CpG island predictions in cold-blooded animals consist primarily of false
772 positives (130), and fish CG methylation occurs mainly in coding regions, where it correlates positively
773 with gene expression levels (131). These curious differences are further enhanced by the seemingly
774 random copy number variation in the *de novo* DNA methyltransferase DNMT3 in teleosts, which do not

775 reflect genome duplication events in teleosts (99). DNMT3 genes display highly spatiotemporal
776 expression patterns particularly during development (132–135), and an in-depth and species-aware
777 exploration of the role of DNA methylation in fish is clearly warranted.
778
779 **Gene expansions**
780
781 A general theme across several of the analyzed gene families is gene expansions. Gene expansions
782 have been linked to invasive potential before (136) and are recurrent in fish genomes, both within
783 (117, 137) and outside (116, 138, 139) the context of whole genome duplications. Many duplicated
784 genes are known to experience rapid neofunctionalization rather than subfunctionalization (137), and
785 have the potential to compensate against mutation even after divergence (140). The round goby and
786 its relatives are definitely strong candidates for further and systematic investigation of a link between
787 gene expansions and colonization or invasion potential. The *Benthophilinae* group is recently
788 diversified crowd of fish with many members inexplicably on the move (141), and *Gobiidae* in general
789 share a remarkable colonization potential (10, 142). Importantly, recent gene expansions can be
790 difficult to resolve with short reads, and genomes based on long read sequencing (as presented here)
791 will be instrumental in this regard.
792
793 Among the receptor families analyzed, the NLRs, TLRs, and olfactory receptors, we identify a couple
794 of particularly beautiful case studies for recent expansions and repeated radiations. Our identification
795 of two previously undescribed NLR-C gene families (88), here termed group 5 and group 6, indicates
796 substantial diversification of NLRs in fish. Different teleost lineages appear to feature different NLR-C
797 subfamilies with large lineage-specific expansions reminiscent of olfactory receptor repertoires.
798 Similarly, we identify interesting cases of parallel expansions across families, and also family-specific
799 expansions, among olfactory receptors. Both cases warrant investigations into the evolution of ligand
800 binding repertoires. For example, 7tm1 subfamily members may be involved in the detection of
801 distinctive types of odors relevant for round goby, and possibly, *Gobiidae* ecology (28–30). Which
802 types of odorants are detected by parallel expanded ORs, and whether these expansions serve to
803 detect similar or different types of odorant molecules in different species, remains to be studied.
804 Finally, the massively expanded TLR22 and TLR23 families warrant an exploration of their ligand
805 binding properties. TLR22 and TLR23 have been suggested to recognize nucleic acid ligands (85), but

806 some also react to protein or lipid pathogen-associated patterns (143–145), and their role in fish is
807 currently unclear.
808
809 In summary, this work provides a solid basis for future research on the genomic, genetic, and
810 epigenetic basis of ecological success. Clearly, many more gene families or pathways may contribute
811 to the round goby's invasion success. For example, the presented analyses barely scratch the surface
812 of epigenetic regulation, innate immunity and transporters (e.g. of toxins). We did not investigate
813 endocrine pathways (which govern growth and reproductive success) nor antimicrobial peptides
814 (which contribute to innate immune defense), areas which may yield fruitful information of the success
815 of this invader. We welcome future research using this novel genomic resource, and encourage
816 experts on those pathways to contribute their knowledge.

817 **Methods**

818

819 A relevant note upfront is that this manuscript is the product of a long-standing collaboration of leading
820 experts in their respective fields. The gene families analyzed differ widely with regard to sequence
821 conservation, the number and similarity of genes within and between species, the scope of questions
822 in the field, etc. Compare, for example, the *de novo* identification of hundreds of virtually identical NLR
823 receptors with the manual annotation of a handful of extremely conserved DNA methyltransferases, or
824 the phylogenetic analysis of the conserved vertebrate CYP gene family with a fish-centered
825 comparison of osmotic balance regulators. Accordingly, each collaborator applied methods that were
826 suited for the respective situation. As a common theme, genes were identified by blast, sequences
827 were extracted and aligned with other fish and/or other vertebrates, trees were constructed with either
828 bayesian or maximum-likelihood methods, and findings were always verified against the mudskipper
829 genomes.

830

831 **Genomic DNA library preparation and PacBio sequencing**

832

833 Genomic DNA was extracted from the liver of one male individual of round goby caught in Basel,
834 Switzerland (47° 35′ 18″ N, 7° 35′ 26″ E). At the Genome Center Dresden, Germany, 300 mg of liver
835 tissue were ground by mortar and pestle in liquid nitrogen and lysed in Qiagen G2 lysis buffer with
836 Proteinase K. RNA was digested by RNase A treatment. Proteins and fat were removed with two
837 cycles of phenol-chloroform extraction and two cycles of chloroform extraction. Then, DNA was
838 precipitated in 100% ice cold ethanol, spooled onto a glass hook, eluted in 1x TE buffer, and stored at
839 4 °C. 10 µg of DNA was cleaned using AMPure beads. From this DNA, five long insert libraries were
840 prepared for PacBio sequencing according to the manufacturer's protocols. Genomic DNA was
841 sheared to 30-40 kb using the Megaruptor device. The PacBio libraries were size selected for
842 fragments larger than 15-17.5 kb using the BluePippin device. PacBio SMRT sequencing was
843 performed with the P6/C4 chemistry using 240 min sequencing runs. Average read length was 11-12
844 kb. In total, 86 SMRT cells were sequenced on the PacBio RSII instrument resulting in 46 gigabases
845 (Gb; an estimated 46x coverage for a putative ~1 Gb genome) polymerase reads.

846

847

848 **Assembly of the round goby genome**

849

850 The round goby genome was assembled at the Heidelberg Institute for Theoretical Studies HITS
851 gGmbH. Raw PacBio reads were assembled using the Marvel (146, 147) assembler with default
852 parameters unless mentioned otherwise. Marvel consisted of three major steps, namely the setup
853 phase, patch phase and the assembly phase. In the setup phase, reads were filtered by choosing only
854 the best read of each Zero-Mode Waveguide as defined by the H5dextract tool (146) and requiring
855 subsequently a minimum read length of 4k. The resulting 3.2 million reads were stored in an internal
856 Marvel database. The patch phase detected and fixed read artefacts including missed adapters,
857 polymerase strand jumps, chimeric reads and long low-quality segments that were the primary
858 impediments to long contiguous assemblies (146). To better resolve those artefacts only low
859 complexity regions were masked (DBdust) and no further repeat masking was done. The resulting
860 patched reads longer than 3k (41x coverage) were then used for the final assembly phase. The
861 assembly phase stitched short alignment artefacts from bad sequencing segments within overlapping
862 read pairs. This step was followed by repeat annotation and the generation of the overlap graph,
863 which was subsequently toured in order to generate the final contigs. By using an alignment-based
864 approach, the final contigs were separated into a primary set and an alternative set containing bubbles
865 and spurs in an overlap graph. To correct base errors, we first used the correction module of Marvel,
866 which made use of the final overlap graph and corrected only the reads that were used to build the
867 contigs. After tracking the raw reads to contigs, PacBio's Quiver (148) algorithm was applied twice to
868 further polish contigs as previously described (146).

869

870 **Automated annotation of the round goby genome**

871

872 The round goby genome assembly was annotated using Maker v2.31.8 (149, 150). Two
873 iterations were run with assembled transcripts from round goby embryonic tissue (46) and data
874 from eleven other actinopterygian species available in the ENSEMBL database (downloaded
875 the 15th February 2016, http://www.ensembl.org, see **Table 5**) as well as the SwissProt protein
876 set from the uniprot database as evidence (downloaded March 2, 2016;
877 https://www.uniprot.org/downloads). In addition, an initial set of reference sequences obtained
878 from a closely related species, the sand goby *Pomatoschistus minutus*, sequenced by the

879 CeMEB consortium at University of Gothenburg, Sweden (https://cemeb.science.gu.se), was
880 included. The second maker iteration was run after first training the gene modeler SNAP
881 version 2006-07-28 (151) based on the results from the first run. Augustus v3.2.2 (152) was
882 run with initial parameter settings from Zebrafish. Repeat regions in the genome were masked
883 using RepeatMasker known elements (153) and repeat libraries from Repbase (154) as well as
884 *de novo* identified repeats from the round goby genome assembly obtained from a
885 RepeatModeler analysis (153).
886
887 **Table 5**. Summary of reference data from Ensembl used for the annotation.

Reference species	Number of protein sequences	Assembly version from ENSEMBL (downloaded 15th Feb 2016)
Astyanax mexicanus	23698	AstMex102
Danio rerio	44487	GRCz10
Gadus morhua	22100	gadMor1
Gasterosteus aculeatus	27576	BROADS1
Lepisosteus oculatus	22483	LepOcu1
Oreochromis niloticus	26763	Orenil1.0
Oryzias latipes	24674	MEDAKA1
Poecilia formosa	30898	PoeFor_5.1.2
Takifugu rubripes	47841	FUGU4
Tetraodon nigroviridis	23118	TETRAODON8
Xiphophorus maculatus	20454	Xipmac4.4.2

888
889 In order to ensure the completeness and quality of the current assembly and the associated gene
890 models, the assembly and the predicted protein sequences were run against reference sets at two
891 different taxonomical levels (303 eukaryotic and 4584 actinopterygian single copy orthologues) using
892 the BUSCO pipeline v2.0 (155, 156).
893
894 The maker annotation results were used to generate a database for JBrowse/Webapollo using the
895 script “maker2jbrowse” included with JBrowse (157, 158). Predicted protein and transcript sequences
896 were used to query the uniprot database, using blastp and blastn respectively, and the best hit
897 descriptions were transferred to the fasta headers with scripts bundled with Maker as described in
898 (150). The annotated genome is currently hosted on a WebApollo genome browser and Blast server at
899 the University of Gothenburg, Sweden at http://albiorix.bioenv.gu.se/.
900 Our analyses reveal that some degree of care is warranted regarding gene models. *De novo*
901 annotation without transcriptome data tends to be biased towards known and conserved genes,
902 homopolymer sequencing errors may cause annotation errors, and fish proteins have diverged faster

903 than mammalian homologs (159). For example, 25% of human genes cannot be identified in the
904 pufferfish (16). Even in the well-characterized zebrafish, targeted approaches have the potential to
905 reveal additional novel genes (160). We therefore encourage researchers to consider genome-wide
906 blast searches in addition to a consultation of round goby gene models, and hope that extensive RNA
907 sequencing data can be generated in the future to improve the predictions.
908
909 **Sex determining regions**
910
911 To investigate whether the round goby genome features large sex determining regions, we analyzed
912 own available RAD sequencing data. We prepared restriction site–associated DNA (RAD) (161)
913 libraries following the protocol used by (162, 163), which is largely based on (166). In short, we used
914 the Sbf1 enzyme on DNA extracted from 57 females, 56 males, and 5 juveniles caught in Basel,
915 Switzerland, and pooled 39-40 individuals per library for SR 100bp sequencing with Illumina. 45
916 females and 47 males retained sufficient numbers of reads (>150000) per sample after cleaning and
917 demultiplexing, were processed with the Stacks pipeline using the genome independent approach
918 (164), and were analyzed for sex-specific loci present exclusively in males or females. Considering a
919 genome size of ~1GB, the presence of 23 chromosomes (165), and a calling success of 21877 loci in
920 95 or 96 individuals (49220 loci in at least 40 individuals), we expected an average density of one
921 RAD locus every 45710 (20316) bp and an average number of 951 (2140) markers for an average
922 sized chromosome. The presence of a sex chromosome should thus be indicated by hundreds of sex-
923 specific RAD loci, while a contiguous sex determining region larger than 45000 bp would be indicated
924 by one or more sex specific RAD loci. Read numbers per locus for each sample were extracted from
925 the *.matches.tsv file output from Stacks and analyzed for sex-specific loci with standard R table
926 manipulations.
927
928 **Vision**
929
930 Opsin genes were extracted from the genome assembly using the Geneious software
931 (http://www.geneious.com) (167) by mapping the genomic scaffolds (Medium Sensitivity, 70% identity
932 threshold) against individual opsin exons of Nile tilapia (*Oreochromis niloticus*; GenBank Acc. no.:
933 MKQE00000000.1). This led to capturing of all scaffolds containing any visual opsin. The genes were

934 then annotated by mapping back of the single exons of tilapia against each scaffold separately (High
935 Sensitivity; 50% identity threshold) combined with the Live Annotate & Predict function as
936 implemented in Geneious, based on the Nile tilapia and mudskipper (25) opsin gene annotation. All
937 regions upstream and downstream from every opsin gene, as well as the intergenic regions were
938 separately tested for presence of any further opsin gene or its fragment (pseudogene). The annotated
939 genes were checked for the reading frame and the putative protein product was predicted.
940
941 We next performed phylogenetic analysis on the visual opsin genes (i.e. SWS1, SWS2, RH2, RH1 and
942 LWS opsins) across vertebrates, with focus on selected model species of teleost fishes. We further
943 specifically focused on the LWS genes from the fish species or lineages known to possess multiple
944 LWS copies, such as livebearers and pupfishes (Cyprinodontiformes) (168), zebrafish (*Danio rerio*)
945 (169), salmon (*Salmo salar*) (170), common carp (*Cyprinus carpio*) (170), cavefish (*Astyanax*
946 *mexicanus*) (171), Northern pike (*Esox lucius*) (170), labyrinth fishes (*Anabas testudineus*) (20), Asian
947 arowana (*Scleropages* formosus) (170) as well as other gobies, such as mudskippers (25) and reef
948 gobies (20). The opsin gene sequences from round goby and other fish species, including outgroup of
949 non-visual opsins (pinopsin, parietopsin, vertebrate-ancestral opsins and opn3 opsin;
950 **Supplemental_Material_S2**) were aligned using the MAFFT (172) plugin (v1.3.5) under the L-ins-i
951 algorithm as implemented in Geneious. Exon 5 (exon 6 in case of LWS) and part of exon 1 (or entire
952 exon 1 in case of LWS), which provided ambiguous alignment due to their higher variability, were
953 discarded. We estimated the model parameters by jModeltest 2.1.6 (173, 174), and subsequently used
954 the bayesian inference to calculate single-gene phylogeny using the MrBayes 3.2.6 (175) software as
955 implemented on the CIPRES Science gateway (176).
956
957 **Olfaction**
958
959 Olfactory receptor (OR) peptide sequences to be used as a reference were extracted from a publicly
960 available *Oreochromis niloticus* protein dataset (177). Those references were blasted (tblastn) against
961 the genomes of the round goby (*Neogobius melanostomus*), the blue-spotted mudskipper
962 (*Boleophthalmus pectinirostris*) (25), the giant mudskipper (*Periophthalmodon magnuspinatus*) (25)
963 and the three-spined stickleback (*Gasterosteus aculeatus*) (178), using an e-value threshold of $10e^{-50}$.
964 Only the hit with highest bit-score for each genomic position with more than one alignment was

965 employed in subsequent steps. Mapped hits belonging to contiguous positions of the protein
966 (maximum overlap of 15 aminoacids) and with a genomic distance smaller than 10kb were joined as
967 exons of the same CDS-gene model. Obtained sequences were translated to proteins using
968 TransDecoder (http://transdecoder.github.io), filtering all models that produce peptides smaller than
969 250 aminoacids. While many ORs are usually around 300 aminoacids long in total, 250 is close to the
970 average size of their main transmembrane domain, which is centrally located in the protein and more
971 suitable to interspecific alignment compared to N-terminal and C-terminal ends. We acknowledge that
972 this method might introduce a reduced proportion of recent pseudogenes that could lead to a small
973 overestimation of OR genes with coding capacity, although all species should be affected equivalently.
974
975 Next, an hmmscan (http://hmmer.org/) was produced against Pfam database to identify the domain
976 with highest score for each obtained protein sequence. We also filtered against false positive detection
977 using blast against confident OR and non-OR protein datasets. For phylogenetic analysis, sequences
978 (**Supplemental_Material_S3**) were aligned with MAFFT (https://mafft.cbrc.jp/alignment/server/) and a
979 Maximum Likelihood methodology was employed to build the tree using W-IQ-TREE software (179)
980 with standard parameters and Ultrafast bootstrap (180). Four adrenergic receptor sequences from
981 *Oreochromis niloticus* were used as an outgroup. Monophyletic groups formed by five or more genes
982 of the same species were considered as lineage-specific gene expansions. Because of the
983 phylogenetic proximity of the two mudskippers and the differences in their genome assembly statistics,
984 only *B. pectinirostris* was considered and *P. magnuspinatus* sequences were allowed to be included in
985 their lineage-specific expansion groups.
986
987 **Detoxification**
988
989 The Basic Local Alignment Search Tool (BLAST, v. 2.2.31) (181) was used to identify local alignments
990 between the round goby genome and a query including all annotated CYPs in humans and zebrafish
991 (vertebrate) and the most dissimilar invertebrate CYPs from *Drosophila melanogaster* (arthropod),
992 *Caenorhabditis elegans* (nematode) and *Capitella teleta* (annelid; **Supplemental_Material_S4**). Only
993 BLAST high scoring pairs with Expect values of 1.0 x 10-10 or smaller were considered significant.
994

995 The JBrowse genome viewer (v1.12.1) was used to manually annotate the significant regions of each
996 genome from the BLAST search, identifying start (ATG) and stop (TGA/TAA/TAG) codons, exon
997 number, and splice site signals (GT/AG) at intron-exon boundaries. The lengths of the potential CYPs
998 were identified and considered full length at ~500 amino acid residues long. Potential genes were
999 matched to the well-curated cytochrome P450 HMM in the Pfam protein family database (182) to
1000 confirm identity. The ScanProsite tool (183) was used to verify the presence of four largely conserved
1001 CYP motifs: the I-helix, K-helix, meander coil and heme loop. Each gene was classified as 'complete'
1002 (proper length with start and stop codon, all motifs present, and match to the HMM) or 'partial'
1003 (presence of at least the entire ~120 amino acid region that contains all motifs but clearly less than full
1004 length). Any potential CYP that was missing at least one of the motifs was considered a gene
1005 'fragment' (**Supplemental_Table_S9**).
1006
1007 All of the 'complete' and 'partial' round goby CYPs (**Supplemental_Table_S9**) were included in further
1008 analyses. Clustal Omega (v1.2.4) (184) was used to generate a multiple sequence alignment of the
1009 round goby sequences and a variety of well-known vertebrate CYPs from humans, *Danio rerio*, *Mus*
1010 *musculus*, *Xenopus laevis*, *Gallus gallus*, and *Rattus norvegicus* (125 sequences in total;
1011 **Supplemental_Material_S5**). Mesquite (v3.10) (185) was utilized to trim the alignment, especially at
1012 the termini of the protein sequences where significant variation is typically observed, leaving only the
1013 portion of the alignment representative of the homology of the sequences. The final 'masked'
1014 alignment (**Supplemental_Material_S6**) was used as input for the Randomized Axelerated Maximum
1015 Likelihood program (RAxML v8.2.10) (186). 100 bootstrap trees were generated with the rapid
1016 generation algorithm (-x) and a gamma distribution. The JTT substitution matrix with empirical
1017 frequencies was implemented in tree generation. The final maximum likelihood phylogenetic tree was
1018 visualized with Figtree (v1.4.3) (187) and rooted with the CYP51 family of enzymes.
1019
1020 **Osmoregulation**
1021
1022 Protein sequences for aquaporins, tight junction proteins, ion transporters, and enzymes in osmolyte
1023 production pathways were retrieved from the round goby genome by BLASTing well-characterized
1024 proteins from zebrafish, downloaded from Uniprot (March 2018), against the round goby gene
1025 models/proteins. Only round goby gene-models/proteins for which the predicted protein covered at

1026 least 70%, with a sequence identity of at least 40% and with E-value < 10^{-20} of the corresponding
1027 protein in zebrafish were used for the phylogenetic analyses. Well-established paralogues belonging
1028 to different subclasses of the respective protein family, based on either literature search or from initial
1029 phylogenetic analysis of that particular protein family, were used as additional query sequences to
1030 minimize the risk of missing relevant round goby sequences. Osmoregulatory genes from human and
1031 zebrafish were used for overall classification of clades in the respective protein family. Some
1032 modifications were made to the retrieved round goby sequences before analysis: i) For NHE ion
1033 transporters, a 780 aa long non-homologous N-terminus from one of the *Neogobius* sequences was
1034 removed before the phylogenetic analysis. ii) Some of the claudin genes were subjected to manual
1035 curation of Maker predicted proteins. The claudin genes in fish consist of several tandem arrays, which
1036 in some cases results in merging of 2-4 claudin genes by the Maker software. Claudins have a typical
1037 trans-membrane (TM) pattern with four distinct TM domains. All manually curated claudin genes from
1038 round goby were examined to have the expected four TM domains by TMHMM searches. Round goby
1039 protein sequences after manual curation are available in the supplement
1040 (**Supplemental_Material_S7**).
1041
1042 No myo-inositol phosphate synthase (MIPS) and sodium/inositol cotransporter (SMIT) proteins from
1043 zebrafish was found in Uniprot. To confirm that there are truly no MIPS and SMIT genes in zebrafish,
1044 the zebrafish genome at NCBI was also searched for homologies using blastp and tblastn using as
1045 query the MIPS and SMIT protein sequences from tilapia as query, and no hits were found. Thus, in
1046 the case of MIPS and SMIT, tilapia sequences were used for searching for round goby homologues.
1047 For the phylogenetic analyses, protein sequences from zebrafish (*Danio rerio*), three spine stickleback
1048 (*Gasterosteus aculeatus*), tilapia (*Oreochromis niloticus*), mudskipper (*Boleophthalmus pectinirostris*)
1049 and *Homo sapiens* (exception for human NKA-beta) were used in comparison to round goby, and
1050 were obtained from Uniprot (zebrafish, stickleback, tilapia, human) or RefSeq (mudskipper;
1051 **Supplemental_Material_S7**). Phylogenetic analyses of osmoregulatory proteins in round goby were
1052 performed using maximum likelihood with PhyML v3.0 with 100 bootstraps and using Gblocks to
1053 eliminate poorly aligned positions and highly divergent regions. PhyML analyses were performed at
1054 the Phylogeny.fr website (http://www.phylogeny.fr) using default settings.
1055
1056 **Immune system**

1057

1058 To perform an overall characterization of key genes related to the immune system, protein queries
1059 representing core components of innate and acquired immunity from several fish species as well as
1060 mammalian reference sequences were downloaded from UniProt and Ensembl. The protein queries
1061 were aligned prior to usage to ensure sequence homology. We also added previously extracted
1062 protein sequences from the Toll-like receptor family, reported by (85), and MHCI sequences reported
1063 by (80). All queries are listed in **Supplemental_Table_S4**. To enable comparative analyses between
1064 sequenced Gobiiformes, the genomes of *Periophthalmodon schlosseri* (GCA_000787095.1),
1065 *Periophthalmus magnuspinatus* (GCA_000787105.1), *Scartelaos histophorus* (GCA_000787155.1)
1066 and *Boleophthalmus pectinirostris* (GCA_000788275.1) were additionally downloaded from NCBI.
1067

1068 All protein queries were used in a tblastn (blast+ v. 2.6.0) towards the round goby genome assembly
1069 using default parameters and a e-value cutoff of 1e-10 (188). Some queries (*caspase-1*, *TLRs*, *IL1*
1070 and *IL8*) were also used in an identical tblastn towards the other Gobiiformes genomes. Genomic hit
1071 regions were extracted using BEDtools (v. 2.17.0) extending both up- and downstream as needed to
1072 obtain full length gene sequences (189). The extracted genomic regions were imported into MEGA7,
1073 the reading frame was adjusted for each exon and aligned as proteins to the corresponding translated
1074 coding sequence of queries using MUSCLE with default parameters. Intronic sequences were
1075 removed leaving an in-frame coding sequence (190, 191). All alignments were subjected to manual
1076 evaluation before subsequent analysis.
1077

1078 To generate phylogenetic trees, protein alignments were made and model tested using the ProtTest3
1079 server (http://darwin.uvigo.es/software/prottest_server.html) specifying BIC and no tree optimization
1080 (server has been disabled but ProtTest is available for download from GitHub) (192). All alignments
1081 reported the JTT model as best hit. Maximum likelihood trees were produced by using RAxML-
1082 PTHREADS (v 8.0.26), PROTCATJTT, rapid bootstrap and 500 bootstrap replicates (193). The final
1083 trees were imported into FigTree (http://tree.bio.ed.ac.uk/software/figtree/), and subsequently Adobe
1084 Illustrator, for presentation purposes.
1085

1086 In order to identify members of the large multigenic family of fish-specific NACHT and Leucine-Rich
1087 Repeats containing genes (NLRs; the fish-specific subset is also known as NLR-C) (87), an alignment

1088 of 368 zebrafish NLR-C proteins was obtained from (88). A combination of tblastn, HMMER3
1089 searches (194) and alignments with MAFFT v7.310 (195) was used to generate first an initial list of
1090 "candidate regions" potentially containing an NLR (**Supplemental_Material_S8**) and then an
1091 annotation of the characteristic domains in round goby NLR-C family members (see
1092 **Supplemental_Material_S9)** and **Supplemental_Table_S8** for details), consisting of 25 PYRIN , 1 N-
1093 terminal CARD, 12 C-terminal CARD, 343 FISNA-NACHT and 178 B30.2 domains. Custom HMM
1094 models for major NLR exons (FISNA-NACHT, and PRY-SPRY/B30.2) were generated and utilized
1095 during this process (Supplementary Methods, **Supplemental_Material_S10**). The majority of
1096 identified FISNA-NACHT exons contained frameshifts or a large insertion, indicating either
1097 pseudogenization, acquisition of new introns, problems with the assembly, or a combination of the
1098 three (196). In any case, for the subsequent phylogenetic analysis, only the 61 clearly intact NLRs
1099 were used. These were aligned with NLRs from human, zebrafish and the mudskipper goby using
1100 MAFFT (**Supplemental_Material_S9**; **Supplemental_Material_S11**); Maximum Likelihood trees were
1101 produced with RAxML-PTHREADS, PROTCATJTT, rapid bootstrap and 500 bootstrap replicates
1102 (193). The final trees were imported into FigTree (http://tree.bio.ed.ac.uk/software/figtree/), and
1103 subsequently Adobe Illustrator. The alignments were inspected manually for presence of the
1104 conserved Walker A motifs and sequence logos for these were generated with WebLogo (197).
1105 Finally, we performed a survey of the PYD domains, Peptidase_C14 domains (Caspases) and CARD.
1106 All cases of a PYD domain followed by an adjacent CARD in the round goby (putative apoptosis-
1107 associated speck-like protein containing a CARD (ASC), also known as PYD-CARD or PYCARD)
1108 were identified from the HMMER3 dataset. The open reading frames containing these were translated,
1109 concatenated, and aligned with similarly structured proteins from human, mouse, lizard, frog and all
1110 the fish in Ensembl, and with PYD-CARDs identified from the other available goby assemblies
1111 (**Supplemental_Material_S12**). A phylogenetic tree was generated as described above. The
1112 annotation for NLR-C genes consists of predicted positions for all of the major conserved NLR-
1113 associated domains (PYD, CARD, FISNA-NACHT-helices, LRRs, B30.2; **Supplemental_Table_S8**).
1114
1115 **Epigenetic regulators**
1116
1117 We focused on two gene expression regulators which are conserved among all eukaryotes: the
1118 Polycomb Repressive Complex 2 (PRC2), which deposits repressive histone methylation marks, and

1119 the DNA methylases, which methylate cytosine in CpG contexts. The presence of both marks is
1120 commonly associated with a downregulation of gene expression. The protein sequences of zebrafish
1121 orthologues of PRC2 components RBBP2, EED, EZH1-2, and SUZ12 (50) and of DNA methylases
1122 DNMT1 and DNMT3 (198) were blasted against the round goby genome using default parameters of
1123 the Albiorix Blast server. The protein sequence of predicted proteins at the hit site was extracted
1124 manually in the round goby genome browser and aligned with mouse, human, and zebrafish protein
1125 sequences. When the first and/or last exon sequences as predicted in the round goby genome differed
1126 significantly from the mouse, human, and zebrafish sequences, we attempted confirmation by 3' and
1127 5'RACE on RNA extracted from whole juvenile animals (see **Supplemental_Material_S13** for primer
1128 sequences and PCR conditions). A putative CDS was combined from automated annotation and
1129 RACE results, and aligned to sequences extracted from a variety of fish taxa, shark, chicken, frog,
1130 lizard, and human (**Supplemental_Material_S14**). Given the high conservation of these proteins in
1131 eukaryotes, and the absence of major unexpected differences between round goby and other
1132 vertebrates, additional Gobiidae were not included in the analyses. In order to perform codon aware
1133 alignment MACSE (199) was used. The model and partitioning scheme used for each phylogenetic
1134 analysis was estimated using PartitionFinder2 (200) using PhyML (201) with corrected AIC scores
1135 (AICc) used for model selection. Phylogenetic analyses were performed using MrBayes 3.2.6 (175,
1136 202) with three independent runs for each gene. Analyses were run for 2,000,000 generations or until
1137 the standard deviation of split frequencies was below 0.01 up to a maximum of 20,000,000
1138 generations. In order to aid convergence in the EZH analyses the temperature parameter was set to
1139 0.05.
1140
1141 **Transposable elements**
1142
1143 A number of different applications were used for the repeat annotation of the genome. They are
1144 described in the repeat annotation report (**Supplemental_Material_S15**). In summary, in addition to
1145 the identification of repeats with RepeatModeler (as described above), we used TRF (203) to predict
1146 tandem repeats. RepeatMasker (153), a homology-based approach was used to produce a genome-
1147 wide overview of interspersed repeats. LTR Finder (204) and LTRharvest (205) in combination with
1148 LTRdigest (206), both de novo approaches, were used to predict LTRs.
1149

1150 **Availability of data and materials**

1151

1152 The Whole Genome Shotgun project has been deposited at DDBJ/ENA/GenBank under the accession
1153 VHKM00000000. The version described in this paper is version VHKM01000000.
1154 Various Illumina reads are available under the accessions indicated in Table 1.
1155 Other datasets supporting the conclusions of this article are included within the article and its
1156 additional files.

1157

1158 **Additional files**

1159

1160 Supplemental Figure S1: .pdf; full opsin phylogenetic tree
1161 Supplemental Figure S2: .pdf; opsin tree constructed with individual exons
1162 Supplemental Figure S3: .pdf; full olfactory receptor phylogenetic tree
1163 Supplemental Figure S4: .pdf; claudin phylogenetic tree
1164 Supplemental Figure S5: .pdf; occludin phylogenetic tree
1165 Supplemental Figure S6: .pdf; sodium transporter phylogenetic trees
1166 Supplemental Figure S7: .pdf; myo-inositol production and accumulation gene phylogenetic trees
1167 Supplemental Figure S8: .pdf; TAP gene phylogenetic tree
1168 Supplemental Figure S9: .pdf; Ig locus schematic
1169 Supplemental Figure S10: .pdf; TLR phylogenetic tree of Gobiidae
1170 Supplemental Figure S11: .pdf; CRP / APCS phylogenetic tree
1171 Supplemental Figure S12: .pdf; SUZ12, EED, and RBBP4 phylogenetic trees
1172 Supplemental Material S1: .gz; annotation tracks for genome
1173 Supplemental Material S2: .txt; opsin sequences used for tree building
1174 Supplemental Material S3: .txt; olfactory receptor sequences used for tree building
1175 Supplemental Material S4: .txt; CYP sequences used as query
1176 Supplemental Material S5: .txt; CYP sequences used for tree building
1177 Supplemental Material S6: .phy; CYP alignment
1178 Supplemental Material S7: .doc; sequences for osmoregulatory proteins
1179 Supplemental Material S8: .fas; NLR candidate regions
1180 Supplemental Material S9: .doc; detailed methods for NLR annotation

Supplemental Material S10: zip of .hmm; hmm models used to identify NLRs

Supplemental Material S11: .fas; NLR sequences used for vertebrate tree building

Supplemental Material S12: .fas; NLR sequences used for Gobiidae tree building

Supplemental Material S13: .doc; detailed methods for RACE

Supplemental Material S14: zip of .nex; dnmt1, dnmt3, eed, ezh, rbbp4, and suz12 alignments

Supplemental Material S15: .txt; detailed methods for repeat annotation

Supplemental Table S1: .xls; overview and results for repeat sequences analysed

Supplemental Table S2: .xls; results for CYP genes (location, sequence, length)

Supplemental Table S3: .doc; overview table of immune genes analysed

Supplemental Table S4: .xls; immune gene sequences used as query

Supplemental Table S5: .doc; results for MHCI

Supplemental Table S6: .doc; results for MHCII

Supplemental Table S7: .txt; results for other immune genes analysed

Supplemental Table S8: .xls; results for NLRs

Supplemental Table S9: .xls; results for CYPs

Funding

ZM was funded by the Czech Science Foundation (16-09784Y) and the Swiss National Science Foundation (PROMYS - 166550). DB was funded by CZ.02.2.69/0.0/0.0/16_027/0008495 - International Mobility of Researchers at Charles University. Genome sequencing was funded with a contribution of the Freiwillige Akademische Gesellschaft Basel to IAK. KP was funded by an Undergraduate Student Research Award and a Discovery grant RGPIN5767-16 (to JYW) from the Natural Sciences and Engineering Research Council of Canada. MT, TL and MAR were funded by the Center for Marine Evolutionary Biology. JS was funded by grants LE 546/9-1 and WI 3081/5-1 within the Deutsche Forschungsgemeinschaft (DFG) - funded Priority Programme SPP1819. MHS was funded by the Norwegian Research Council (grant numbers 199806/S40 and 222378/F20). AB was funded by the Swedish Research Council (VR; #2017-04559).

Acknowledgements

1212 We are grateful to Prof. Patricia Burkhardt-Holm for her continuous support and encouragement. We
1213 thank Bernd Egger, Astrid Böhne, Philipp Hirsch and Patricia Burkhardt-Holm for critically reading the
1214 manuscript. We thank Fabio Cortesi for his insightful comments and the Center for Marine
1215 Evolutionary Biology for hosting a Blast server and a genome browser. Computational resources were
1216 provided by the CESNET LM2015042 and the CERIT Scientific Cloud LM2015085, provided under the
1217 programme "Projects of Large Research, Development, and Innovations Infrastructures". We thank
1218 Maria Leptin for her helpful comments and advice during annotation of the inflammasome
1219 components.
1220

1221 **Author contributions**

1222

1223 Sylke Winkler isolated DNA and generated PacBio reads, Martin Pippel and Siegfried Schloissnig
1224 assembled the genome sequence, and Tomas Larsson, Mats Tölpel and Magnus Alm Rosenblad
1225 performed automated annotation and provided the genome browser and Blast server.
1226

1227 Jean-Claude Walser provided transposable element analyses, Silvia Gutnik, Claire Peart, and Irene
1228 Adrian-Kalchhauser provided DNA methyltransferase and PRC2 analyses, Anders Blomberg provided
1229 osmoregulation analyses, Monica Hongroe Solbakken and Jaanus Suurväli provided immune gene
1230 analyses, Zuzana Musilova and Demian Burguera provided vision and olfaction analyses, Joanna
1231 Yvonne Wilson and Kirill Pankov provided CYP gene analyses, Nico Michiels investigated red
1232 fluorescence.
1233

1234 Irene Adrian-Kalchhauser initiated, designed, and supervised the project, acquired the necessary
1235 funding, coordinated annotation efforts, compiled the manuscript and handled the submission process.
1236

1237 **Permissions**

1238

1239 Fish used in this work were caught in accordance with permission 2-3-6-4-1 from the Cantonal Office
1240 for Environment and Energy, Basel Stadt.

1241 ## References

1242 1. Bock DG *et al. (*2014) What we still don't know about invasion genetics. *Molecular Ecology*.

1243 2. Prentis PJ, Wilson JRU, Dormontt EE, RICHARDSON DM, Lowe AJ (2008) Adaptive evolution in
1244 invasive species. *Trends in Plant Science* 13:288–294.

1245 3. Tsutsui ND, Suarez AV, Holway DA, Case TJ (2000) Reduced genetic variation and the success
1246 of an invasive species. *Proceedings of the National Academy of Sciences* 97:5948.

1247 4. Lee CE (2002) Evolutionary genetics of invasive species. *TRENDS IN ECOLOGY & EVOLUTION*
1248 17:386–391.

1249 5. Jude DJ, Reider RH, Smith GR (1992) Establishment of Gobiidae in the Great Lakes Basin. *Can.*
1250 *J. Fish. Aquat. Sci.* 49:416–421.

1251 6. Michalek M, Puntila R, Strake S, Werner M (2012) *HELCOM Baltic Sea Environment Fact Sheet*
1252 *2012*.

1253 7. Roche KF, Janac M, Jurajda P (2013) A review of Gobiid expansion along the Danube-Rhine
1254 corridor - geopolitical change as a driver for invasion. *KNOWLEDGE AND MANAGEMENT OF*
1255 *AQUATIC ECOSYSTEMS*.

1256 8. Hirsch PE, N'Guyen A, Adrian-Kalchhauser I, Burkhardt-Holm P (2015) What do we really know
1257 about the impacts of one of the 100 worst invaders in Europe? A reality check. *Ambio*.

1258 9. Dufour BA, Hogan TM, Heath DD (2007) Ten polymorphic microsatellite markers in the invasive
1259 round goby (Neogobius melanostomus) and cross-species amplification. *MOLECULAR*
1260 *ECOLOGY NOTES* 7:1205–1207.

1261 10. Adrian-Kalchhauser I *et al. (*2017) The mitochondrial genome sequences of the round goby and
1262 the sand goby reveal patterns of recent evolution in gobiid fish. *BMC GENOMICS* 18:177.

1263 11. Feldheim KA *et al. (*2009) Microsatellite loci for Ponto-Caspian gobies: markers for assessing
1264 exotic invasions. *Molecular Ecology Resources* 9:639–644.

1265 12. Neilson ME, Stepien CA (2009) Escape from the Ponto-Caspian: Evolution and biogeography of
1266 an endemic goby species flock (Benthophilinae: Gobiidae: Teleostei). *Molecular Phylogenetics*
1267 *and Evolution* 52:84–102.

13. Bowley LA, Alam F, Marentette JR, Balshine S, Wilson JY (2010) Characterization of vitellogenin gene expression in round goby (Neogobius melanostomus) using a quantitative polymerase chain reaction assay. *Environmental toxicology and chemistry / SETAC* 29:2751–2760.

14. Thacker CE, Roje DM (2011) Phylogeny of Gobiidae and identification of gobiid lineages. *Systematics and Biodiversity* 9:329–347.

15. Thacker CE, Thompson AR, Roje DM (2011) Phylogeny and evolution of Indo-Pacific shrimp-associated gobies (Gobiiformes: Gobiidae). *Molecular Phylogenetics and Evolution* 59:168–176.

16. Aparicio S *et al. (*2002) Whole-Genome Shotgun Assembly and Analysis of the Genome of <em>Fugu rubripes</em&gt. *Science* 297:1301.

17. Amemiya CT *et al. (*2013) The African coelacanth genome provides insights into tetrapod evolution. *NATURE* 496:311 EP -.

18. Star B *et al. (*2011) The genome sequence of Atlantic cod reveals a unique immune system. *NATURE* 477:207–210.

19. Li J-T *et al. (*2015) The fate of recent duplicated genes following a fourth-round whole genome duplication in a tetraploid fish, common carp (Cyprinus carpio). *Scientific reports* 5:8199 EP -.

20. Musilova Z *et al. (*2019) Vision using multiple distinct rod opsins in deep-sea fishes. *Science* 364:588.

21. Seehausen O, van Alphen JJM, Witte F (1997) Cichlid Fish Diversity Threatened by Eutrophication That Curbs Sexual Selection. *Science* 277:1808.

22. Seehausen O *et al. (*2008) Speciation through sensory drive in cichlid fish. *NATURE* 455:620-U23.

23. Barth FG; Schmid A; Douglas RH, eds (2001) *The Ecology of Teleost Fish Visual Pigments: a Good Example of Sensory Adaptation to the Environment? Ecology of Sensing* (Springer Berlin Heidelberg).

24. Hornsby MAW, Sabbah S, Robertson RM, Hawryshyn CW (2013) Modulation of environmental light alters reception and production of visual signals in Nile tilapia. *JOURNAL OF EXPERIMENTAL BIOLOGY* 216:3110–3122.

25. You X *et al. (*2014) Mudskipper genomes provide insights into the terrestrial adaptation of amphibious fishes. *NATURE COMMUNICATIONS* 5.

26. Busserolles F de *et al.* (2017) Pushing the limits of photoreception in twilight conditions. The rod-like cone retina of the deep-sea pearlsides. *SCIENCE ADVANCES* 3.

27. Kenaley CP, Devaney SC, Fjeran TT (2014) The complex evolutionary history of seeing red. Molecular phylogeny and the evolution of an adaptive visual system in deep-sea dragonfishes (Stomiiformes: Stomiidae). *Evolution; international journal of organic evolution* 68:996–1013.

28. Corkum LD *et al.* (2006) Evidence of a Male Sex Pheromone in the Round Goby (Neogobius melanostomus). *Biol Invasions* 8:105–112.

29. Farwell M *et al.* (2017) Differential female preference for individual components of a reproductive male round goby (Neogobius melanostomus) pheromone. *JOURNAL OF GREAT LAKES RESEARCH* 43:379–386.

30. Tierney KB *et al.* (2012) Invasive male round gobies (Neogobius melanostomus) release pheromones in their urine to attract females. *Can. J. Fish. Aquat. Sci.* 70:393–400.

31. Laframboise AJ, Katare Y, Scott AP, Zielinski BS (2011) The Effect of Elevated Steroids Released by Reproductive Male Round Gobies, Neogobius melanostomus, on Olfactory Responses in Females. *JOURNAL OF CHEMICAL ECOLOGY* 37:260–262.

32. Marentette JR *et al.* (2010) Signatures of contamination in invasive round gobies (Neogobius melanostomus): A double strike for ecosystem health? *ECOTOXICOLOGY AND ENVIRONMENTAL SAFETY* 73:1755–1764.

33. Marentette JR, Balshine S (2012) Altered Prey Responses in Round Goby from Contaminated Sites. *ETHOLOGY* 118:812–820.

34. McCallum ES *et al.* (2014) Persistence of an invasive fish (Neogobius melanostomus) in a contaminated ecosystem. *BIOLOGICAL INVASIONS* 16:2449–2461.

35. Goldstone JV *et al.* (2006) The chemical defensome. Environmental sensing and response genes in the Strongylocentrotus purpuratus genome. *DEVELOPMENTAL BIOLOGY* 300:366–384.

36. Whitfield AK (2015) Why are there so few freshwater fish species in most estuaries? *J Fish Biol* 86:1227–1250.

37. Lee KA, Klasing KC (2004) A role for immunology in invasion biology. *TRENDS IN ECOLOGY & EVOLUTION* 19:523–529.

1324 38. David GM *et al. (*2018) A minimalist macroparasite diversity in the round goby of the Upper Rhine
1325 reduced to an exotic acanthocephalan lineage. *Parasitology* 145:1020–1026.

1326 39. Jaenisch R, Bird A (2003) Epigenetic regulation of gene expression. How the genome integrates
1327 intrinsic and environmental signals. *Nature genetics* 33:245 EP -.

1328 40. Zamudio N *et al. (*2015) DNA methylation restrains transposons from adopting a chromatin
1329 signature permissive for meiotic recombination. *Genes & development* 29:1256–1270.

1330 41. Choi J, Lyons DB, Kim Y, Moore JD, Zilberman D (2019) *DNA methylation and histone H1*
1331 *cooperatively repress transposable elements and aberrant intragenic transcripts. Supplemental*
1332 *Information*.

1333 42. Feinberg AP, Irizarry RA (2010) Stochastic epigenetic variation as a driving force of development,
1334 evolutionary adaptation, and disease. *PROCEEDINGS OF THE NATIONAL ACADEMY OF*
1335 *SCIENCES OF THE UNITED STATES OF AMERICA* 107:1757–1764.

1336 43. Herman JJ, Sultan SE (2016) DNA methylation mediates genetic variation for adaptive
1337 transgenerational plasticity. *Proceedings of the Royal Society B: Biological Sciences*
1338 283:20160988.

1339 44. Cortijo S *et al. (*2014) Mapping the Epigenetic Basis of Complex Traits. *Science* 343:1145.

1340 45. Wellband KW, Heath DD (2017) Plasticity in gene transcription explains the differential
1341 performance of two invasive fish species. *Evol Appl* 10:563–576.

1342 46. Adrian-Kalchhauser I, Walser J-C, Schwaiger M, Burkhardt-Holm P (2018) RNA sequencing of
1343 early round goby embryos reveals that maternal experiences can shape the maternal RNA
1344 contribution in a wild vertebrate. *BMC EVOLUTIONARY BIOLOGY* 18:34.

1345 47. Somerville V *et al. (*2019) *DNA Methylation Patterns in the Round Goby Hypothalamus Support an*
1346 *On-The-Spot Decision Scenario for Territorial Behavior*.

1347 48. Grimm SA *et al. (*2019) DNA methylation in mice is influenced by genetics as well as sex and life
1348 experience. *NATURE COMMUNICATIONS* 10:305.

1349 49. Weyrich A *et al. (*2016) Paternal heat exposure causes DNA methylation and gene expression
1350 changes of in Wild guinea pig sons. *Ecology and evolution*.

1351 50. Margueron R, Reinberg D (2011) The Polycomb complex PRC2 and its mark in life. *NATURE*
1352 469:343–349.

1353 51. Gibbs DJ *et al. (*2018) Oxygen-dependent proteolysis regulates the stability of angiosperm
1354 polycomb repressive complex 2 subunit VERNALIZATION 2. *NATURE COMMUNICATIONS*
1355 9:5438.

1356 52. Martinez P *et al. (*2014) Genetic architecture of sex determination in fish. Applications to sex ratio
1357 control in aquaculture. *Frontiers in genetics* 5.

1358 53. Hardie DC, Hebert PDN (2003) The nucleotypic effects of cellular DNA content in cartilaginous
1359 and ray-finned fishes. *GENOME* 46:683–706.

1360 54. Hardie DC, Hebert PDN (2004) Genome-size evolution in fishes. *Can. J. Fish. Aquat. Sci.*
1361 61:1636–1646.

1362 55. Gregory TR (2019) Animal Genome Size Database.

1363 56. Bowmaker JK, Hunt DM (2006) Evolution of vertebrate visual pigments. *Current Biology* 16:R484-
1364 R489.

1365 57. Cortesi F *et al. (*2015) Ancestral duplications and highly dynamic opsin gene evolution in
1366 percomorph fishes. *PROCEEDINGS OF THE NATIONAL ACADEMY OF SCIENCES OF THE*
1367 *UNITED STATES OF AMERICA* 112:1493–1498.

1368 58. Liu D-W *et al. (*2019) The Cone Opsin Repertoire of Osteoglossomorph Fishes. Gene Loss in
1369 Mormyrid Electric Fish and a Long Wavelength-Sensitive Cone Opsin That Survived 3R.
1370 *MOLECULAR BIOLOGY AND EVOLUTION* 36:447–457.

1371 59. Yokoyama S (2008) in *Linkage disequilibrium and association mapping*, ed Weir BS, pp 259–282.

1372 60. Niimura Y (2012) Olfactory receptor multigene family in vertebrates. From the viewpoint of
1373 evolutionary genomics. *Current genomics* 13:103–114.

1374 61. Niimura Y (2009) On the Origin and Evolution of Vertebrate Olfactory Receptor Genes.
1375 Comparative Genome Analysis Among 23 Chordate Species. *GENOME BIOLOGY AND*
1376 *EVOLUTION* 1:34–44.

1377 62. Nelson DR (2003) Comparison of P450s from human and fugu. 420 million years of vertebrate
1378 P450 evolution. *Archives of Biochemistry and Biophysics* 409:18–24.

1379 63. Goldstone JV *et al. (*2010) Identification and developmental expression of the full complement of
1380 Cytochrome P450 genes in Zebrafish. *BMC GENOMICS* 11:643.

1381 64. Kirischian N, McArthur AG, Jesuthasan C, Krattenmacher B, Wilson JY (2011) Phylogenetic and
1382 functional analysis of the vertebrate cytochrome p450 2 family. *JOURNAL OF MOLECULAR*
1383 *EVOLUTION* 72:56–71.

1384 65. Dejong CA, Wilson JY (2014) The Cytochrome P450 Superfamily Complement (CYPome) in the
1385 Annelid Capitella teleta. *PLoS ONE* 9:e107728.

1386 66. Luch A, Baird WM in *The carcinogenic effects of polycyclic aromatic hydrocarbons*, pp 19–96.

1387 67. Yan J, Cai Z (2010) Molecular evolution and functional divergence of the cytochrome P450 3
1388 (CYP3) Family in Actinopterygii (ray-finned fish). *PLoS ONE* 5:e14276.

1389 68. Yokoyama C *et al. (*1996) Human Gene Encoding Prostacyclin Synthase (PTGIS). Genomic
1390 Organization, Chromosomal Localization, and Promoter Activity. *Genomics* 36:296–304.

1391 69. Li Y-C *et al. (*2008) Structures of prostacyclin synthase and its complexes with substrate analog
1392 and inhibitor reveal a ligand-specific heme conformation change. *JOURNAL OF BIOLOGICAL*
1393 *CHEMISTRY* 283:2917–2926.

1394 70. Finn RN, Cerdà J (2011) Aquaporin evolution in fishes. *Frontiers in physiology* 2:44.

1395 71. Finn RN, Chauvigné F, Hlidberg JB, Cutler CP, Cerdà J (2014) The Lineage-Specific Evolution of
1396 Aquaporin Gene Clusters Facilitated Tetrapod Terrestrial Adaptation. *PLoS ONE* 9:e113686.

1397 72. Loh YH, Christoffels A, Brenner S, Hunziker W, Venkatesh B (2004) Extensive Expansion of the
1398 Claudin Gene Family in the Teleost Fish, Fugu rubripes. *GENOME RESEARCH* 14:1248–1257.

1399 73. Hwang P-P, Chou M-Y (2013) Zebrafish as an animal model to study ion homeostasis. *Pflügers*
1400 *Archiv - European Journal of Physiology* 465:1233–1247.

1401 74. Ronkin D, Seroussi E, Nitzan T, Doron-Faigenboim A, Cnaani A (2015) Intestinal transcriptome
1402 analysis revealed differential salinity adaptation between two tilapiine species. *Comparative*
1403 *biochemistry and physiology. Part D, Genomics & proteomics* 13:35–43.

1404 75. Rim JS *et al. (*1998) Transcription of the sodium/myo-inositol cotransporter gene is regulated by
1405 multiple tonicity-responsive enhancers spread over 50 kilobase pairs in the 5 '-flanking region.
1406 *JOURNAL OF BIOLOGICAL CHEMISTRY* 273:20615–20621.

1407 76. Wang X, Kültz D (2017) Osmolality/salinity-responsive enhancers (OSREs) control induction of
1408 osmoprotective genes in euryhaline fish. *PROCEEDINGS OF THE NATIONAL ACADEMY OF*
1409 *SCIENCES OF THE UNITED STATES OF AMERICA* 114:E2729-E2738.

1410 77. Sacchi R, Gardell AM, Chang N, Kültz D (2014) Osmotic regulation and tissue localization of the
1411 myo-inositol biosynthesis pathway in tilapia (Oreochromis mossambicus) larvae. *J. Exp. Zool.*
1412 321:457–466.

1413 78. Sacchi R, Li J, Villarreal F, Gardell AM, Kültz D (2013) Salinity-induced regulation of the
1414 myo-inositol biosynthesis pathway in tilapia gill epithelium. *J. Exp. Biol.*
1415 216:4626.

1416 79. Flajnik MF (2018) A cold-blooded view of adaptive immunity. *Nature reviews. Immunology* 18:438–
1417 453.

1418 80. Grimholt U *et al. (*2015) A comprehensive analysis of teleost MHC class I sequences. *BMC*
1419 *EVOLUTIONARY BIOLOGY* 15:32.

1420 81. McConnell SC *et al. (*2016) Alternative haplotypes of antigen processing genes in zebrafish
1421 diverged early in vertebrate evolution. *PROCEEDINGS OF THE NATIONAL ACADEMY OF*
1422 *SCIENCES OF THE UNITED STATES OF AMERICA* 113:E5014-E5023.

1423 82. Mashoof S, Criscitiello MF (2016) Fish Immunoglobulins. *Biology* 5:45.

1424 83. Riera Romo M, Perez-Martinez D, Castillo Ferrer C (2016) Innate immunity in vertebrates. An
1425 overview. *Immunology* 148:125–139.

1426 84. Guo H, Callaway JB, Ting JP-Y (2015) Inflammasomes. Mechanism of action, role in disease, and
1427 therapeutics. *NATURE MEDICINE* 21:677–687.

1428 85. Solbakken MH *et al. (*2016) Evolutionary redesign of the Atlantic cod (Gadus morhua L.) Toll-like
1429 receptor repertoire by gene losses and expansions. *Scientific reports* 6:25211 EP -.

1430 86. Solbakken MH, Voje KL, Jakobsen KS, Jentoft S (2017) Linking species habitat and past
1431 palaeoclimatic events to evolution of the teleost innate immune system. *Proceedings. Biological*
1432 *sciences* 284.

1433 87. Laing KJ, Purcell MK, Winton JR, Hansen JD (2008) A genomic view of the NOD-like receptor
1434 family in teleost fish. Identification of a novel NLR subfamily in zebrafish. *BMC EVOLUTIONARY*
1435 *BIOLOGY* 8.

1436 88. Howe K *et al. (*2016) Structure and evolutionary history of a large family of NLR proteins in the
1437 zebrafish. *Open biology* 6:160009.

1438 89. Tørresen OK *et al. (*2018) Genomic architecture of haddock (Melanogrammus aeglefinus) shows
1439 expansions of innate immune genes and short tandem repeats. *BMC GENOMICS* 19:240.

1440 90. Li J-Y *et al. (*2018) Characterization of an NLRP1 Inflammasome from Zebrafish Reveals a Unique
1441 Sequential Activation Mechanism Underlying Inflammatory Caspases in Ancient Vertebrates.
1442 *Journal of immunology (Baltimore, Md. : 1950)* 201:1946–1966.

1443 91. Kuri P *et al. (*2017) Dynamics of in vivo ASC speck formation. *The Journal of Cell Biology*
1444 216:2891–2909.

1445 92. Schwartz YB, Pirrotta V (2013) A new world of Polycombs. Unexpected partnerships and
1446 emerging functions. *Nature Reviews Genetics* 14:853 EP -.

1447 93. Mu W, Starmer J, Shibata Y, Della Yee, Magnuson T (2017) EZH1 in germ cells safeguards the
1448 function of PRC2 during spermatogenesis. *DEVELOPMENTAL BIOLOGY* 424:198–207.

1449 94. Xu J *et al. (*2015) Developmental control of polycomb subunit composition by GATA factors
1450 mediates a switch to non-canonical functions. *Molecular cell* 57:304–316.

1451 95. San B *et al. (*2016) Normal formation of a vertebrate body plan and loss of tissue maintenance in
1452 the absence of ezh2. *Scientific reports* 6:24658.

1453 96. Völkel P *et al. (*2019) Ezh1 arises from Ezh2 gene duplication but its function is not required for
1454 zebrafish development. *Scientific reports* 9:4319.

1455 97. Jeltsch A, Jurkowska RZ (2014) New concepts in DNA methylation. *Trends in Biochemical*
1456 *Sciences* 39:310–318.

1457 98. Ponger L, Li W-H (2005) Evolutionary Diversification of DNA Methyltransferases in Eukaryotic
1458 Genomes. *MOLECULAR BIOLOGY AND EVOLUTION* 22:1119–1128.

1459 99. Wang F-L *et al. (*2018) Genome-wide identification, evolution of DNA methyltransferases and their
1460 expression during gonadal development in Nile tilapia. *COMPARATIVE BIOCHEMISTRY AND*
1461 *PHYSIOLOGY B-BIOCHEMISTRY & MOLECULAR BIOLOGY* 226:73–84.

1462 100. Stapley J, Santure AW, Dennis SR (2015) Transposable elements as agents of rapid
1463 adaptation may explain the genetic paradox of invasive species. *Mol Ecol* 24:2241–2252.

1464 101. Pysek P *et al. (*2018) Small genome separates native and invasive populations in an
1465 ecologically important cosmopolitan grass. *Ecology* 99:79–90.

1466 102. Pezold FL (1984) Evidence for multiple sex-chromosomes in THE FRESH-WATER GOBY,
1467 GOBIONELLUS-SHUFELDTI (PISCES, GOBIIDAE). *COPEIA*:235–238.

1468 103. Bitton P-P, Christmann SAY, Santon M, Harant UK, Michiels NK (2018) Visual modelling
1469 validates prey detection by means of diurnal active photolocation in a small cryptobenthic fish.
1470 *bioRxiv*:338640.

1471 104. Carleton KL, Dalton BE, Escobar-Camacho D, Nandamuri SP (2016) Proximate and ultimate
1472 causes of variable visual sensitivities. Insights from cichlid fish radiations. *genesis* 54:299–325.

1473 105. Marshall J, Johnsen S (2017) Fluorescence as a means of colour signal enhancement.
1474 *Philosophical Transactions of the Royal Society B: Biological Sciences* 372.

1475 106. Michiels NK *et al. (*2008) Red fluorescence in reef fish. A novel signalling mechanism? *BMC*
1476 *ECOLOGY* 8:14pp.

1477 107. Olsson KH *et al. (*2017) Dark eyes in female sand gobies indicate readiness to spawn. *PLoS*
1478 *ONE* 12:e0177714.

1479 108. Anthes N, Theobald J, Gerlach T, Meadows MG, Michiels NK (2016) Diversity and Ecological
1480 Correlates of Red Fluorescence in Marine Fishes. *FRONTIERS IN ECOLOGY AND EVOLUTION*
1481 4.

1482 109. Vélez-Espino LA, Koops MA, Balshine S (2010) Invasion dynamics of round goby (Neogobius
1483 melanostomus) in Hamilton Harbour, Lake Ontario. *BIOLOGICAL INVASIONS* 12:3861–3875.

1484 110. Young JAM *et al. (*2010) Demography and substrate affinity of the round goby (Neogobius
1485 melanostomus) in Hamilton Harbour. *JOURNAL OF GREAT LAKES RESEARCH* 36:115–122.

1486 111. Behrens JW, van Deurs M, Christensen EAF (2017) Evaluating dispersal potential of an
1487 invasive fish by the use of aerobic scope and osmoregulation capacity. *PLoS ONE* 12:e0176038.

1488 112. Hirsch PE *et al. (*2016) A tough egg to crack: recreational boats as vectors for invasive goby
1489 eggs and transdisciplinary management approaches. *Ecology and evolution* 6:707–715.

1490 113. Miladi H, Elabed H, Ben Slama R, Rhim A, Bakhrouf A (2017) Molecular analysis of the role of
1491 osmolyte transporters opuCA and betL in Listeria monocytogenes after cold and freezing stress.
1492 *Archives of microbiology* 199:259–265.

1493 114. Vigoder FM *et al. (*2016) Inducing Cold-Sensitivity in the Frigophilic Fly Drosophila montana by
1494 RNAi. *PLoS ONE* 11:e0165724.

1495 115. Wu C *et al. (*2014) The draft genome of the large yellow croaker reveals well-developed innate
1496 immunity. *NATURE COMMUNICATIONS* 5.

1497 116. Liu Z *et al. (*2016) The channel catfish genome sequence provides insights into the evolution
1498 of scale formation in teleosts. *NATURE COMMUNICATIONS* 7.

1499 117. Berthelot C *et al. (*2014) The rainbow trout genome provides novel insights into evolution after
1500 whole-genome duplication in vertebrates. *NATURE COMMUNICATIONS* 5:3657.

1501 118. Reis MIR, do Vale A, Pereira PJB, Azevedo JE, dos Santos NMS (2012) Caspase-1 and IL-1
1502 beta Processing in a Teleost Fish. *PLoS ONE* 7.

1503 119. Vojtech LN, Scharping N, Woodson JC, Hansen JD (2012) Roles of inflammatory caspases
1504 during processing of zebrafish interleukin-1β in Francisella noatunensis infection. *INFECTION*
1505 *AND IMMUNITY* 80:2878–2885.

1506 120. Richter K *et al. (*2018) C-Reactive Protein Stimulates Nicotinic Acetylcholine Receptors to
1507 Control ATP-Mediated Monocytic Inflammasome Activation. *Frontiers in immunology* 9:1604.

1508 121. Cao R, Zhang Y (2004) SUZ12 is required for both the histone methyltransferase activity and
1509 the silencing function of the EED-EZH2 complex. *Molecular cell* 15:57–67.

1510 122. Ciferri C *et al. (*2012) Molecular architecture of human polycomb repressive complex 2. *eLife*
1511 1:e00005.

1512 123. Chittock EC, Latwiel S, Miller TCR, Müller CW (2017) Molecular architecture of polycomb
1513 repressive complexes. *Biochemical Society transactions* 45:193–205.

1514 124. Cao Q *et al. (*2014) The central role of EED in the orchestration of polycomb group
1515 complexes. *NATURE COMMUNICATIONS* 5:3127.

1516 125. Liu X, Yang J, Wu N, Song R, Zhu H (2015) Evolution and Coevolution of PRC2 Genes in
1517 Vertebrates and Mammals. *Advances in protein chemistry and structural biology* 101:125–148.

1518 126. Davidovich C, Cech TR (2015) The recruitment of chromatin modifiers by long noncoding
1519 RNAs. Lessons from PRC2. *RNA (New York, N.Y.)* 21:2007–2022.

1520 127. Cross S, Kovarik P, Schmidtke J, Bird A (1991) Non-methylated islands in fish genomes are
1521 GC-poor. *NUCLEIC ACIDS RESEARCH* 19:1469–1474.

1522 128. Jiang N *et al. (*2014) Conserved and Divergent Patterns of DNA Methylation in Higher
1523 Vertebrates. *GENOME BIOLOGY AND EVOLUTION* 6:2998–3014.

1524 129. Han L, Zhao Z (2008) Comparative analysis of CpG islands in four fish genomes. *Comparative*
1525 *and functional genomics*:565631.

1526 130. Huska M, Vingron M (2016) Improved Prediction of Non-methylated Islands in Vertebrates
1527 Highlights Different Characteristic Sequence Patterns. *PLOS COMPUTATIONAL BIOLOGY* 12.

1528 131. McGaughey DM, Abaan HO, Miller RM, Kropp PA, Brody LC (2014) Genomics of CpG
1529 methylation in developing and developed zebrafish. *G3 (Bethesda, Md.)* 4:861–869.

1530 132. Campos C, Valente LMP, Fernandes JMO (2012) Molecular evolution of zebrafish dnmt3
1531 genes and thermal plasticity of their expression during embryonic development. *GENE* 500:93–
1532 100.

1533 133. Takayama K, Shimoda N, Takanaga S, Hozumi S, Kikuchi Y (2014) Expression patterns of
1534 dnmt3aa, dnmt3ab, and dnmt4 during development and fin regeneration in zebrafish. *GENE*
1535 *EXPRESSION PATTERNS* 14:105–110.

1536 134. Firmino J *et al. (*2017) Phylogeny, expression patterns and regulation of DNA
1537 Methyltransferases in early development of the flatfish, Solea senegalensis. *BMC*
1538 *DEVELOPMENTAL BIOLOGY* 17:11.

1539 135. Wood RK, Crowley E, Martyniuk CJ (2016) Developmental profiles and expression of the DNA
1540 methyltransferase genes in the fathead minnow (Pimephales promelas) following exposure to di-2-
1541 ethylhexyl phthalate. *Fish Physiol Biochem* 42:7–18.

1542 136. Wu N *et al. (*2019) Fall webworm genomes yield insights into rapid adaptation of invasive
1543 species. *Nature ecology & evolution* 3:105–115.

1544 137. Lien S *et al. (*2016) The Atlantic salmon genome provides insights into rediploidization.
1545 *NATURE* 533:200 EP -.

1546 138. Kim B-M *et al. (*2019) Antarctic blackfin icefish genome reveals adaptations to extreme
1547 environments. *Nature ecology & evolution* 3:469–478.

1548 139. Mu Y *et al. (*2018) An improved genome assembly for Larimichthys crocea reveals hepcidin
1549 gene expansion with diversified regulation and function. *Communications biology* 1:195.

1550 140. El-Brolosy MA *et al. (*2019) Genetic compensation triggered by mutant mRNA degradation.
1551 *NATURE* 568:193–197.

1552 141. Roche K *et al. (*2015) A newly established round goby (Neogobius melanostomus)
1553 population in the upper stretch of the river Elbe. *Knowl. Manag. Aquat. Ecosyst.*:33.

1554 142. Patzner RA; VanTassel J.L.; Kovačić M; Kapoor BG, eds (2011) *The biology of gobies*
1555 (Science Publishers, Enfield, NH).

1556 143. Xing J, Zhou X, Tang X, Sheng X, Zhan W (2017) Characterization of Toll-like receptor 22 in
1557 turbot (Scophthalmus maximus). *FISH & SHELLFISH IMMUNOLOGY* 66:156–162.

1558 144. Paria A, Makesh M, Chaudhari A, Purushothaman CS, Rajendran KV (2018) Toll-like receptor
1559 (TLR) 22, a non-mammalian TLR in Asian seabass, Lates calcarifer. Characterisation, ontogeny
1560 and inductive expression upon exposure with bacteria and ligands. *Developmental & Comparative*
1561 *Immunology* 81:180–186.

1562 145. Qi Z *et al. (*2018) Molecular characterization of three toll-like receptors (TLR21, TLR22, and
1563 TLR25) from a primitive ray-finned fish Dabry's sturgeon (Acipenser dabryanus). *FISH &*
1564 *SHELLFISH IMMUNOLOGY* 82:200–211.

1565 146. Nowoshilow S *et al. (*2018) The axolotl genome and the evolution of key tissue formation
1566 regulators. *NATURE* 554:50–55.

1567 147. Grohme MA *et al. (*2018) The genome of Schmidtea mediterranea and the evolution of core
1568 cellular mechanisms. *NATURE* 554:56–61.

1569 148. Chin C-S *et al. (*2013) Nonhybrid, finished microbial genome assemblies from long-read
1570 SMRT sequencing data. *NATURE METHODS* 10:563.

1571 149. Cantarel BL *et al. (*2008) MAKER. An easy-to-use annotation pipeline designed for emerging
1572 model organism genomes. *GENOME RESEARCH* 18:188–196.

1573 150. Campbell MS, Holt C, Moore B, Yandell M (2014) Genome Annotation and Curation Using
1574 MAKER and MAKER-P. *Current protocols in bioinformatics* 48:4.11.1-39.

1575 151. Korf I (2004) Gene finding in novel genomes. *BMC BIOINFORMATICS* 5.

1576 152. Stanke M, Diekhans M, Baertsch R, Haussler D (2008) Using native and syntenically mapped
1577 cDNA alignments to improve de novo gene finding. *Bioinformatics (Oxford, England)* 24:637–644.

1578 153. Smit AFA, Hubley R, Green P (2013-2015) *RepeatMasker Open-4.0*.

1579 154. Bao W, Kojima KK, Kohany O (2015) Repbase Update, a database of repetitive elements in
1580 eukaryotic genomes. *MOBILE DNA* 6.

1581 155. Waterhouse RM *et al. (*2017) BUSCO Applications from Quality Assessments to Gene
1582 Prediction and Phylogenomics. *MOLECULAR BIOLOGY AND EVOLUTION* 35:543–548.

1583 156. Kriventseva EV, Zdobnov EM, Simão FA, Ioannidis P, Waterhouse RM (2015) BUSCO.
1584 Assessing genome assembly and annotation completeness with single-copy orthologs.
1585 *BIOINFORMATICS* 31:3210–3212.

1586 157. Dunn NA *et al.* GMOD/Apollo: 2.2.0 JB#1.15.4-release.

1587 158. Lee E *et al. (*2013) Web Apollo. A web-based genomic annotation editing platform. *Genome*
1588 *biology* 14:R93.

1589 159. Jaillon O *et al. (*2004) Genome duplication in the teleost fish Tetraodon nigroviridis reveals the
1590 early vertebrate proto-karyotype. *NATURE* 431:946–957.

1591 160. Pauli A *et al. (*2012) Systematic identification of long noncoding RNAs expressed during
1592 zebrafish embryogenesis. *GENOME RESEARCH* 22:577–591.

1593 161. Baird NA *et al. (*2008) Rapid SNP Discovery and Genetic Mapping Using Sequenced RAD
1594 Markers. *PLoS ONE* 3:e3376.

1595 162. Roesti M, Hendry AP, Salzburger W, Berner D (2012) Genome divergence during evolutionary
1596 diversification as revealed in replicate lake-stream stickleback population pairs. *Mol Ecol* 21:2852–
1597 2862.

1598 163. Roesti M, Kueng B, Moser D, Berner D (2015) The genomics of ecological vicariance in
1599 threespine stickleback fish. *NATURE COMMUNICATIONS* 6:8767.

1600 164. Rochette NC, Catchen JM (2017) Deriving genotypes from RAD-seq short-read data using
1601 Stacks. *NATURE PROTOCOLS* 12:2640–2659.

1602 165. Ocalewicz K, Sapota M (2011) Cytogenetic characteristics of the round goby Neogobius
1603 melanostomus (Pallas, 1814) (Teleostei. Gobiidae: Benthophilinae). *Marine Biology Research*
1604 7:195–201.

1605 166. Hohenlohe PA *et al. (*2010) Population Genomics of Parallel Adaptation in Threespine
1606 Stickleback using Sequenced RAD Tags. *PLOS GENETICS* 6:e1000862.

1607 167. Kearse M *et al. (*2012) Geneious Basic. An integrated and extendable desktop software
1608 platform for the organization and analysis of sequence data. *BIOINFORMATICS* 28:1647–1649.

1609 168. Ward MN *et al. (*2008) The molecular basis of color vision in colorful fish. Four long wave-
1610 sensitive (LWS) opsins in guppies (Poecilia reticulata) are defined by amino acid substitutions at
1611 key functional sites. *BMC EVOLUTIONARY BIOLOGY* 8:210.

1612 169. Rennison DJ, Owens GL, Taylor JS (2012) Opsin gene duplication and divergence in ray-
1613 finned fish. *Molecular Phylogenetics and Evolution* 62:986–1008.

1614 170. Lin J-J, Wang F-Y, Li W-H, Wang T-Y (2017) The rises and falls of opsin genes in 59 ray-
1615 finned fish genomes and their implications for environmental adaptation. *Scientific reports* 7.

1616 171. Register EA, Yokoyama R, Yokoyama S (1994) Multiple origins of the green-sensitive opsin
1617 genes in fish. *JOURNAL OF MOLECULAR EVOLUTION* 39:268–273.

1618 172. Katoh K, Kuma K, Toh H, Miyata T (2005) MAFFT version 5. Improvement in accuracy of
1619 multiple sequence alignment. *NUCLEIC ACIDS RESEARCH* 33:511–518.

1620 173. Darriba D, Taboada GL, Doallo R, Posada D (2012) jModelTest 2. More models, new
1621 heuristics and parallel computing. *NATURE METHODS* 9:772.

1622 174. Guindon S, Gascuel O (2003) A simple, fast, and accurate algorithm to estimate large
1623 phylogenies by maximum likelihood. *Systematic biology* 52:696–704.

1624 175. Ronquist F, Huelsenbeck JP (2003) MrBayes 3. Bayesian phylogenetic inference under mixed
1625 models. *BIOINFORMATICS* 19:1572–1574.

1626 176. Hajkova P *et al. (*2010) Genome-Wide Reprogramming in the Mouse Germ Line Entails the
1627 Base Excision Repair Pathway. *Science* 329:78.

1628 177. Brawand D *et al. (*2014) The genomic substrate for adaptive radiation in African cichlid fish.
1629 *NATURE* 513:375–381.

1630 178. Peichel CL, Sullivan ST, Liachko I, White MA (2017) Improvement of the Threespine
1631 Stickleback Genome Using a Hi-C-Based Proximity-Guided Assembly. *The Journal of heredity*
1632 108:693–700.

1633 179. Trifinopoulos J, Nguyen L-T, Haeseler A von, Minh BQ (2016) W-IQ-TREE. A fast online
1634 phylogenetic tool for maximum likelihood analysis. *NUCLEIC ACIDS RESEARCH* 44:W232-5.

1635 180. Hoang DT, Chernomor O, Haeseler A von, Minh BQ, Le Vinh S (2018) UFBoot2. Improving
1636 the Ultrafast Bootstrap Approximation. *MOLECULAR BIOLOGY AND EVOLUTION* 35:518–522.

1637 181. Altschul S (1990) Basic Local Alignment Search Tool. *Journal of Molecular Biology* 215:403–
1638 410.

1639 182. Finn RD *et al. (*2010) The Pfam protein families database. *NUCLEIC ACIDS RESEARCH*
1640 38:D211-22.

1641 183. Sigrist CJA *et al. (*2010) PROSITE, a protein domain database for functional characterization
1642 and annotation. *NUCLEIC ACIDS RESEARCH* 38:D161-6.

1643 184. Sievers F *et al. (*2011) Fast, scalable generation of high-quality protein multiple sequence
1644 alignments using Clustal Omega. *MOLECULAR SYSTEMS BIOLOGY* 7:539.

1645 185. Maddison WP, Maddison MP (2016) Mesquite: a modular system for evolutionary analysis.
1646 Version 3.10.

1647 186. Stamatakis A (2014) RAxML version 8. A tool for phylogenetic analysis and post-analysis of
1648 large phylogenies. *Bioinformatics (Oxford, England)* 30:1312–1313.

1649 187. Rambaut A (2016) Figtree v1.4.3: Tree figure drawing tool.

1650 188. Camacho C *et al. (*2009) BLAST+. Architecture and applications. *BMC BIOINFORMATICS*
1651 10:421.

1652 189. Quinlan AR, Hall IM (2010) BEDTools. A flexible suite of utilities for comparing genomic
1653 features. *BIOINFORMATICS* 26:841–842.

1654 190. Edgar RC (2004) MUSCLE. A multiple sequence alignment method with reduced time and
1655 space complexity. *BMC BIOINFORMATICS* 5:113.

1656 191. Kumar S, Stecher G, Tamura K (2016) MEGA7: Molecular Evolutionary Genetics Analysis
1657 version 7.0 for bigger datasets. *MOLECULAR BIOLOGY AND EVOLUTION*.

1658 192. Darriba D, Taboada GL, Doallo R, Posada D (2011) ProtTest 3. Fast selection of best-fit
1659 models of protein evolution. *Bioinformatics (Oxford, England)* 27:1164–1165.

1660 193. Stamatakis A (2006) RAxML-VI-HPC. Maximum likelihood-based phylogenetic analyses with
1661 thousands of taxa and mixed models. *Bioinformatics (Oxford, England)* 22:2688–2690.

1662 194. Eddy SR (2011) Accelerated Profile HMM Searches. *PLOS COMPUTATIONAL BIOLOGY* 7.

1663 195. Katoh K, Standley DM (2013) MAFFT multiple sequence alignment software version 7.
1664 Improvements in performance and usability. *MOLECULAR BIOLOGY AND EVOLUTION* 30:772–
1665 780.

1666 196. Wang P *et al. (*2018) Factors Influencing Gene Family Size Variation Among Related Species
1667 in a Plant Family, Solanaceae. *GENOME BIOLOGY AND EVOLUTION* 10:2596–2613.

1668 197. Crooks GE, Hon G, Chandonia J-M, Brenner SE (2004) WebLogo. A sequence logo
1669 generator. *GENOME RESEARCH* 14:1188–1190.

1670 198. Edwards JR, Yarychkivska O, Boulard M, Bestor TH (2017) DNA methylation and DNA
1671 methyltransferases. *EPIGENETICS & CHROMATIN* 10:23.

1672 199. Ranwez V, Harispe S, Delsuc F, Douzery EJP (2011) MACSE. Multiple Alignment of Coding
1673 SEquences accounting for frameshifts and stop codons. *PLoS ONE* 6:e22594.

1674 200. Lanfear R, Frandsen PB, Wright AM, Senfeld T, Calcott B (2017) PartitionFinder 2. New
1675 Methods for Selecting Partitioned Models of Evolution for Molecular and Morphological
1676 Phylogenetic Analyses. *MOLECULAR BIOLOGY AND EVOLUTION* 34:772–773.

1677 201. Guindon S *et al. (*2010) New algorithms and methods to estimate maximum-likelihood
1678 phylogenies. Assessing the performance of PhyML 3.0. *Systematic biology* 59:307–321.

1679 202. Huelsenbeck JP, Ronquist F (2001) MRBAYES. Bayesian inference of phylogenetic trees.
1680 *BIOINFORMATICS* 17:754–755.

1681 203. Benson G (1999) Tandem repeats finder. A program to analyze DNA sequences. *NUCLEIC*
1682 *ACIDS RESEARCH* 27:573–580.

1683 204. Xu Z, Wang H (2007) LTR_FINDER. An efficient tool for the prediction of full-length LTR
1684 retrotransposons. *NUCLEIC ACIDS RESEARCH* 35:W265-W268.

1685 205. Ellinghaus D, Kurtz S, Willhoeft U (2008) LTRharvest, an efficient and flexible software for de
1686 novo detection of LTR retrotransposons. *BMC BIOINFORMATICS* 9:18.

1687 206. Steinbiss S, Willhoeft U, Gremme G, Kurtz S (2009) Fine-grained annotation and classification
1688 of de novo predicted LTR retrotransposons. *NUCLEIC ACIDS RESEARCH* 37:7002–7013.

1689

Supplemental_Fig_S1
The round goby genome

Phylogenetic tree of vertebrate opsin protein sequences. Maximum-likelihood phylogenetic tree with VA opsins and pinopbsins as outgroup. Round goby is indicated in orange. Non-teleost species and the outgroup (VA opsins and pinopsins) are indicated in grey.

Supplemental_Fig_S2
The round goby genome

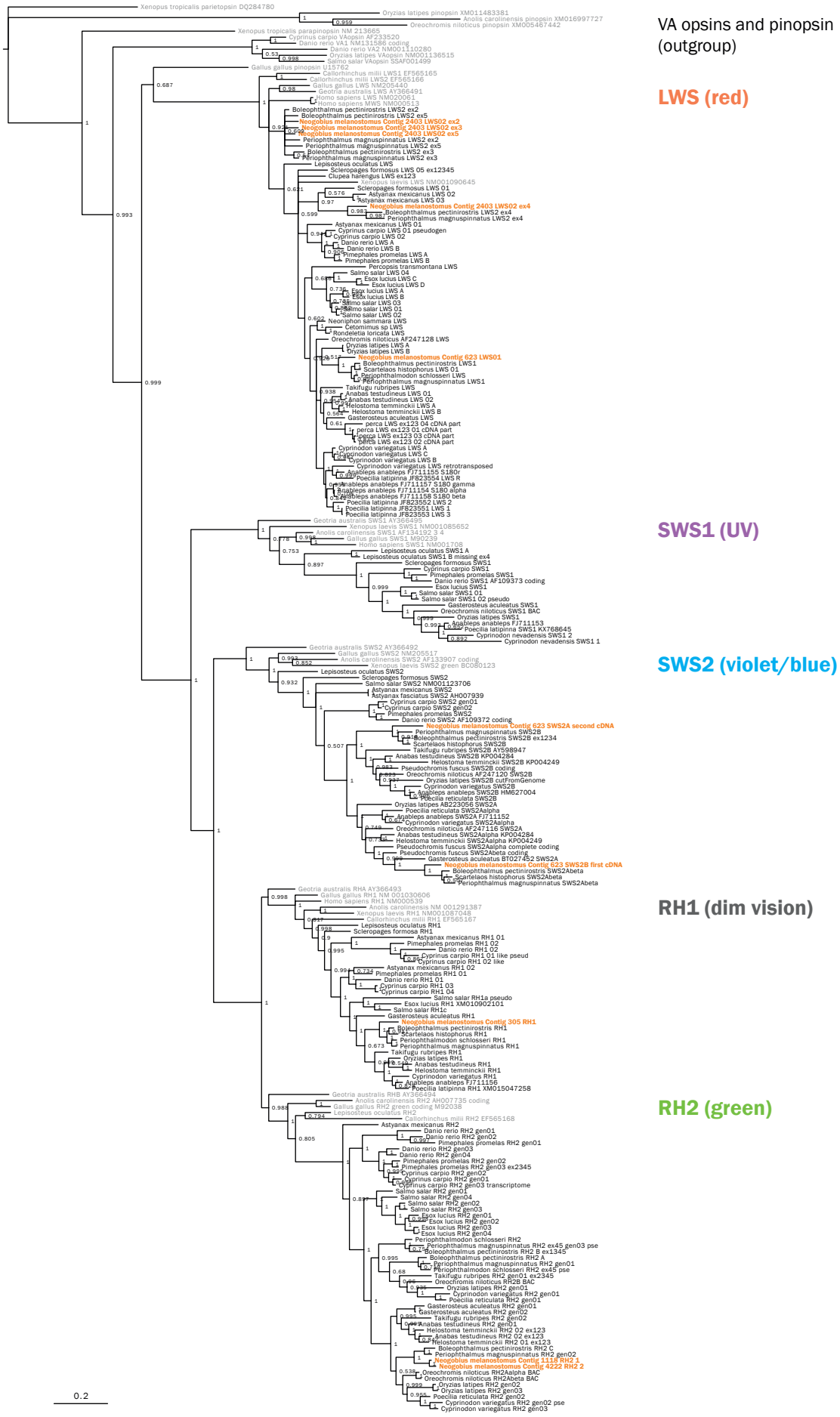

Phylogenetic tree of vertebrate opsin protein sequences, using single exons. Maximum-likelihood phylogenetic tree with VA opsins and pinopbsins as outgroup. Round goby is indicated in orange. Non-teleost species and the outgroup (VA opsins and pinopsins) are indicated in grey.

Supplemental_Fig_S3
The round goby genome

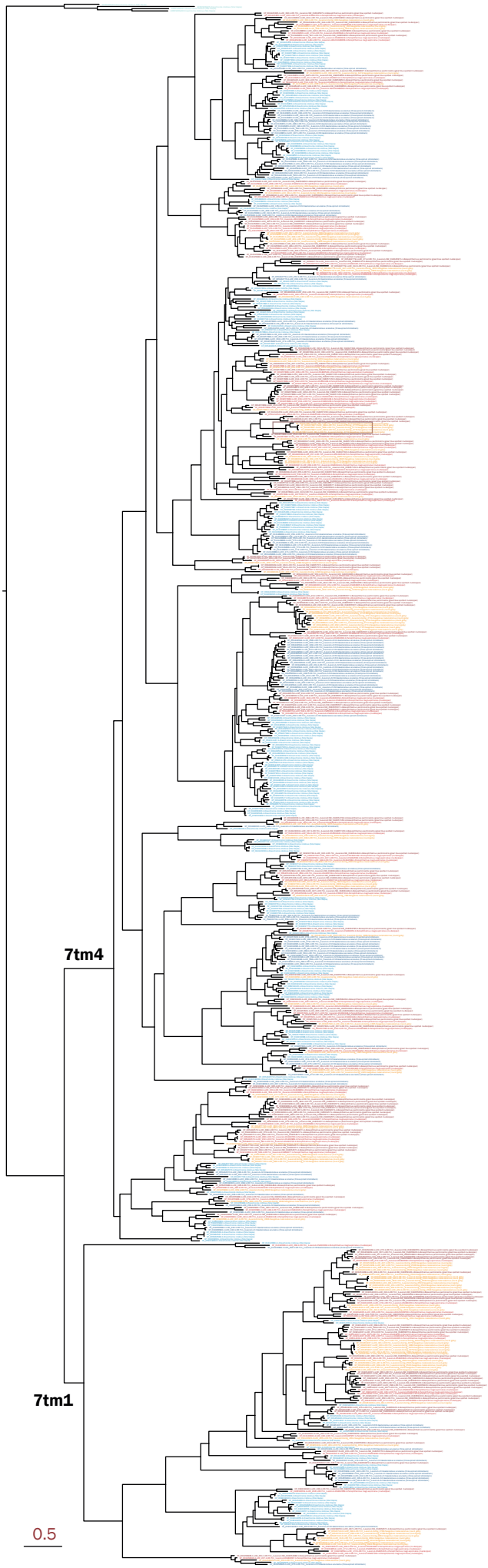

Maximum-likelihood phylogenetic tree of percomorph olfactory receptor protein sequences.

Supplemental_Fig_S4
The round goby genome

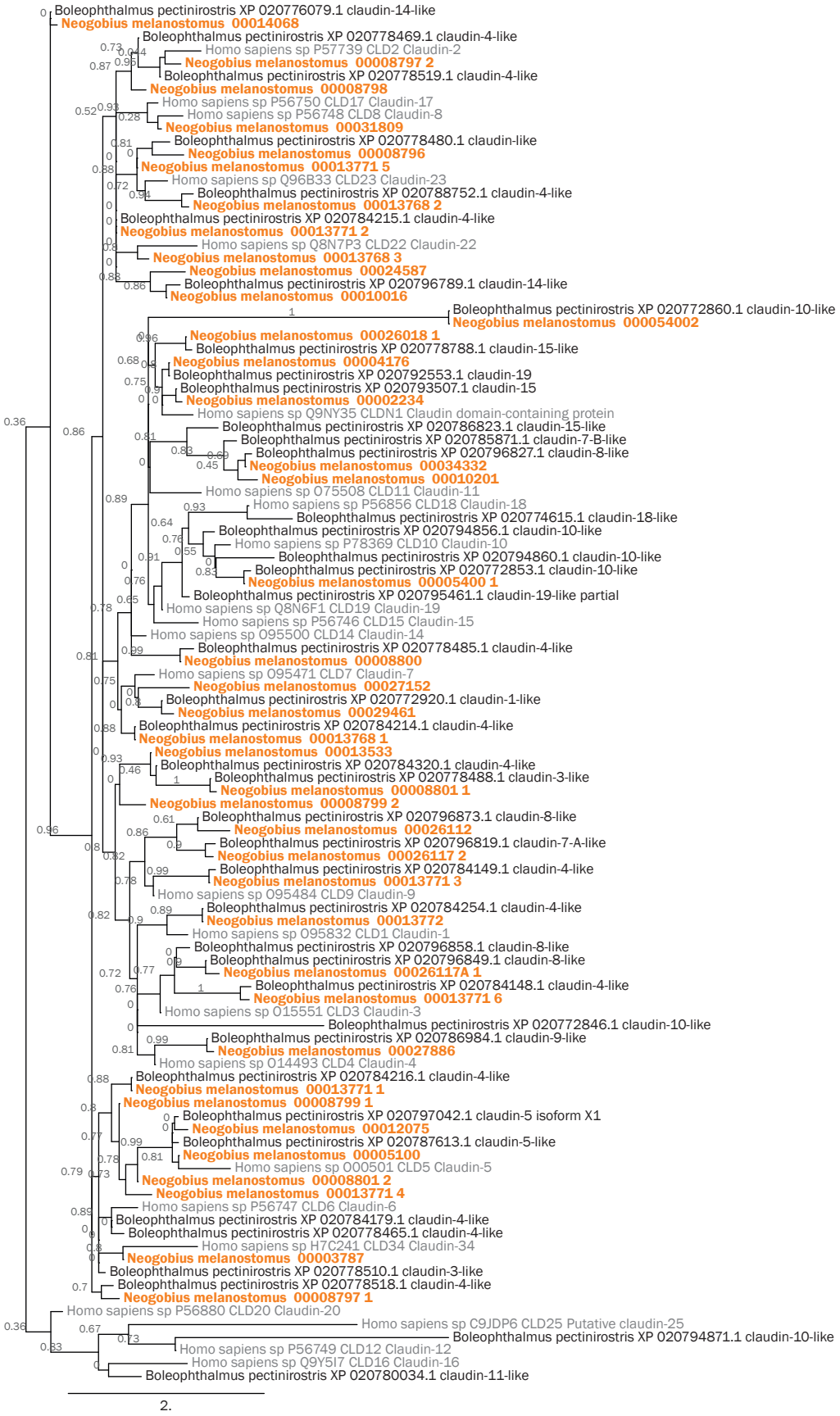

Phylogenetic tree of vertebrate claudin genes. Maximum-likelihood tree with 100 bootstraps of round goby (Neogobius melanostomus, orange) in relation to great blue-spotted mudskipper (Boleophthalmus pectinirostris) and human (Homo sapiens, grey).

Supplemental_Fig_S5
The round goby genome

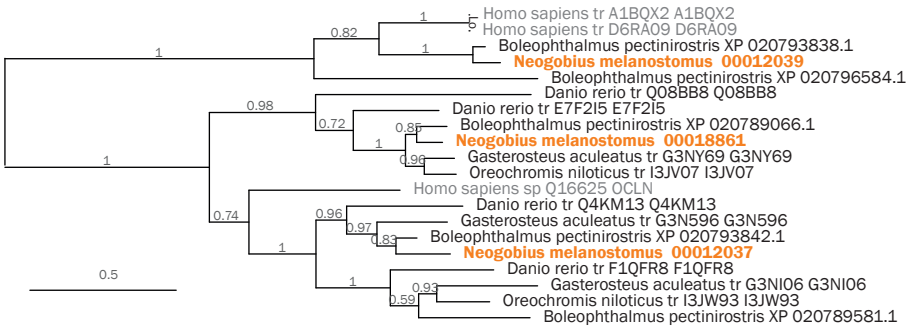

Phylogenetic tree of vertebrate occludin genes. Maximum-likelihood tree with 100 bootstraps of round goby (Neogobius melanostomus, orange) in relation to great blue-spotted mudskipper (Boleophthalmus pectinirostris), stickleback (Gasterosteus aculeatus), nile tilapia (Oreochromis niloticus), zebrafish (Danio rerio), and human (Homo sapiens, grey).

Supplemental_Fig_S6
The round goby genome

Na+/H+ exchanger

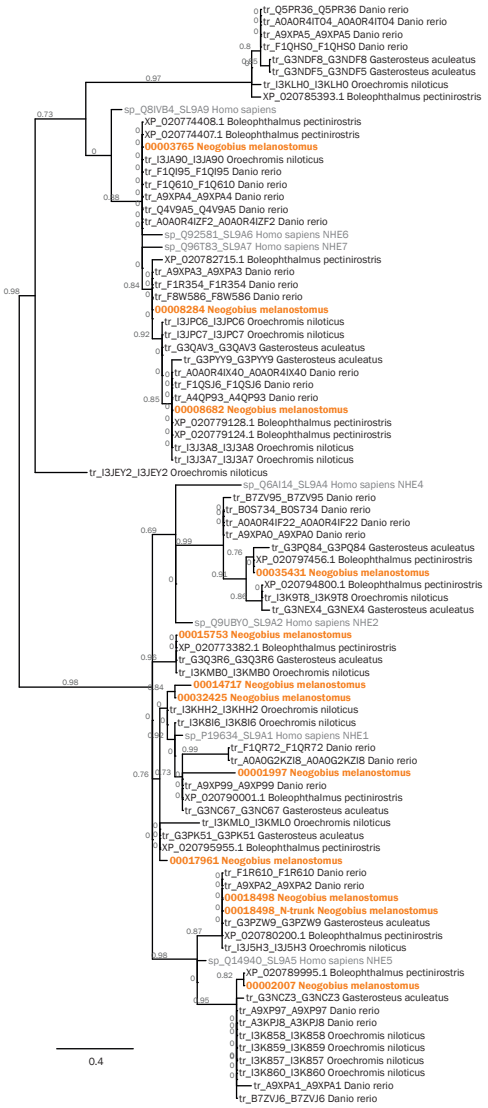

Na+-K+-ATPase alpha

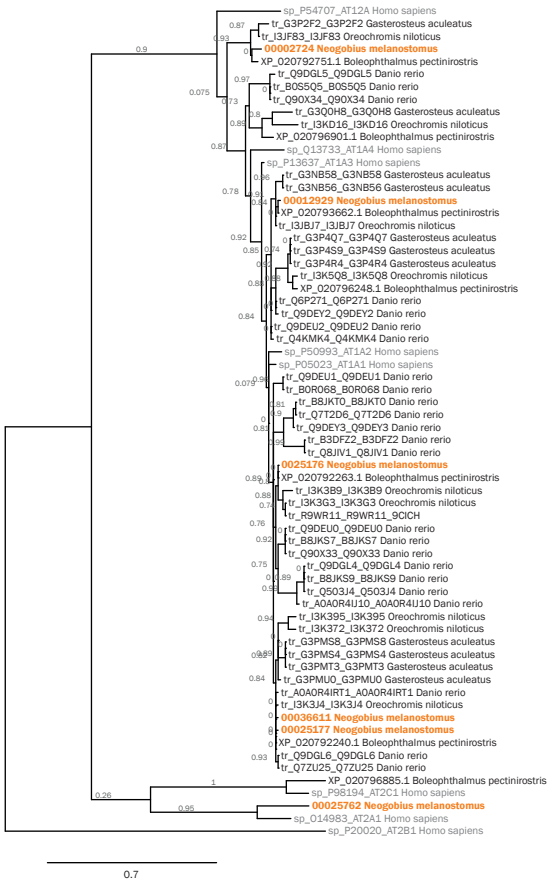

Na+-K+-ATPase beta

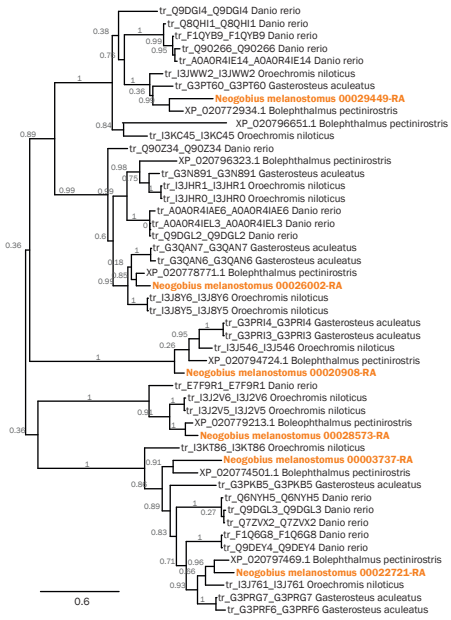

Phylogenetic tree of vertebrate ion transporters. Maximum-likelihood tree with 100 bootstraps of round goby (Neogobius melanostomus, orange) in relation to great blue-spotted mudskipper (Boleophthalmus pectinirostris), stickleback (Gasterosteus aculeatus), nile tilapia (Oreochromis niloticus), zebrafish (Danio rerio), and human (Homo sapiens, grey)

Supplemental_Fig_S7
The round goby genome

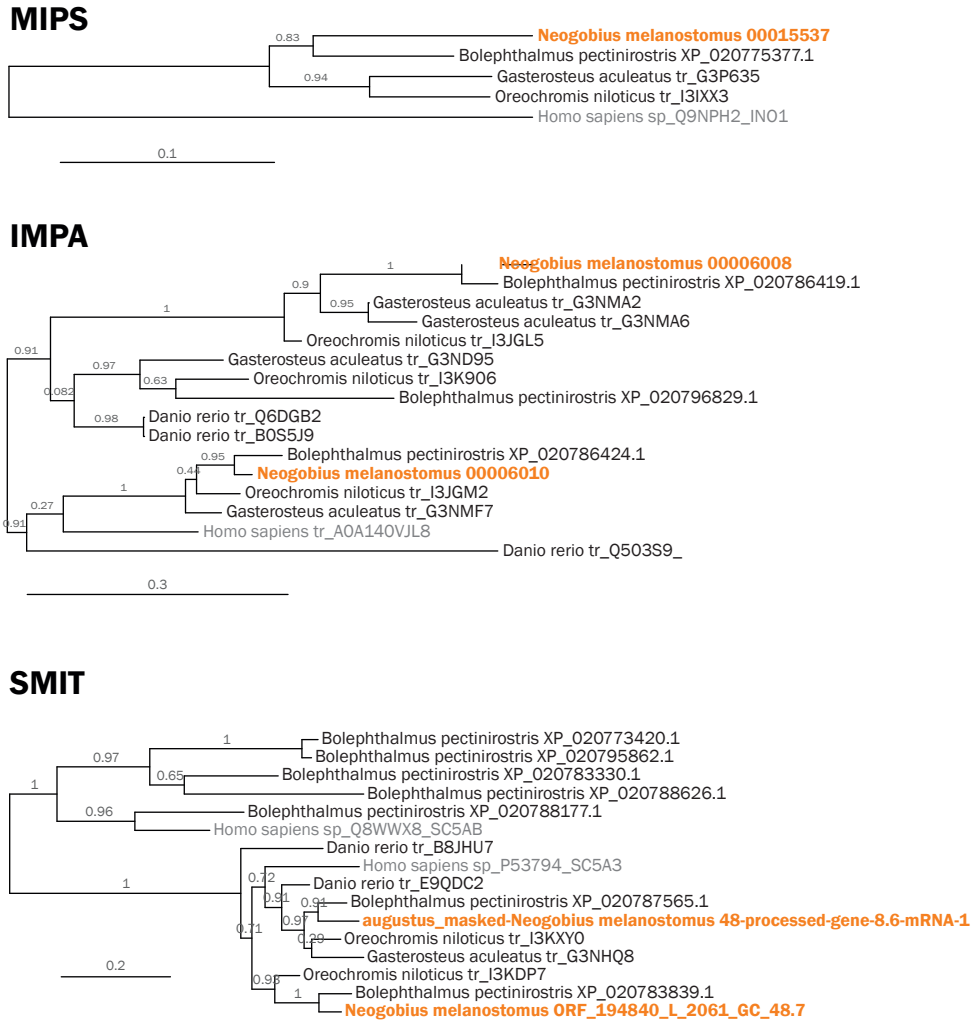

Phylogenetic tree of vertebrate genes promoting osmolyte production. Maximum-likelihood tree with 100 bootstraps of round goby (Neogobius melanostomus, orange) in relation to great blue-spotted mudskipper (Boleophthalmus pectinirostris), stickleback (Gasterosteus aculeatus), nile tilapia (Oreochromis niloticus), zebrafish (Danio rerio), and human (Homo sapiens, grey)

Supplemental_Fig_S8
The round goby genome

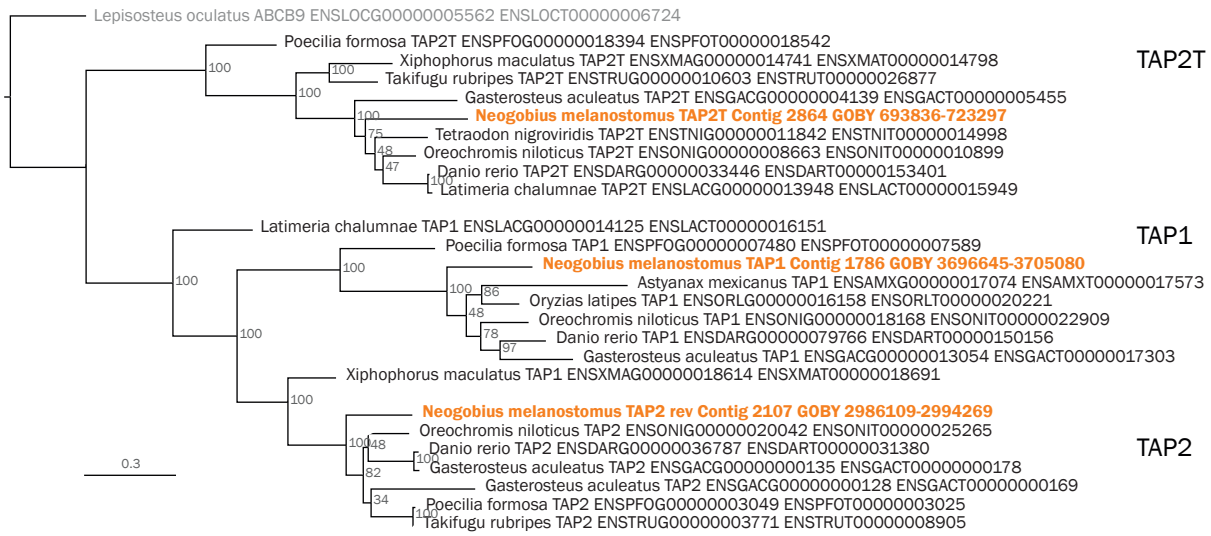

Phylogenetic tree of fish TAP genes. Maximum-likelihood tree with 500 bootstraps. Round goby (Neogobius melanostomus) is labeled orange. Outgroup: Lepistosteus oculatus ABC transporter.

Supplemental_Fig_S9
The round goby genome

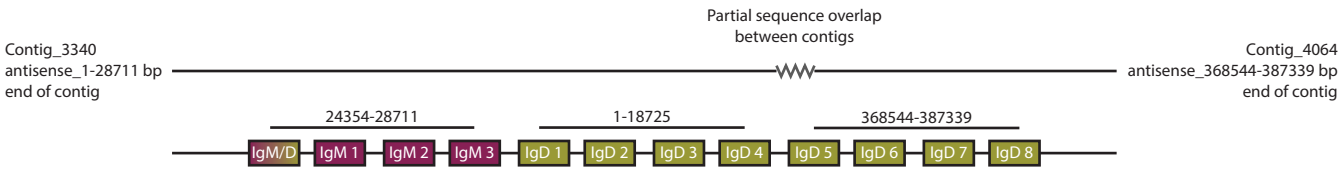

The Ig locus spans two contigs and contains IgM and IgD domains.

Supplemental_Fig_S10
The round goby genome

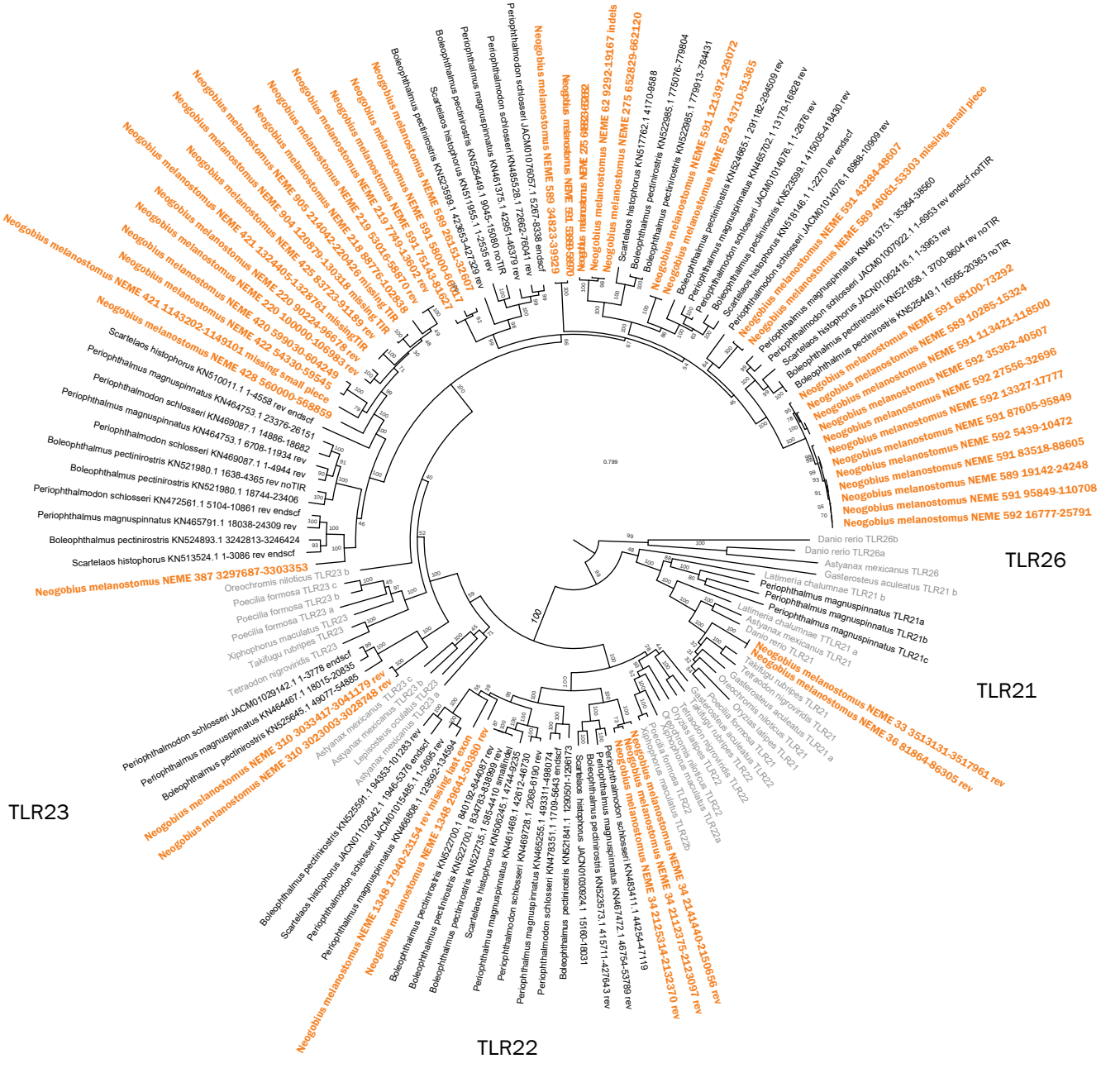

Phylogenetic tree of Gobiidae Toll Like Receptor protein sequences. A maximum likelihood phylogenetic tree run with the JTT substitution model and 500 bootstrap replicates on the transmembrane, linker and TIR domain of all TLRs found in Gobiiformes (Neogobius melanostomus, orange; other Gobiidae, black) and selected other fish (grey) for context.

Supplemental_Fig_S11
The round goby genome

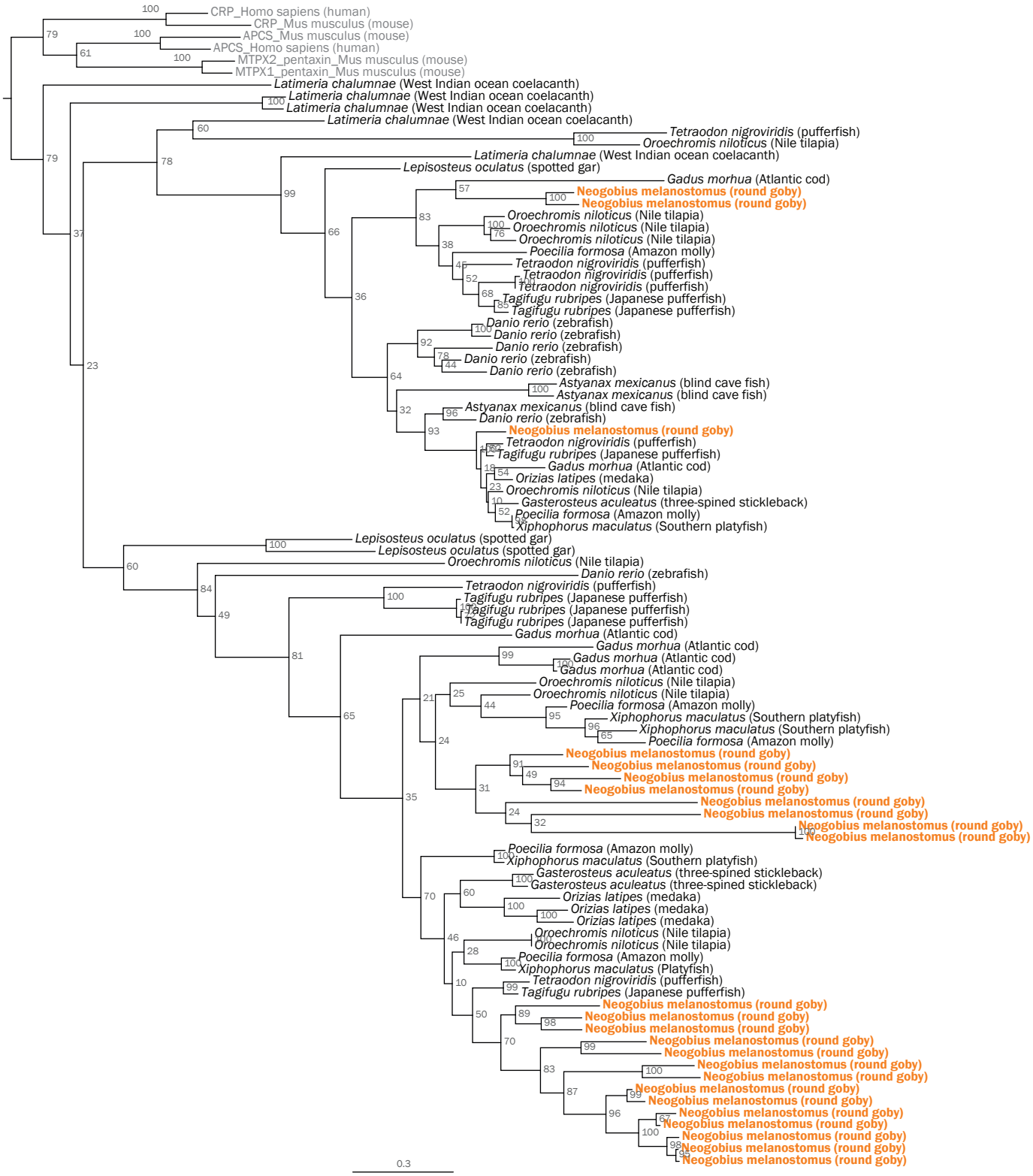

Phylogenetic tree of fish CRP/APCS sequences. Maximum Likelihood phylogenetic tree with 500 bootstraps rooted at the split between tetrapods and ray-finned fish. Tetrapods were used as outgroup and are indicated in grey. Round goby is indicated in orange.

Supplemental_Fig_S12
The round goby genome

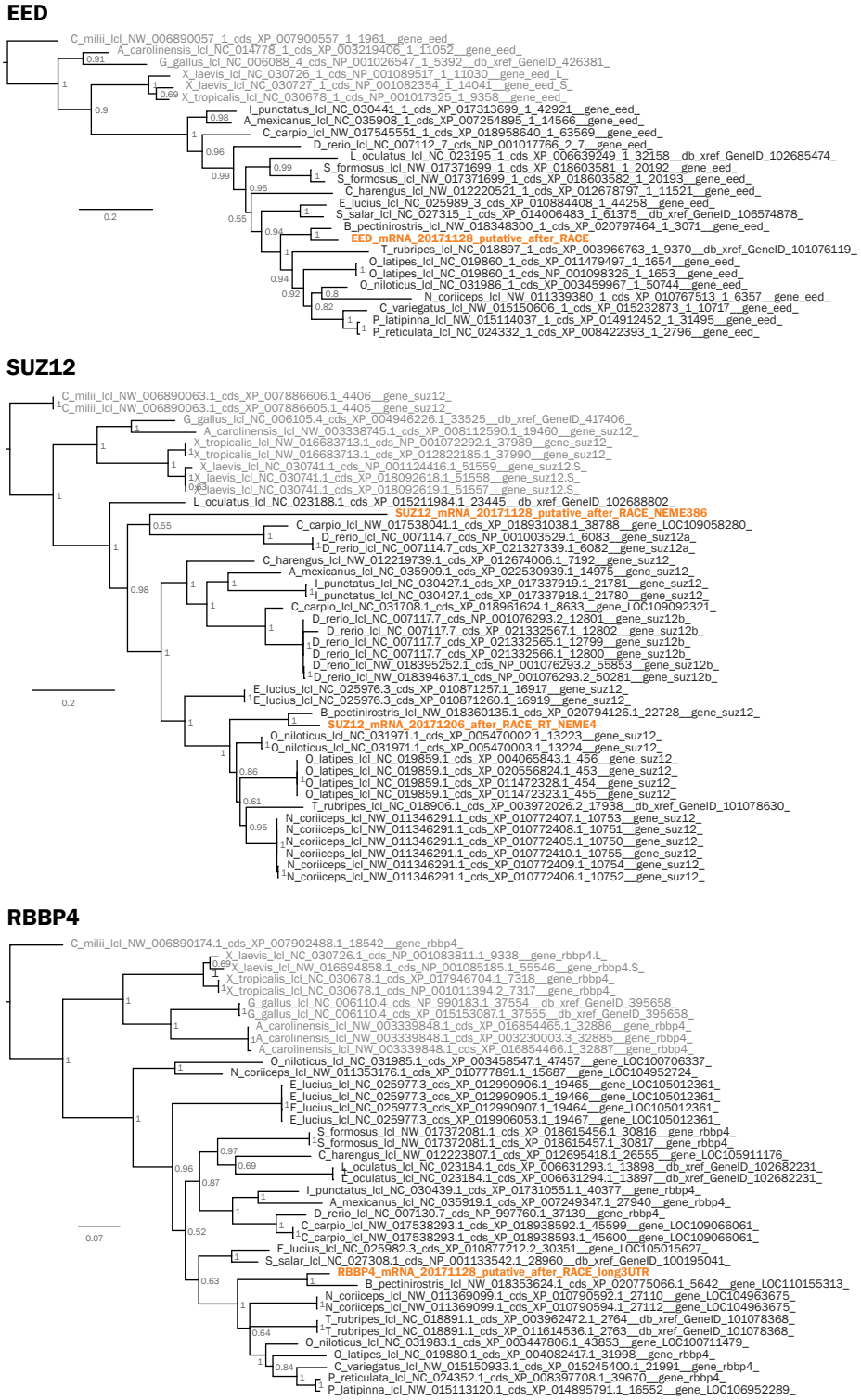

Phylogenetic tree of vertebrate PRC2 components EED, SUZ12, and RBBP4. Bayesian phylogenetic tree rooted with Australian ghostshark (C. milii). Round goby is indicated in orange.